ISSN: 2161-6795 Volume 9, Number 2, April 2019

Scientific Research Publishing

World Journal of Nuclear Science and Technology

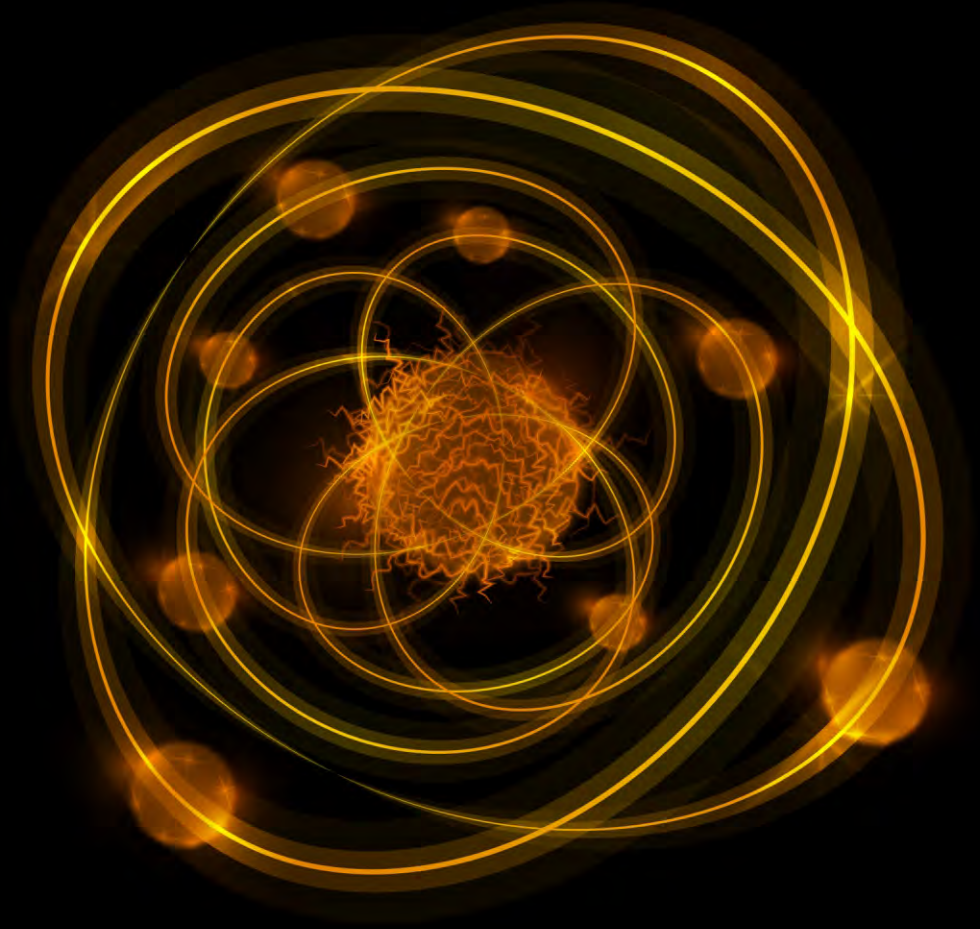

ISSN: 2161-6795

www.scirp.org/journal/wjnst

Journal Editorial Board

ISSN 2161-6795 (Print) ISSN 2161-6809 (Online)
http://www.scirp.org/journal/wjnst

Editor-in-Chief

Editorial Board

Scientific Research Publishing

World Journal of Nuclear Science and Technology, 2019, 9, 27-111
http://www.scirp.org/journal/wjnst
ISSN Online: 2161-6809
ISSN Print: 2161-6795

Table of Contents

Volume 9 Number 2 April 2019

World Journal of Nuclear Science and Technology (WJNST)
Journal Information

SUBSCRIPTIONS

The *World Journal of Nuclear Science and Technology* (Online at Scientific Research Publishing, www.SciRP.org) is published quarterly by Scientific Research Publishing, Inc., USA.

Subscription rates:
Print: $79 per issue.
To subscribe, please contact Journals Subscriptions Department, E-mail: sub@scirp.org

SERVICES

Advertisements
Advertisement Sales Department, E-mail: service@scirp.org

Reprints (minimum quantity 100 copies)
Reprints Co-ordinator, Scientific Research Publishing, Inc., USA.
E-mail: sub@scirp.org

COPYRIGHT

PRODUCTION INFORMATION

For manuscripts that have been accepted for publication, please contact:
E-mail: wjnst@scirp.org

World Journal of Nuclear Science and Technology, 2019, 9, 27-66
http://www.scirp.org/journal/wjnst
ISSN Online: 2161-6809
ISSN Print: 2161-6795

Radiotracers and Nucleonic Control Systems Applied in Industry—Polish Case

Andrzej G. Chmielewski, Tomasz Smoliński, Marcin Rogowski

Institute of Nuclear Chemistry and Technology (INCT), Warsaw, Poland
Email: a.chmielewski@ichtj.waw.pl

How to cite this paper: Chmielewski, A.G., Smoliński, T. and Rogowski, M. (2019) Radiotracers and Nucleonic Control Systems Applied in Industry—Polish Case. *World Journal of Nuclear Science and Technology*, **9**, 27-66.
https://doi.org/10.4236/wjnst.2019.92003

Received: February 11, 2019
Accepted: March 4, 2019
Published: March 7, 2019

Abstract

Nuclear and radiation technologies play an important role in Polish power sector, oil industry and mining sector, starting from fossil fuels exploitation, their transport and distribution and finally power generation. Application of environmental isotopes, stable and radioactive, in ground water monitoring in the vicinity of open cast lignite mine, and radon monitor applied for miner's safety in deep coal mines and nucleonic control systems for ash in coal quality control is often used in mining industry. Other applications of nuclear techniques reviewed, concern the oil industry, oil field recovery, transportation pipelines and refineries. Finally, the application of beta radiation-based gauges for air borne fly ash monitoring and radiation technology for flue gas treatment are the examples of using this technique in power sector equipped with coal and oil fired boilers [1]. The radiotracers techniques were used also in glass industry (determination and optimization parameters of the furnaces), cement industry (test of aggregates for the production of cement and optimization media transport in pipelines), metallurgy of Cu, Pb, Zn (investigation of pyrometallurgy processes and new techniques), cellulose industry, environmental and (mainly hydrological) research etc. [2]. The article is brief review of present status of radiotracer and nucleonic gauges techniques as applied to polish industry.

Keywords

Radiotracers, Nucleonic Control Systems, Coal Mining, Oil Industry

1. Introduction

First application of nuclear techniques in Poland was reported nearly 45 years ago, and in 1961, about 200 radioisotope gauges were already installed in Polish industry [3]. During the next thirty years, manufacturing, installation and servicing facilities have been built enabling application of the nucleonic control

systems (NCS) and radiotracer techniques in the industry on the relatively large scale [4]. A main sector where radiation and nuclear technologies in Poland are used:

- Medical sealed sources and accelerators,
- Industrial and geological field research,
- Radioisotope gauges,
- Industrial and research laboratories (open sources),
- Industrial and research laboratories (sealed sources),
- Production, transport and sales of radioactive materials.

Since the 90's decade, profound reconstruction of the Polish economy has started. Introduction of the market economy rules, the gradual introduction of new regulations on the use of radioisotopes and development of new non-radioisotope technologies caused reduced demand from the industry on the radiotracer testing. Such situation influenced that radiotracer techniques had to be considerably reduced. Moreover, competition of the other techniques, strict environmental protection standards and the rise of the anti-nuclear movements had significant impact on the position of radiotracer techniques.

At the moment radiotracers for industrial application mainly are used for leakage tests in refinery (INCT group). Metals recovery application investigated by radiotracers methods are under development as well [5] [6]. Radiometric methods are used also for waste water treatment application [7]. Sealed sources technologies such as: production and application of radioisotope gauges used for measurements and/or automatic control of such quantities as level, density, thickness, coating thickness, mass flow, ash content, acid concentration and airborne dust are still used as well. There are some specific branches of industry where "traditionally" nucleonic gauges are readily installed, such as sugar-factories (density), sulfuric acid production lines (concentration gauges) or coal mines (ash). The numbers of licenses for using radioisotope and radiation sources are shown in **Table 1**.

2. Present Status of Radiotracer and Nucleonic Gauges Techniques as Applied in Industry

The short summary of the present status of using radiotracers and NCS in Poland is showed in **Table 2**.

2.1. Radionuclide Source

National Centre or Nuclear Research POLATOM Radioisotope Centre [8] is a Polish manufacturer and distributor of the isotope used in medicine, science, industry and environmental protection. The Centre produces wide range of products for medicine and for research, and development, technology and environment protection such as:

- Radiopharmaceuticals for diagnostic and therapy,
- Kits for labelling with Tc-99m,
- Radiochemicals (pharmaceutical grade),

- Radiopharmaceutical precursor (for the radiolabeling of carrier molecules),
- Radionuclide generators,
- Wide range of radiochemicals,
- Sealed radiation sources for gamma radiography and industrial process control, (Ytterbium-169, Selenium-75, Iridium-192, Cobalt-60),
- Standard solutions and sources for electronic measurement devices calibration.

Radioisotopes in Poland are produced at MARIA research nuclear reactor which is currently the sole operated in Poland. Its power amounts to 30 MW. Current main reactor applications [9]:

Table 1. According to data of the National Atomic Energy Agency, the following numbers of licenses for using radioisotope and radiation sources were issued till the end of 2016 [3].

Activity type	Symbol	Number of entities	Number of activity types
Class I laboratory	I	1	1
Class II laboratory	II	94	107
Class III laboratory	III	124	242
Class Z laboratory	Z	108	199
Smoke detector service	UIC	372	372
Device service	UIA	168	197
Isotope devices	AKP	556	696
Manufacture of isotope sources and devices	PRO	28	32
Trade in isotope sources and devices	DYS	76	85
Accelerator	AKC	77	156
Isotope applicators	APL	37	53
Telegamma therapy	TLG	5	5
Radiation device	URD	36	37
Gamma graphic apparatus	DEF	111	113
Storage facility of isotope sources	MAG	120	145
Work with sources outside registered laboratory	TER	56	62
Transport of sources or waste	TRN	488	499
Chromatograph	CHR	227	275
Veterinary X-ray apparatus	RTW	1083	1128
X-ray scanner	RTS	471	609
X-ray defectoscope	RTD	206	229
Other X-ray apparatus	RTG	399	592
Total			5834

ANNUAL REPORT 2016 National Atomic Energy Agency

Table 2. Status of radiotracer and nucleonic gauges in Poland.

Radioactive source	Open sources	Sealed sources
Permission for the application in the country	Yes	Yes
Current status	Used	Used
Examples of present application	Leakage tests in refinery	Level gauges Density gauges Thickness gauges Coating thickness gauges Nucleonic balances (bulk flow meter) Concentration gauge Gamma scanning Analyzers and monitors
Requirements	National Atomic Energy Agency permission	National Atomic Energy Agency permission for use
Special requirements and restrictions	Provincial Sanitary and Epidemiological Station permission Office of Technical Inspection permission for pressure tests	Certificates PN-EN norms, ISO standards

- Production of radioisotopes,
- Testing of fuel and structural materials for nuclear power engineering,
- Neutron transmutation doping of silicon,
- Neutron modification of materials,
- Research in neutron and condensed matter physics,
- Neutron radiography,
- Neutron activation analysis,
- Neutron beams in medicine,
- Training in the field of reactor physics & technology.

2.2. Present Examples of Using Radiotracer and Nucleonic Control Systems Applied to Industry

2.2.1. Leakage Tests

The Institute of Nuclear Chemistry and Technology has been performing for many years in control of the leak-proof-ness of production systems and facilities, underground and ground tanks and underground gas and liquid pipelines by radioisotope marker methods. The field group comprises experienced staff, licensed by the National Atomic Energy Agency. They have got specialized equipment for field generation of various radioisotope markers suitable for marking different types of media. The hardware includes dosing and measuring equipment and detectors for leak-proof-ness tests performed by pig moving inside pipelines. They use special absorptive materials matching the markers [10].

The method is basing on filling the tested facility with (primarily) gaseous methyl bromide labelled with bromine Br-82 (**Figure 1**). Following mixing with the control or working medium the marker flows to the leak site and is captured

by either natural (soil, thermal insulation) or artificial (special materials installed before test) adsorbent. In case of soil adsorption, the marker migrates towards the surface. Radiometric detection can be carried out through layers of soil up to 5 meters thick and enables identification and precise positioning of the leak. Special follow-up detectors moving inside the pipeline together with the control medium are used for tests of underground pipelines with cleanout chambers. No absorbents are used for tests of valves and exchangers. They are performing leak-proof-ness tests including precise localization of leaks using radioisotope marker methods at [11]:

- underground liquid and gas pipelines (Φ200 - 600 mm) with cleanout chambers—with sensitivity of up to 0.5 dcm^3/h for liquids and 5 g/h for gases (output from the smallest detected at localized leak) and underground liquid and gas pipelines ($\Phi \geq$ 600 mm) without cleanout chambers—with sensitivity of up to 1.0 dcm^3/h for liquids and 10 g/h for gases,
- underground and ground pipelines (of all diameters) for gas and liquids without cleanout chambers with sensitivity up to 1.0 dcm^3/h for liquids and 10 g/h for gas (**Figure 2**),
- gate valves in pipelines for all media,
- underground tanks and ground tank bottoms with sensitivity related to the tank volume,

Figure 1. Equipment needed for generation of gaseous methyl bromide from pre-activated potassium bromide.

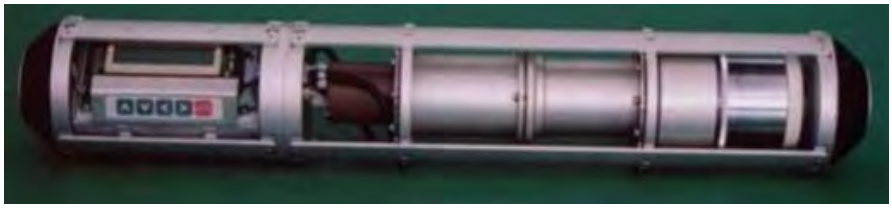

Figure 2. Detector for detection of leaks in underground pipelines with cleanout chambers.

- petrochemical and chemical industry installations with sensitivity of 30 cm^3/h. Tests are performed without removal of inner and outside lining, installation of scaffoldings and removal of catalysts,
- other installations and structures subject to individual arrangements.

The methods are recognized by the Office of Technical Inspection. A long experience gained during various projects carried out for PKN Orlen Płock, Gdańsk Refinery, Przedsiębiorstwo Eksploatacji Rurociągów Naftowych (PERN) in Płock and other clients stands evidence to the quality of results and efficiency of the method. In terms of costs, using radioisotope markers for leak-proof=ness tests is cheaper than traditional methods.

2.2.2. Radiotracer in Biotechnology Process Investigations

Radiotracer in the form of tritium water ($T_{1/2}$ = 4510 days, β radiation—0.018 MeV) was used for determination of residence time distribution (RTD) of materials in installation with 42 dm^3 volume and flow rate 0.6 dm^3/day for biogas production during anaerobic digestion of selected agricultural material or municipal wastes. The scanning technique was applied for measurement of density distribution inside the fermenter and eventually presents of foam inside the fermenter (**Figure 3**) [12].

These experiments were a base for construction of industry scale technology for biogas generation (230 kW).

2.2.3. Coal Mining Industry

Sealed radioactive sources steel is used into polish coal mines. Examples of the use of radioisotope techniques in mines are presented below (**Figure 4** and **Figure 5**).

Carbon enrichment involves the separation of coal from the stone. This occurs in a thick suspension fluid. To maintain the appropriate density of this liquid, isotopic densitometers are used. The densitometers are most often used when measuring the density of the product flowing in pipeline, detector and container with the source are mounted on a special frame, after both sides of the pipe and is part of the pipeline [2].

3. Regulations on Radiation Protection and Use of Radiation

3.1. Legal Basis

The legal basis for regulating the use of radioactive materials is: Atomic Law. Act of Parliament of 29 November 2000 on the Atomic Law introduced a consistent system ensuring nuclear safety and radiological protection of workers and general public in Poland [14].

Key provisions of the Atomic Law Act regard licensing of activities which involve exposure to ionizing radiation (*i.e.* licenses issued for activities specified in section "Definition, structure and functions of nuclear safety and radiological protection system") [15], powers vested within heads of organizational entities conducting activities with the use of radiation and powers of the President of

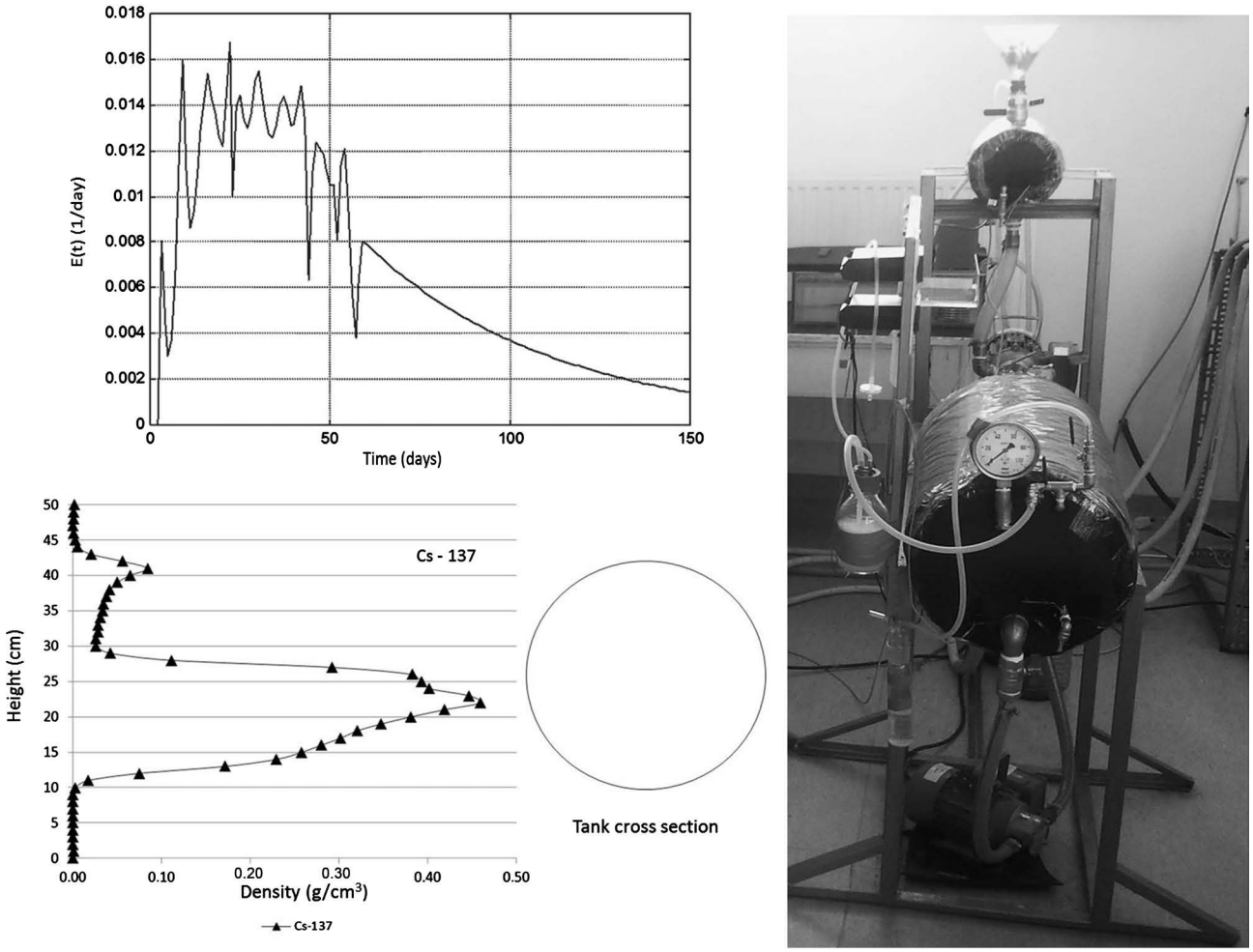

Figure 3. Comparison of experimental and model RTD results and scheme of scanning measurement and distribution of the density inside the fermenter [12].

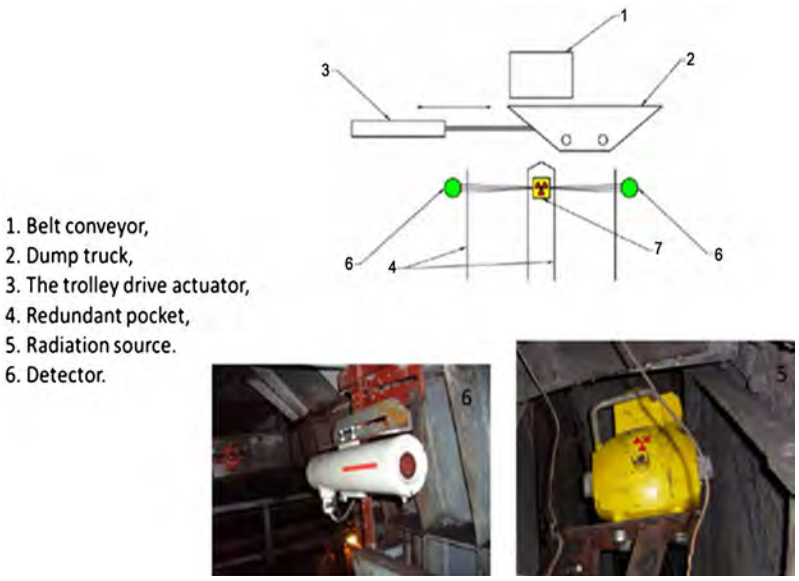

Figure 4. Loading of skip pocket [13].

Figure 5. Density gauges into coal enrichment installation (source Cs-137) [13].

National Atomic Energy Agency to control and supervise these activities. The Act also identifies other tasks of the PAA President concerning, inter alia, assessment of national radiation situation and procedures applied in radiation emergency. The most important provisions of the aforementioned Act concern issuance of licenses for activities connected with exposure to ionizing radiation (*i.e.* licenses for activities specified above in the subchapter "Definition, structure and functions of the nuclear safety and radiological protection system"), obligations of heads of organizational units conducting activities which involve radiation and prerogatives of the President of the National Atomic Energy Agency to exercise regulatory control and supervision of these activities [3].

Other Acts of Parliament

Apart from the Atomic Law Act, Polish laws set forth provisions indirectly connected with the issues of nuclear safety and radiological protection, which are included in other Acts of Parliament, in particular in [16]:

- Act of Parliament on Shipment of Hazardous Goods,
- Act of Parliament on Marine Safety,
- Act of Parliament on Technical Supervision,
- Plus 34 secondary legislation to the Atomic Law for example:

- Regulation of the Council of Ministers of July 12, 2006 on detailed conditions of safe work with sources of ionizing radiation (Journal of Laws from 2006 No. 140 item 994),
- Regulation of the Council of Ministers of December 23, 2002 on the requirements for dosimetric equipment (Journal of Laws of 2002 No. 239, item 2032),

- Regulation of the Council of Ministers of December 3, 2002 on radioactive waste and spent nuclear fuel (Journal of Laws of 2002 No. 230 item 1925),
- Regulation of the Council of Ministers of February 20, 2007 on basic requirements for controlled and supervised areas (Journal of Laws of 2007 No. 131, item 910).

3.2. How to Perform Industrial Research Using Radioisotopes in Poland—An Example of a Path

The first step is to get permission for work with isotopes from the PAA President [17].

Drafts of the PAA President's licenses for performance of activities involving exposure to ionizing radiation and other decisions in matters considered important for nuclear safety and radiological protection were prepared by the Radiological Protection Department (DOR) of PAA. Issuance of a license, an annex to a license or receipt of a notification is always preceded by the analysis and assessment of the documentation submitted by users of ionizing radiation sources. Apart from the said documentation, a detailed analysis is also conducted to cover the following issues: substantiation for the commencement of the activity involving exposure, utility dose limits proposed, quality assurance program in connection with the activity conducted Supervision of the use of ionizing radiation sources and an internal emergency plan for cases of radiation emergency. In cases, in which activity involving ionization radiation exposure does not require a license, decisions are issued on acceptance of notification of activity involving exposure to ionizing radiation. These cases have been listed in the Regulation of the Council of Ministers of 6 August 2002 concerning cases, in which activity involving exposure to ionizing radiation is not subject to the license or notification obligation and cases, in which it may be conducted on the basis of a notification (Journal of Laws No. 137, item 1153 as amended).

In the application for a permit, there must be a description of the test procedure—Technological Instruction. There is a description of the isotope and its form, activity, radioactive waste management, justification of the method, possessed dosimetry equipment, type of source (open, closed), name of the tested installation, what will be tested, how and by what method, how the activity measurement will be performed. With the use of unsealed sources, special attention should be paid to storage and handling of sources and to the potential for contamination of workers and equipment.

The procedure differs slightly when sealed radioactive sources is used. Heads of organizational units performing activity which involves use or storage of sealed radioactive sources or equipment featuring such sources under the relevant authorization granted are obliged to submit copies of records concerning the radioactive sources to the PAA President. Such documents include record sheets containing the following data about sources: radioactive isotope name, activity according to a source certificate, date when the activity was established, certificate number and source type, storage vessel type or device name and place

of the source use or storage. It is also needed emergency procedure if the source is unsealed. Data extracted from the accountancy cards are entered into the register of sealed radioactive sources, used to verify information about individual sources. The information contained in the said register is used to supervise organizational units conducting activity involving exposure to ionizing radiation. The supervision consists in comparing accountancy cards entries with the scope of the given authorization issued.

The application is verified by the Nuclear Supervision Inspector. After the substantive analysis, a permit is issued.

The second step of "the path" is preparation of Technical Procedure of the planned work. This document needs:

- Positive opinion of the competent State Sanitary Inspector of technological work instructions,
- Permission of the PAA President to conduct works radioactive source in the field,
- Written consent of the site administrator to perform works on its premises with source of radiation,
- Notification of the competent State Sanitary Inspector on the date and place of performing works with radioactive source,
- The program of protection against ionizing radiation in the transport of radioactive materials,
- Emergency plan.

Certain types of measurements (e.g. leak tests under pressure) may require additional permits such as: Office of Technical Inspection permission for pressure tests. Such permission requires the preparation of many additional documents and procedures, and the UDT certificate procedure may take up to 12 months!

In the next step radioisotope must be ordered from supplier (Maria Reactor) and transported to the laboratory for synthesis of radiotracer (if needed). The contractor performing work with the isotope must be equipped with a radiological laboratory. A special transport must be organized to deliver the isotope to the laboratory and test site.

Only a qualified employee may be allowed to work with the isotope. During fieldwork, a radiological protection inspector must attend them all the time. After completing the work, the inspector has to perform dosimetry measurements and prepare report for PAA inspector.

Additional information:

Radioactive waste: if a short-lived isotope is used for tests, it is waiting for its expiration. If it is a long-lived isotope, the waste should be collected and transported to the Radioactive Waste Management Plant,

Open sources: usually the activity of the initial isotope is strictly limited, so that after it's spreading in the installation its activity decreases below the norm of acceptable contamination,

Time: the measurements on the site in case leak detections take 1 - 2 weeks

but whole procedure with may take even several months.

Permissions: The Laboratory of Diagnostic Methods at INCT has PAA permission and UDT certificate, which is valid for 2 years (Figure 6). It authorizes to carry out research in the field—leak testing of technical facilities using isotope tracers. Technical devices and objects in industrial installations may be examined like petrochemical and chemical, e.g. pipelines, apparatus, columns, exchangers, boilers, etc.

3.3. Norms and Standards Used in Poland [18]

- PN-EN ISO/IEC 17025 General requirements for the competence of testing and calibration laboratories,
- ISO 2975/I-1976 Measurement of water flow in closed conduits-Tracer methods-Part I: General,
- ISO 2975/III-1976 Measurement of water flow in closed conduits-Tracer methods-Part III: Constant rate injection method using radioactive tracers,
- ISO 553/3-1982 Liquid flow measurement in open channels—Dilution methods for measurement of steady flow—Part 3: Constant rate injection method and integration method using radioactive tracers,
- PN-ISO 7205:1997 Isotopic control and measurement devices—Fixed devices,

URZĄD DOZORU TECHNICZNEGO

ŚWIADECTWO UZNANIA LABORATORIUM

nr **LBU-267/27-18**

Urząd Dozoru Technicznego
poświadcza, że

Instytut Chemii i Techniki Jądrowej
ul. Dorodna 16, 03-195 Warszawa
Laboratorium Technik Jądrowych
Pracownia Metod Diagnostycznych
ul. Dorodna 16, 03-195 Warszawa

spełniając wymagania normy PN-EN ISO/IEC 17025:2005
uzyskało uznanie Urzędu Dozoru Technicznego
do wykonywania badań laboratoryjnych

Szczegółowy zakres metod badawczych objętych uznaniem określony jest w załączniku do niniejszego świadectwa

Data uzyskania uznania: **16 maja 2018 r.**
Data ważności uznania: **15 maja 2020 r.**

Prezes
Urzędu Dozoru Technicznego
Andrzej Ziółkowski

Warszawa, dnia 16 maja 2018 r.

Załącznik do
ŚWIADECTWA UZNANIA LABORATORIUM
nr **LBU-267/27-18**
z dnia 16 maja 2018 r.
Zakres metod badawczych objętych uznaniem
Instytut Chemii i Techniki Jądrowej
ul. Dorodna 16, 03-195 Warszawa
Laboratorium Technik Jądrowych
Pracownia Metod Diagnostycznych
ul. Dorodna 16, 03-195 Warszawa

Lp.	Metoda badawcza/ pomiarowa	Badane obiekty/ grupa obiektów	Badane cechy	Norma i/lub udokumentowana procedura/instrukcja
1.	Kontrola szczelności obiektów technicznych metodą znaczników izotopowych	Urządzenia techniczne, obiekty w instalacjach przemysłu m. in. petrochemicznego i chemicznego, np: rurociągi, aparaty, kolumny, wymienniki, kotły, cold-boxy	Wykrywanie nieszczelności określanie wielkości nieszczelności i lokalizacja nieszczelności	Procedura Badawcza PB-PMD: Kontrola Szczelności Obiektów Technicznych Metodą Znaczników Izotopowych. Wydanie 3. Data wydania: styczeń 2018 r

Nadzór nad świadectwem uznania laboratorium

1. Zmiana zakresu metod badawczych następuje na wniosek laboratorium i wymaga przeprowadzenia oceny laboratorium przez UDT.
2. Przedłużenie ważności świadectwa uznania UDT następuje na wniosek laboratorium, który powinien być złożony nie później 3 miesiące przed upływem jego ważności i wymaga ponownej oceny laboratorium przez UDT.
3. W przypadku nieprzedłużenia ważności świadectwa uznania, laboratorium, jest usuwane z rejestru uznanych laboratoriów.
4. W przypadku nieprzestrzegania warunków określonych w niniejszym świadectwie lub wykonywania przez laboratorium badań w sposób niewłaściwy, mający negatywny wpływ na bezpieczną eksploatację urządzeń technicznych, Prezes UDT może zawiesić świadectwo uznania laboratorium. Informacja o zawieszeniu świadectwa uznania zamieszczana jest w rejestrze uznanych laboratoriów.
5. Prezes UDT, zawieszając świadectwo uznania laboratorium, wyznacza termin usunięcia uchybień stanowiących podstawę zawieszenia, po którego upływie, w razie ich nieusunięcia, cofa świadectwo uznania laboratorium.
6. UDT może przeprowadzać niezapowiedziane kontrole w siedzibie laboratorium lub w miejscu wykonywania badań laboratoryjnych. Podczas tych kontroli UDT może przeprowadzać lub zlecać przeprowadzenie badań mających na celu weryfikację badań wykonywanych przez uznane laboratorium.
7. Kontrole o których mowa w punkcie 6 nie są przeprowadzane w przypadku laboratoriów, których działalność objęta jest systemem jakości zgodnym z Polskimi Normami, zatwierdzonym i nadzorowanym przez Prezesa UDT.
8. UDT zastrzega sobie prawo uczestnictwa w badaniach i bezpośredniego nadzoru nad badaniami, których wyniki brane są pod uwagę przez UDT, przy wydawaniu decyzji w sprawie eksploatacji urządzeń.

Departament Techniki
Dyrektor
Jacek Kocięcki

Warszawa, 16 maja 2018 r.

Figure 6. UDT Certificate.

- PN-EN 60846:2004 Apparatus of radiation protection. Meters and/or monitors for the spatial and/or directional equivalent dose (or power) of beta, X-ray and gamma radiation,
- PN-EN 60846:2004 Apparatus of radiation protection. Measurement of individual Hp (10) and Hp (0.07) dose equivalent of X-rays, gamma, neutron and beta radiation. Direct reading of individual dose equivalent measures,
- PN-EN 60325:2007 Instrumentation for radiological protection. Meters and monitors of radioactive contamination, alpha, beta and alpha/beta (beta energy > 60 keV),
- PN-ISO 9978:1999 Radiological protection—Closed-cell radioactive sources—Leak testing methods.

4. Local Companies, Manufacturing NCS and Institutions

4.1. Institute of Nuclear Chemistry and Technology (INCT) [19]

(Instytut Chemii i Techniki Jądrowej) Dorodna 16, 03-195 Warsaw, Poland http://www.ichtj.waw.pl, phone: +48 22 504 10 00, e-mail: sekdyrn@ichtj.waw.pl. Services:

- Detection irradiated foods,
- Radiation Sterilization Plant,
- Nuclear Techniques Laboratory, Diagnostic Methods Group:
- underground liquid and gas pipelines (Φ200 - 600 mm) with cleanout chambers—with sensitivity of up to 0.5 dcm^3/h for liquids and 5 g/h for gases (output from the smallest detected at localized leak) and underground liquid and gas pipelines ($\Phi \geq 600$ mm) without cleanout chambers—with sensitivity of up to 1.0 dcm^3/h for liquids and 10 g/h for gases,
- underground and ground pipelines (of all diameters) for gas and liquids without cleanout chambers with sensitivity up to 1.0 dcm^3/h for liquids and 10 g/h for gas,
- gate valves in pipelines for all media,
- underground tanks and ground tank bottoms with sensitivity related to the tank volume,
- petrochemical and chemical industry installations with sensitivity of 30 cm^3/h. Tests are performed without removal of inner and outside lining, installation of scaffoldings and removal of catalysts,
- other installations and structures subject to individual arrangements,
- Laboratory of Nuclear Analytical Methods,
- Food and Environmental Laboratory,

Other activities are presented in [4] [5] [6] [7] and [20] [21].

4.2. National Centre or Nuclear Research (NCBJ) [22]

(Narodowe Centrum Badań Jądrowych) Str. Andrzeja Sołtana 7, 05-400 Otwock, Świerk, Poland https://www.ncbj.gov.pl/en, phone: +48 22 27 31 001, e-mail: ncbj@ncbj.gov.pl.

NCBJ offers a broad range of research/engineering services for both domestic and foreign customers. They have accumulated vast experience in producing ionizing radiation detectors and materials for their construction; the detectors are used by the most eminent equipment manufacturers and research labs in the world. They have been constructing unique electronic instruments to cooperate with ionizing radiation detectors, including individual circuits and entire systems for LHC in CERN, Geneva, which is the largest research facility built by the mankind. The Institute is also operator of the Maria Reactor. The part of the institute is POLATOM Radioisotope Centre which is a Polish manufacturer and distributor of the isotope used in medicine, science, industry and environmental protection. Research is a research and development. The Centre produces wide range of products for medicine and for research and development, technology and environment protection.

4.3. EMAG [13]

Institute of Innovative Technologies EMAG, and Centre of Technology Transfer EMAG Ltd. (CTT EMAG, http://www.cttemag.pl/, Leopolda 31, 40-189 Katowice).

For over 40 years, the Institute of Innovative Technology EMAG has specialized in the development and construct of systems and equipment for on-line monitoring and laboratory measurements of coal quality parameters, as well as in the implementation of these devices in mines and power plants. The systems based inter alia on the radiation detection techniques, such as: backscattering of gamma radiation (ALFA-06 and ALFA-06/T systems) and absorption of a dual energy gamma ray transmission (ALFA-06/2E ash meter, ALFA-06/3E system), have found wide application in Poland. At present, over 100 systems and devices for analysis are used in Polish hard and brown coal mines.

ALFA-06/T—ash meter and calculating calorific value, use backscattering.

ALFA-06/2E—on-line ash monitor, use absorption of a dual energy gamma ray transmission. Makes it possible to measure ash content in coal with a grain size of 0 - 200 mm and in carbon layers with a thickness of 50 - 300 mm. The ash content is determined by measuring the attenuation of two concentrated beams of radiation passing through the coal layer, which come from two different radiation sources placed between the conveyor belts. This ash meter can be used in a situation where different coal sizes lie on a belt in a layered system.

ALFA-06/3E—Absorption system for on-line monitoring of coal quality (ash content, moisture) and calculating calorific value of coal transported on conveyor belt. Use absorption of a dual energy gamma ray transmission utilized in loading places and controlling the enrichment process (**Figure 7**).

Modern versions of density meters have been developed at the EMAG Centre. Accurate measurement of density and values being density functions for a substance with an altered chemical composition was obtained thanks to applied measuring method using of absorbing and scattering radiation gamma. A cha-

racteristic feature of the meters is that the isotope gauge is an element a pipeline with an internal diameter equal to the internal diameter of pipeline. The EMAG Centre was developed several types of gauge intended for various applications. C and CA (caesium and americium) type isotope density meter are designed for measurement of high density substances.

C-type gauge provides continuous measurement of the density of substances transported by pipelines; measurement of other qualities of these substances calculated on the basis of the measured density (**Figure 8**).

Technical information:

- measuring method: gamma ray absorption,
- pressure of the measured substance: ≤1 MPa,
- outside diameter of the pipeline: 100 - 400 mm,
- range of density measurement: 0.1 - 2.5 g/cm^3,

Figure 7. ALFA 06/3E at the coal processing plant Radiation source: 137Cs (0.555 GBq) and 241Am (11.1 GBq) [13].

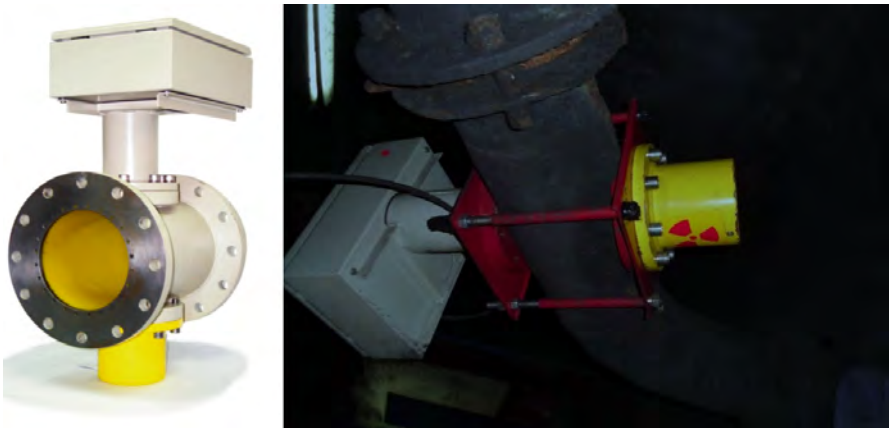

Figure 8. C-type isotope density meter [13].

- time of measurement: 3 - 100 s,
- radiation source: Cs-137 with activity 37 - 555 MBq (1 - 10 mCi).

B and BA (133Ba and 241Am) type density meter are provided for measuring of substances with slightly larger or smaller density than water.

CA-type density meter gauge was applied in "Jaworzno" mining where it is utilized for automatic control work of pumps which receive a concentrated sludge from a radial thickener and for control the process of preparing a backfilling mixture.

These devices ensure full safety of use—no restricted zone due to the use of isotope with very low activity. Application in automation systems process control:

- flotation,
- coal enrichment in a heavy liquid (especially C-type gauge),
- water and mud circuit,
- preparation and transport mixtures flooring.

Previously generation of devices produced by EMAG-MPKF radiometric ash meter: enable fast (100 s) measurement of ash content in samples with granulation 0 - 10 (20) mm. The measurement is based on low-energy forward-scattering gamma rays of Am-241. This type of fully automated devices is used in 18 mining plants to control the quality of raw coal and enrichment products (**Figure 9**).

Figure 9. MPKF radiometric ash meter [13].

4.4. Industrial Implementation Company "WILPO" Ltd. [23]

Mikołowska 29, 41 - 400 Mysłowice (Poland), http://www.wilpo.pl/.

The company was founded in 1988 and offers stationary devices as well a series of on-line devices for work directly on belt conveyors and devices co-operating with coal samplers. In the field of on-line measuring, the WILPO offers a number of solutions, adapted to various installation and measurement conditions.

WILPO C 212—radiometric under belt ash meter (**Figure 10**) is especially prepared for ash content measurement in a run of a mine of hard and brown coal. It can be employed in an open pit (*i.e.* directly on excavators), power stations and mines. The WILPO C212UG version is the first ash meter in Poland approved for operation in underground conditions (sign WUG: DE-111/99).

Technical specifications:

- Granulation of tested carbon: 0 - 300 mm,
- Required thickness of the carbon layer: min. 100 mm (homogeneous, without a layer of coal),
- Radiation source: Cs-137 with activity 3.7 GBq.

WILPO C 411A—radiometric ash meter is designed for continuous measurement of the ash content in coal directly on the conveyor belt, especially in carbonaceous mixtures with a layered structure and in the coal with the layer height on the conveyor belt from 50 to 250 mm and grains up to 80 mm (**Figure 11**). The measurement is possible on sloping, reversing and even passable belts. The small size and the non-contact measurement method predispose it to be used in technological nodes of mines, as well as in power plants, heating plants, coking plants, etc.

Technical specifications:

- Coal type: hard and brown,

Figure 10. WILPO C 212 ash meter [23].

- Granulation of tested carbon: 0 - 80 mm,
- Height of the carbon layer: 50 - 250 mm,
- Radiation source: Am-241 (3.7 GBq and 40 kBq), Cs-137 with activity 3.7 GBq.

WILPO C 431—measuring system designed for on-line measurements of ash content, moisture content and determination of the calorific value directly on the conveyor belt (Figure 12). The basic applications of the system are related to the measurement possibilities, among others: carbon mixtures with a layered structure, variable granulation coal, technological nodes, points with relatively small amounts of coal, etc.

Technical specifications:

- Granulation of tested carbon: 0 - 80 mm,
- Required thickness of the carbon layer: 50 - 250 mm,
- Radiation source: Am-241 and Cs-137 with activity < 4 GBq.

WILPO C 512 and HC version-radiometric ash meters. Are intended for continuous measurements of ash content in hard (especially C 512 HC) and brown coal, for virtually any layer height and coal granulation, directly on a belt conveyor

Figure 11. WILPO C 411A ash meter [23].

Figure 12. WILPO C 431 ash meter [23].

of any construction width. The innovative, scattering-absorbing measuring method used in the ash meter makes it possible to carry out measurements, which is a complete novelty, on conveyor belts with steel cords. This predisposes this type of ash meter for applications on long, open transport routes, especially in open-cast coal mines (Figure 13).

Technical specifications:

- Coal type: hard and brown,
- Granulation of carbon: 0-300 mm,
- Required thickness of the carbon layer: 100-500 (temporarily up to 750) mm,
- Radiation source: Am-241 with activity 3.7-37 GBq (3.7 - 18.5 GBq for HC version).

WILPO C 532hc—coal quality parameters measurement system. Continuous measurement of ash content in coal is conducted using the innovative radiometric scattering and absorption method developed by WILPO in 2009 (Figure 14).

Figure 13. WILPO C 512 ash meter [23].

Figure 14. WILPO C 532 [23].

The method is based on irradiating a layer of coal (from above) with low-energy gamma rays and on recording the intensity of gamma radiation reaching a set of detectors arranged under the conveyor belt. Instead of one detector, a system of two appropriately positioned detectors has been introduced: one to measure scattered radiation, the other to measure absorbed radiation. This enabled the gathering of data on ash content variability and surface density of the coal analysed using one radiation source. The applied configuration provided measurement advantages which were unattainable until now, while retaining the valuable features of radiometric ash meters used before. Continuous measurement of moisture content in coal is carried out with use of the technology that consists in absorption of microwaves.

Technical specifications:

- Coal type: hard,
- Granulation of carbon: 0 - 70 mm,
- Required thickness of the carbon layer: 50 - 250 mm (500 mm if only ash content),
- Radiation source: Am-241 with activity 3.7 - 18.5 GBq and energy 60 keV.

The new design of the measuring system, most importantly that of the ash meter which includes a single and low-energy (60 keV) Am-241 radiation source, is perfectly safe. The device has been approved for manufacturing by WILPO by the Polish National Atomic Energy Agency (PAA) in Warsaw (permit No. D-17222 of 24 June 2009).

WILPO also holds a permit issued by PAA for the turnover, installation and transportation of equipment comprising sources of radiation (permit No. D-15512 of 14 January 2005, annex No.1 of 26 May 2008).

WILPO C 732 measurement system (**Figure 15**). This rapid measurement system of coal quality parameters which can cooperate with the samplers is designed

Figure 15. WILPO C 732 [23].

for direct measurement of ash and moisture content and calculation of the calorific value of coal in redundant, averaged and crushed material, returned to the main conveyor belt after each sampling by the sampler.

Technical specifications:

- Coal type: hard,
- Granulation of carbon: issued by the sampler crusher,
- Volume of the measuring chamber: 5 L,
- Measuring method of ash content: dispersion of gamma radiation,
- Radiation source: Am-241 with activity 3.7 GBq.

WILPO CG 111—isotope density meter is designed for on-line determination of density of liquids or slurries transported in industrial pipelines, especially in ash slurries. Density meter is practically maintenance-free device, mounted directly on the pipelines transporting the slurries. The measuring system consists of controller unit, which can work autonomously or work together with an external PC unit as well as consist of the isotope head and detection unit.

Technical specifications:

- Measured material: slurries, liquids,
- Method of measurement: absorption of gamma radiation,
- Radiation source: Cs-137.

The on-line coal quality monitors and users are shown in Table 3 and Table 4.

Table 3. Installations-on-line coal quality monitors by WILPO [23].

USERS		ADDRESS	TYPE OF DEVICE
"BEŁCHATÓW"	Coal Mine	97 - 400 Bełchatów, skr. pocztowa 100	C 212 (5 pieces) C 512 (4 pieces)
"BOBREK"	Coal Mine	41 - 905 Bytom, ul. Konstytucji 76	C 431 (2 pieces), C 112A, C 212
"CENTRUM"	Coal Mine	41 - 902 Bytom, ul. Łużycka 7	C 132
"BOLESŁAW ŚMIAŁY"	Coal Mine	43 - 174 Łaziska G, ul. Pstrowskiego 12	C 411A, C 431, 532hc (3 pieces)
"BRZESZCZE"	Coal Mine	43 - 270 Brzeszcze, ul. Kościuszki 1	C 132, C 212 (3 pieces)
"BUDRYK"	Coal Mine	43 - 178 Onontowice, ul. Zamkowa 10	C 411A (2 pieces), C 132, C 212, C 532hc (3 pieces)
"CHWAŁOWICE"	Coal Mine	44 - 206 Rybnik 6, ul. 1 Maja 26	C 411A (3 pieces) C 532hc (2 pieces)
"HALEMBA-WIREK" Ruch Halemba	Coal Mine	41 - 706 Ruda Śląska, ul. Kłodnicka 54	C 411A
"JANINA"	Coal Mine	32 - 590 Libiąż, ul. Górnicza 23	C 532 hc
"JANKOWICE"	Coal Mine	44 - 253 Rybnik, ul. Jastrzębska 12	C 132 (3 pieces), C 411A, C 532 hc (2 pieces)
"KRUPIŃSKI"	Coal Mine	43 - 267 Suszec, ul. Piaskowa 35	C 532hc (3 pieces)

Continued

"KAZIMIERZ JULIUSZ"	Coal Mine	42 - 540 Sosnowiec, ul. Ogrodowa 1	C 431
"KNURÓW-SZCZYGŁOWICE" Ruch Knurów	Coal Mine	42 - 220 Knurów, ul. Dworcowa 1	C 411A, C 213
"KNURÓW-SZCZYGŁOWICE" Ruch Szczygłowice	Coal Mine	44 - 193 Knurów 3, ul. Górnicza 1	C 411A, C 431 (4 pieces)
"KONIN"	Coal Mine	62 - 540 Kleczew, ul. 600-lecia 9	C 212 (3 pieces), C 512
"SOŚNICA"	Coal Mine	44 - 103 Gliwice, ul. Błonie 6	C 213, C 411A, C 431 (2 pieces), C 532hc (2 pieces)
"MAKOSZOWY"	Coal Mine	41 - 800 Zabrze, ul. Makoszowska 24	C 132, C 431, C 212, C 532hc
"MARCEL"	Coal Mine	44 - 310 Radlin, ul. Korfantego 52	C 411A (2 pieces), C 132, C 732 (2 pieces)
"MARPO" (BB POL)	Sp.j	70 - 675 Szczecin, Grudzińskiego 12	C 532hc
"MYSŁOWICE-WESOŁA"	Coal Mine	41 - 408 Mysłowice, ul. Kopalniana 5	C 132 C 532hc
"PIAST" Ruch II	Coal Mine	43 - 225 Wola, ul. Kopalniana 10	C 132 (4 pieces)
"PIEKARY"	Coal Mine	41 - 949 Piekary Śląskie, ul. Brzechwy 13	C 132, C 431 (3 pieces)
"PNIÓWEK"	Coal Mine	43 - 251 Pawłowice Śl., ul. Krucza 18	C 532hc (2 pieces)
"RADLIN"	Coking plant	44 - 310 Radlin, ul. Hutnicza 1	C 132
"RYDUŁTOWY-ANNA" Ruch I-Rydułtowy	Coal Mine	44 - 280 Rydułtowy, ul. Leona 2	C 411A
"SILESIA"	Coal Mine	43 - 502 Czechowice Dz., ul. Górnicza 60	C 132
"MURCKI-STASZIC" Ruch Staszic	Coal Mine	40 - 167 Katowice, ul. Karolinki 1	C 112A (2 pieces)
"TURÓW"	Coal Mine	59 - 916 Bogatynia 3	C 612
"TURÓW"	Power station	ul. Młodych Energetyków 12 59 - 916 Bogatynia 3	C 212 (2 pieces), C 512 (4 pieces)
"WIECZOREK"	Coal Mine	40 - 432 Katowice, ul. Szopienicka 58	C 212
"WUJEK" Ruch Wujek	Coal Mine	40 - 598 Katowice, ul. W. Pola 65	C 132, C 532hc
"WUJEK" Ruch Śląsk	Coal Mine	41 - 707 Ruda Śląska, ul. Kalinowa 12	C 132, C 212, C 411A, C 431

Continued

"ZIEMOWIT"	Coal Mine	43 - 143 Lędziny, ul. Pokoju 4	C 132, C 431 (2 pieces), C 532hc
"SOBIESKI"	Coal Mine	43 - 600 Jaworzno, ul. Grunwaldzka 37	C 532hc
ZE PAK	S.A.	52 - 510 Konin, ul. Kazimierska 45	C 512
USERS		ADDRESS	TYPE OF DEVICE
"BEŁCHATÓW"	Coal Mine	97 - 400 Bełchatów, skr. pocztowa 100	C 212 (5 pieces) C 512 (4 pieces)
"BOBREK"	Coal Mine	41 - 905 Bytom, ul. Konstytucji 76	C 431 (2 pieces), C 112A, C 212
"CENTRUM"	Coal Mine	41 - 902 Bytom, ul. Łużycka 7	C 132
"BOLESŁAW ŚMIAŁY"	Coal Mine	43 - 174 Łaziska G, ul. Pstrowskiego 12	C 411A, C 431, 532hc (3 pieces)
"BRZESZCZE"	Coal Mine	43 - 270 Brzeszcze, ul. Kościuszki 1	C 132, C 212 (3 pieces)
"BUDRYK"	Coal Mine	43 - 178 Onontowice, ul. Zamkowa 10	C 411A (2 pieces), C 132, C 212, C 532hc (3 pieces)
"CHWAŁOWICE"	Coal Mine	44 - 206 Rybnik 6, ul. 1 Maja 26	C 411A (3 pieces) C 532hc (2 pieces)
"HALEMBA-WIREK" Ruch Halemba	Coal Mine	41 - 706 Ruda Śląska, ul. Kłodnicka 54	C 411A
"JANINA"	Coal Mine	32 - 590 Libiąż, ul. Górnicza 23	C 532hc
"JANKOWICE"	Coal Mine	44 - 253 Rybnik, ul. Jastrzębska 12	C 132 (3 pieces), C 411A, C 532hc (2 pieces)
"KRUPIŃSKI"	Coal Mine	43 - 267 Suszec, ul. Piaskowa 35	C 532hc (3 pieces)
"KAZIMIERZ JULIUSZ"	Coal Mine	42 - 540 Sosnowiec, ul. Ogrodowa 1	C 431
"KNURÓW-SZCZYGŁOWICE" Ruch Knurów	Coal Mine	42 - 220 Knurów, ul. Dworcowa 1	C 411A, C 213
"KNURÓW-SZCZYGŁOWICE" Ruch Szczygłowice	Coal Mine	44 - 193 Knurów 3, ul. Górnicza 1	C 411A, C 431 (4 pieces)
"KONIN"	Coal Mine	62 - 540 Kleczew, ul. 600-lecia 9	C 212 (3 pieces), C 512
"SOŚNICA"	Coal Mine	44 - 103 Gliwice, ul. Błonie 6	C 213, C 411A, C 431 (2 pieces), C 532hc (2 pieces)
"MAKOSZOWY"	Coal Mine	41 - 800 Zabrze, ul. Makoszowska 24	C 132, C 431, C 212, C 532hc

Continued

"MARCEL"	Coal Mine	44 - 310 Radlin, ul. Korfantego 52	C 411A (2 pieces), C 132, C 732 (2 pieces)
"MARPO" (BB POL)	Sp.j	70 - 675 Szczecin, Grudzińskiego 12	C 532 hc
"MYSŁOWICE-WESOŁA"	Coal Mine	41 - 408 Mysłowice, ul. Kopalniana 5	C 132 C 532 hc
"PIAST" Ruch II	Coal Mine	43 - 225 Wola, ul. Kopalniana 10	C 132 (4 pieces)
"PIEKARY"	Coal Mine	41 - 949 Piekary Śląskie, ul. Brzechwy 13	C 132, C 431 (3 pieces)
"PNIÓWEK"	Coal Mine	43 - 251 Pawłowice Śl., ul. Krucza 18	C 532hc (2 pieces)
"RADLIN"	Coking plant	44 - 310 Radlin, ul. Hutnicza 1	C 132
"RYDUŁTOWY-ANNA" Ruch I-Rydułtowy	Coal Mine	44 - 280 Rydułtowy, ul. Leona 2	C 411A
"SILESIA"	Coal Mine	43 - 502 Czechowice Dz., ul. Górnicza 60	C 132
"MURCKI- -STASZIC" Ruch Staszic	Coal Mine	40 - 167 Katowice, ul. Karolinki 1	C 112A (2 pieces)
"TURÓW"	Coal Mine	59 - 916 Bogatynia 3	C 612
"TURÓW"	Power station	ul. Młodych Energetyków 12 59 - 916 Bogatynia 3	C 212 (2 pieces), C 512 (4 pieces)
"WIECZOREK"	Coal Mine	40 - 432 Katowice, ul. Szopienicka 58	C 212
"WUJEK" Ruch Wujek	Coal Mine	40 - 598 Katowice, ul. W. Pola 65	C 132, C 532hc
"WUJEK" Ruch Śląsk	Coal Mine	41 - 707 Ruda Śląska, ul. Kalinowa 12	C 132, C 212, C 411A, C 431
"ZIEMOWIT"	Coal Mine	43 - 143 Lędziny, ul. Pokoju 4	C 132, C 431 (2 pieces), C 532hc
"SOBIESKI"	Coal Mine	43 - 600 Jaworzno, ul. Grunwaldzka 37	C 532hc
ZE PAK	S.A.	52 - 510 Konin, ul. Kazimierska 45	C 512

Table 4. Installations—Export by WILPO [23].

USERS		ADDRESS	TYPE OF DEVICE
"CORESTI"	Plant	Petrosani, ROMANIA	WILPO C 212
"CORESTI"	Plant	Petrosani, ROMANIA	WILPO C 431
KOSTOLAC	Power Station	Pożarevac, SERBIA	WILPO C 212

According to data from 2009, in national mining works about 100 on-line radiometric ash meters from various companies, based on transmission and backscattering methods of gamma radiation, including over 60 WILPO solutions. There are currently 10 continuous ash meters in the Polish brown coal mining industry, all production of "WILPO" Sp. z o.o. (WILPO C 212 sub-belt ash meters).

4.5. "SYSKON—Systemy Kontroli Procesów Przemysłowych" Henryk Zastawny [24]

Kościerzyńska 7, 51 - 416 Wrocław, http://www.syskon.eu.

Company operating since 1995. Designs, creates and implements systems for continuous measurement of coal quality on belt conveyors and testing the content of flammable particles in flue gas.

The radiation level on the surface of the source container is well below the level allowed by the PAA regulations, *i.e.* 2 mSv/h. Measurements are made automatically and no employee is required near the device.

SysKon 50—is a control device that allows on-line measure the density of fluids, pulp, mules, etc. transported in pipelines (**Figure 16**).

The measurement principle is based on the determination of the high energy gamma radiation absorption by the material under study. The gauge is installed directly on the ascending section of the pipeline, which guarantees that the pipe cross-section is filled with the tested material.

Technical specifications:

- pipeline width: unlimited,

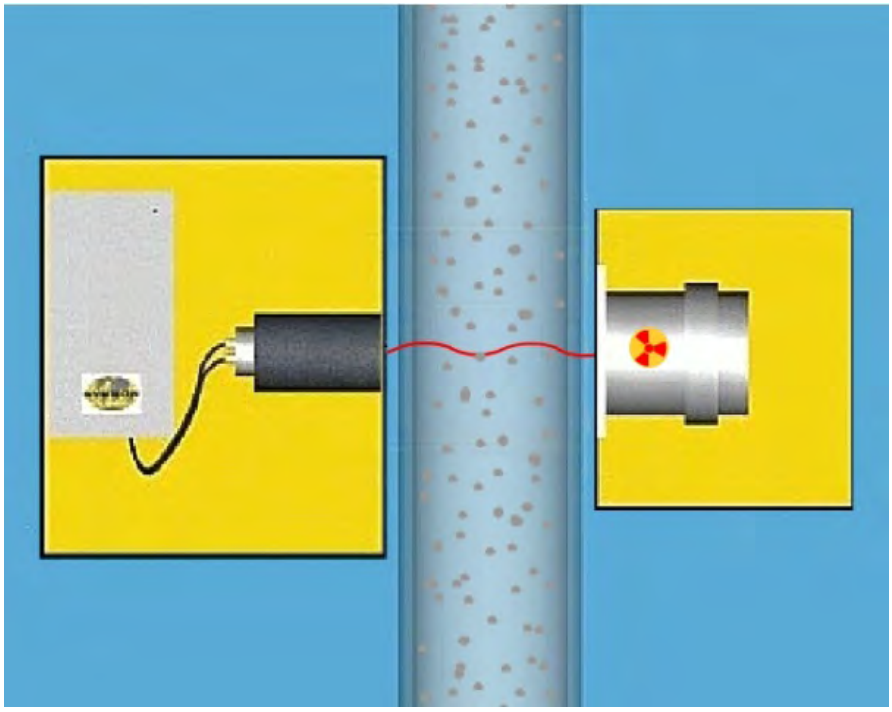

Figure 16. SysKon50 [24].

- liquid flow speed: unlimited,
- transport performance: unlimited,
- maximum granulation: unlimited,
- density range: unlimited,
- measurement time: about 1 min,
- radiation source: Cs-137.

SysKon 202—a control device that measures a content of flammable parts in fly ash. The probe is installed in the flue gas duct, using the negative pressure prevailing there, continuously samples the ash. The sample weighing about 10 g is directed to the measuring container, where it is scanned with gamma radiation, while its dielectric parameters are measured. From the relation between the absorption of gamma radiation and dielectric properties, the content of flammable parts is calculated. After measurement, the sample is expelled back into the flue gas duct and a new cycle begins.

Technical specifications:

- range of flammable parts: 0% - 16%,
- measurement time: 3 - 5 min,
- radiation sources: Cs-137.

SysKonSystem (**Figure 17**) and SysKonSystemSkan (**Figure 18**)—a devices controlling the quality of coal transported by a belt conveyor (ash content, moisture, calculation of calorific value). The device measures the coal in the middle of the conveyor belt—this is the main feature that differs from the SysKonSystem-Skan. The Skan version of device, in the case of a non-uniform stream of material on the conveyor, thanks to the lateral scanning of this stream, better averages the measured values—this is the main feature that differs from

Figure 17. SysKonSystem in Lubelski Węgiel "BOGDANKA" [24].

the SysKonSystem device.

Technical specifications:

- type of coal: hard,
- granulation: 0-300 mm,
- layer height: 50-300 mm,
- radiation sources: Am-241, Cs-137.

SysKon400—a device with nucleonic weighers that controls the quality of coal transported by a belt conveyor (ash and moisture content, mass of coal). The device is optionally mounted with an additionally technological scale. The device is adapted for use in underground mining plants in methane explosive areas (**Figure 19**).

Figure 18. SysKonSystem-Skan in "Brzeszcze" Coal Mine [24].

Figure 19. SysKon400 in Lubelski Węgiel "BOGDANKA" [24].

Technical specifications:

- type of coal: hard,
- granulation: 0 - 300 mm,
- layer height: 50 - 300 mm,
- radiation sources: Am-241, Cs-137.

SysKon500—the device that controls the quality of coal transported by a belt conveyor (Figure 20). The measurement of coal is carried out using the activation method. Individual elements included in coal, under the influence of neutron with energies of 1 - 10 MeV they generate a characteristic energy spectrum. Through his examination it can be determined the content of coal, ash, moisture and calorific value of the examined coal.

The device allows to determine the content of elements such as: carbon, hydrogen, oxygen, calcium, chlorine, silicon, sulfur, iron and aluminum. The design of the analyzer is built-up around a conveyor belt. Under the carrier tape, in the bottom tunnel of the device, an isotopic neutron source is placed (Am-Be). Over the tape, in the upper tunnel devices, detectors are placed gamma radiation. The design contains system of protective covers against neutron and gamma radiation.

Technical specifications:

- type of coal: hard,
- granulation: 0 - 300 mm,
- layer height: from 100 mm,
- neutron source: Am-Be.

Installed de4vices and users are shown in Table 5.

Figure 20. SysKon500 [24].

Table 5. Installed devices by SYSKON [24].

USERS	LOCATION	TYPE OF DEVICE
"Łęczyńska Energetyka"	Bogdanka	SysKonSystem: 1
Lubelski Węgiel "BOGDANKA"	Bogdanka	SysKonSystem: 3 SysKonSystemSkan: 7 SysKonSystemLab: 1 SysKon 400: 5
Przedsiębiorstwo Górnicze "SILESIA"	Czechowice-Dziedzice	SysKonSystem: 2 SysKonSystemSkan: 2
Zakład Górniczy "Sobieski"	Jaworzno	SysKonSystem: 1
Kopalnia Węgla Kamiennego "Mysłowice-Wesoła"	Mysłowice	SysKonSystem: 2
Kopalnia Węgla Kamiennego "Brzeszcze"	Brzeszcze	SysKonSystemSkan: 3
ENEA Wytwarzanie S.A.	Kozienice	SysKon 202: 8
PGE Górnictwo i Energetyka Konwencjonalna Spółka Akcyjna, Elektrownia Dolna Odra	Nowe Czarnowo	SysKon 202: 6
Zespół Elektrociepłowni Wrocławskich KOGENERACJA S.A.	Wrocław	SysKon 202: 6
PGE Energia Ciepła S.A.	Rybnik	SysKon 202: 4
Ostravská těžební, a.s.	Śląska Ostrawa (Czech Republic)	SysKonSystem: 2

4.6. TD-ELECTRONICS Tomasz Dudek [25]

Blatona 1/63, 01-494 Warszawa, http://www.td-electronics.pl.

Exists since 1998 and specializes in software development, construction and implementation of electronic, isotope, measuring equipment for industry, laboratories and environmental measurements.

Isotope measurements are carried out by means of the TDI series. These are meters containing a radioactive source and an ionizing radiation detector. It is possible to measure (where xx can be Am-241, Cs-137, Co-60, Kr-85, Cd-109, Pm-147, Sr-90):

TDI-xx-GT—Traversing thickness or basis weight (**Figure 21**) is intended for continuous, non-contact measurement of the thickness profile of film, paper, and sheets (depending on the radiation source used). It uses the absorption method of measurement. The radioactive source is placed under while the detector assembly over the measured of material tape. The traverse mechanism (scanner) enables synchronous movement of the source-head system, across the produced tape, between the parametrically determined turning points.

TDI-xx-GR—Stationary thicknesses or basis weight is designed for continuous, non-contact measurement of thickness or basic weight of film, paper, sheets, and plates (depending on the radiation source used) directly on the production line. It uses the absorption method of measurement.

The measuring head system (source-detector) of the thickness or basis weight

Figure 21. Traversing thickness gauge [25].

gauge is installed on a fixed structure and measures along the band of measured material moving between the source and the detector. On one production line, it is possible to install one or several measuring heads. Depending on the thickness and type of band material being measured and the required metrological parameters of the gauge, the appropriate radiation source, its activity, the protective container and the type of detector are selected.

TDI-xx-GE—Density or concentration in the pipe is intended for continuous, non-contact density measurement and derivative parameters of liquids, solutions and suspensions in pipelines. For the measurement, an attenuated gamma radiation by medium variable density or concentration is used.

Technical parameters:

- measurement range: 0.4 - 5.0 g/cm^3,
- outer diameter of steel pipes: 100 - 500 mm,
- outer diameter of PVC pipes: 40 - 90 mm,
- radiation sources: Am-241 (0.5 - 4 GBq) or Cs-137 (0.5 - 15 GBq).

TDI-xx-GZ—Density and concentrations in the tank.

Gauges are designed to measure the density or concentration of liquid media and suspensions in tanks. They use the absorption method of measurement. The measurement head of the densitometer or concentration meter is made up of a system of source and radiation detector assemblies installed on a suitable mechanical construction. Measured medium must completely fill the space between the source and detector assembly in the tank. Depending on the thickness of the tank wall, the distance between the source and the detector, the type and density of the medium being measured and the meter's required metrological parame-

ters, the appropriate radiation source, its activity, protective container and type of detector are selected.

TDI-xx-OG—Thickness, density and concentration (Figure 22).

These meters use a scattering method for their work. They are utilized primarily where it is not possible to use the absorption method, because (e.g. due to technological reasons) access to the measuring medium is possible only on one side.

TDI-xx-WA—Mass on conveyors (Figure 23).

Nucleonic weigher's belt conveyors are meters intended for measuring the mass of loose media transported by conveyor belts. They use the absorption method of measurement. The measuring head is a fixed frame located across the moving conveyor belt. On the frame above the conveyor there are installed sources (source) of radiation in a suitable container. A linear detector is installed under the conveyor belt. Depending on the width of the conveyor belt and the amount and type of material on the belt, the appropriate radiation source, its activity, protective container and the type of detector are selected.

TDI-xx-PL-Level (linear) and TDI-xx-PP-Level (point).

Isotopic level gauges used for linear measurement of media levels in a given

Figure 22. Backscattering densitometer for PE foam [25].

range, while point level measuring devices (isotopic level relays) are used to signal the exceeding of a given level by the measured medium at the meter head installation location. In these gauges, the measured medium completely covers (cuts off) part of the radiation beam. Linear and point level gauges do not differ in principle, but only in terms of collimation of the radiation beam and the detector's active length.

TDI-xx-SF—Analysis of the composition of the medium and coating thickness.

These meters use fluorescent method for their work. They are used to analyze the percentage of various elements in the measuring medium (e.g. iron, zinc, lead, nickel, copper), as well as to measure the thickness of thin coatings covering thicker substrates.

4.7. POLON-IZOT Sp. z o.o. [26]

Michała Spisaka 31, 02 - 495 Warszawa, http://www.polonizot.pl.

POLON-IZOT is a leading domestic producer of apparatus using X-rays and isotopic phenomena. It can boast over 50 years of technical achievements. Polon-Izot has many years of experience in the field of construction and production of measuring devices, control systems for technological processes, metrology (laboratory measurements, off-on line) and apparatus for the needs of environmental

Figure 23. Nucleonic weighers [25].

protection. They provided control and measurement devices to over 300 companies in Poland and abroad.

Industrial dust gauge

To measure the concentration of dust in the air, the device uses the attenuation of ionizing radiation through the measured medium. In principle, the system is therefore a density meter. To extract the dust content from the sample, it is necessary to know the current air density, which is calculated on the basis of the values collected by the temperature, pressure and humidity meters. The collimated radiation beam emanating from the container with the isotope source passes the measurement space and goes to the detection unit, where the intensity of radiation is converted into an electrical signal in the detector. The signal is amplified and processed into a digital form—in this post it goes through the serial interface to the controller, which calculates the concentration of dust based on the difference in air density and the density of the measurement space. The controller has outputs for switching on the visual and acoustic signaling in case of exceeding the permissible dust levels (**Figure 24**).

Area of applications: measurement of industrial concentrations of dust in channels and chimneys; measurement of dust concentrations in hazardous areas explosion; processes related to heat treatment in furnaces industrial; monitoring of filters; chemical, foundry and metallurgical industry. Technical specifications of MPP are shown in **Table 6**.

Level gauge

The entire class of level recording devices is based on the tendency of the material to reflect or absorb radiation. The main advantage of the level meter is the

Figure 24. Dust monitoring system in the mine. Detector and radiation emitter (ATEX performance) [26].

lack of moving parts and the ability to detect level without physical contact with the tested medium. The gauge registers changes in the radiation dose rate as a result of the presence of the medium in the measurement space between the isotope source and the detector. The gauges are used for contactless, continuous level measurements of liquid, powders, aggregates and solids.

Area of applications: measuring the level of concentrated acids, bases, salt solutions and suspensions; monitoring the crystallization process and polymerization; measuring the level of solids including aggregates on conveyor belts; powder level measurement; measurement of filling level of tanks, cylinders. Technical specifications of MP are shown in **Table 7**.

Industrial gauges of thickness and basis weight

The industrial (on-line) thickness and basis weight gauges operate in a non-contact manner and do not destroy of the tested sample (**Figure 25**). The partial absorption of radiation by the sample is used for the measurement—after passing through the tested medium falls on detector that converts radiation

Table 6. Technical specifications of MPP type gauges [26].

MPP-xx	Measurement range [g/cm^3]	Function
01	0 - 60	The system of continuous measurement of coal dust concentration, composed of three density gauges type GM-01C, intended for application in storage rooms, mines, etc.

Table 7. Technical specifications of MP type gauges [26].

MP-xx	Measurement range [mm]	Isotope used	Function
01 to 04	0 - 18,000	Cs-137, Co-60	measurement and signalling of exceeding the set level in tanks, clogging of through channels, etc. by a process medium

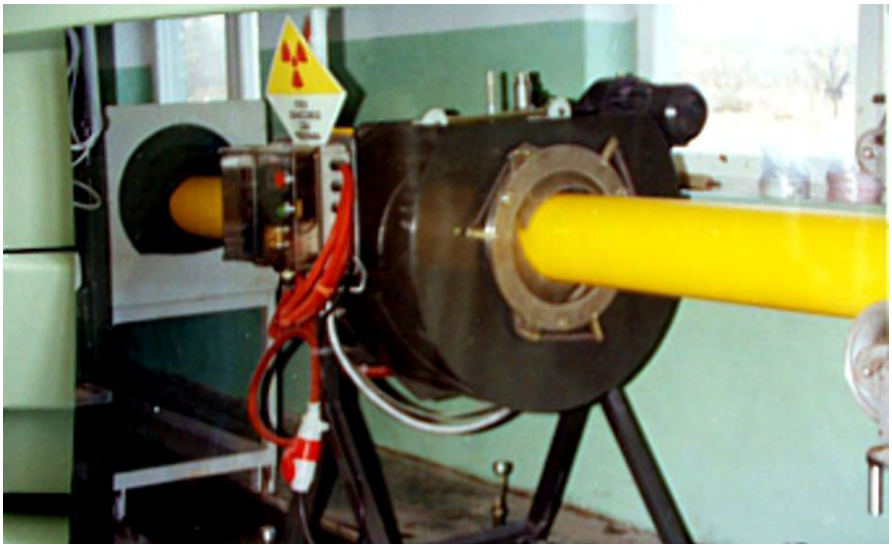

Figure 25. Thickness gauge of plastic pipes walls, MM-04 type [26].

changes into a signal electric. Changing the thickness or basis weight of the measured material changes the current of the detector that is sent to microprocessor controller. The information provided in real time influence for increasing productivity and saving of raw materials. The online meters allow remote control production process, often under extreme conditions, e.g. at high temperature, in high humidity or in large dust (Figure 26). Technical specifications of MM are shown in Table 8.

Industrial density and/or concentration gauges

Emitted ionizing radiation is absorbed when passing through the tested material. The level of absorption depends on the length optical path which overcomes the radiation in a given substance and from the parameters of the substance:

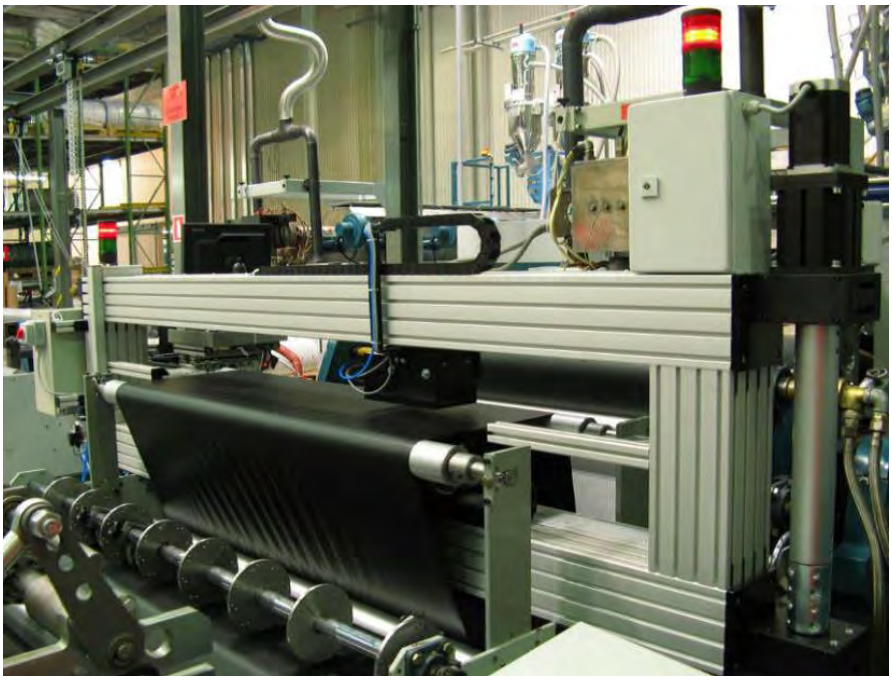

Figure 26. Radiometric profile meter—head with traverse, MM-06 type [26].

Table 8. Technical specifications of MM type gauges [26].

MM-xx	Measurement range [mm]	Measurement range [g/m^2]	Function
02	0.1 - 8.0	-	Rolled sheets thickness measurement
03	-	250 - 950	Basis weight of paper, cardboard, mineral wool, fiberboard, non-woven, chipboard, etc.
04	1.8 - 60.0 (for outer diameter ≤ 630 - 1200 mm depends on thickness)	-	Surrounding, continuous measurement of the plastic pipes wall thickness during the production process, adapted for operation with different types of extruding machines
06	0.01 - 4.0	-	Measuring the thickness of film, lining, rubber and similar materials using a traverse head across the band
08 and 09	0.5 - 10.0	-	Thickness across the glass pane with a traverse head
12	0.02 - 0.5	-	Thickness of rolled steel sheets

density, concentration, chemical composition, temperature (Figure 27 and Figure 28). The constant distance of the emitter from the detector allows the measurement of the measured parameters in radiation absorption function in the material under study. The device allows non-contact measurement of the density or concentration of liquids in pipelines or tanks with complete filling of the measuring space. They can be used in the building industry (lime and gypsum slurries), sugar and alcohol (diffusion juice) and related industries. The EX is designed for applications in potentially explosive areas. Technical specifications of GM are shown in Table 9.

Nucleonic weighers

Provide contactless mass measurement of bulk materials transported on belt conveyors in the chemical, mining, food, and other industries. Technical specifications of MPP are shown in Table 10.

Figure 27. Density gauge GM-01 type [26].

Figure 28. Concentration gauge, GM-06 type [26].

Table 9. Technical specifications of GM type gauges [26].

GM-xx	Measurement range [g/cm^3]	Outer diameter of pipe [mm]	Temperature measuring range [˚C]
01	0.6 - 3.5	100 - 298	−25 - 200
02	0.6 - 3.5	300 - 406	−25 - 200
04		40 - 75	0 - 100
06	0.7 - 1.6 (or the corresponding percentages of concentration)	40 - 75 (up to 250 for special design)	−25 - 200
01 or 02EX	0.6 - 3.5	100 - 298 (for 01) 300 - 406 (for 02)	−25 - 200

Table 10. Technical specifications of GM type gauges [26].

TW-xx	Measurement range [kg/m]	Typical yield [Mg/h]
03	3 - 20 (for 500 mm belt) 10 - 50 (for 650 mm belt)	20 - 300 100 - 650
04	20 - 80 (for 800 mm belt)	120 - 1000
05	30 - 120 (for 1200 mm belt)	180 - 1500

4.8. Ośrodek Techniki Jądrowej Polon Wrocław Sp z o. o. ("POLON" Nuclear Technology Centre in Wrocław, Ltd.) [27]

Na Grobli 6, 50-421 Wrocław, http://www.polon-otj.pl.

In terms of the subject of its operation and continuity of obligations, it is a successor to the "Polon" Department of Applied Nuclear Techniques in Wrocław (operating in the years 1965-1992). The department was established in the sixties with the mission to implement isotopic techniques in the industry. It successfully performed the tasks involving designing, implementation and maintenance of industrial equipment containing sources of ionizing radiation. Along with the emergence of fire detection systems, in which smoke detectors containing radioactive material are an important element, the scope of business operation was expanded to include the design, construction and maintenance of fire detection systems. In 1992, a group of the Company's employee transformed the state-owned company into a limited liability company through employee privatization. The Company continues its activity in its traditional areas, however, due to the natural evolution of the market demand, it has expanded the range of the services offered that now include: development, production of electronic devices made to single orders of the customers; design, installation, maintenance of building security systems, *i.e.* hazardous gas detection equipment, intrusion alarm systems, smoke ventilation systems, access control systems and CCTV systems.

Signalling Devices: ISP-03S, ISP-02G, ISP-01 (**Figure 29**).

They are used for the non-contact control of tanks filling with liquid or loose material. Isotopic signaling devices are used to perform tasks that are impossible or very difficult to accomplish with other measurement methods. With proper selection of the source of radiation, it is possible to control the presence of the

medium enclosed in the shell, e.g. 0.5 m of concrete or 200 mm of steel.

ISP-01, ISP-02G are the Geiger counters, moreover 02G type can be mounted in potentially explosive areas. The special feature of the ISP-03S signaling device is its scintillation detector NaI(Tl) instead of the G-M meter, which makes it about 15 times more sensitive than ISP-01 for 60Co sources and about 50 times more sensitive for 137Cs sources. For example, the ISP-01 radiometric probe is installed in the SOLBET production facility and controls the cement tank filling system.

Isotopic Level Transmitter IPSPZ-3 (**Figure 30**).

Isotopic level signal transmitter is designed for non-contact measurement of the level of various substances in tanks. In cooperation with the controller, it allows for precise level stabilization, and thus simplifies the technological process control. If the emergency level is exceeded, it activates the tank filling blockade. Geiger counters are used as the radiation detector. Their number and position of

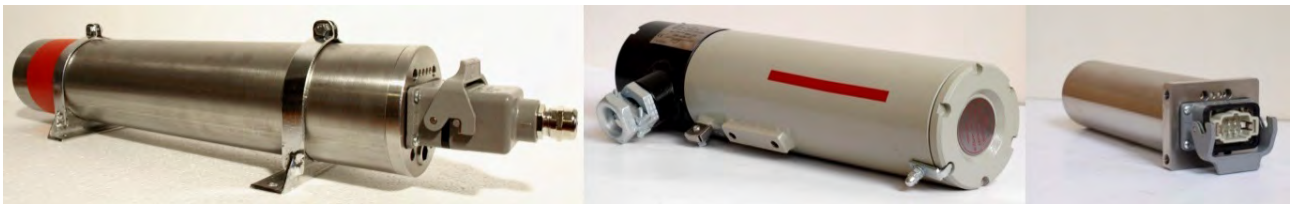

Figure 29. ISP-03S, ISP-02G ISP-01 [27].

Figure 30. IPSPZ-3 [27].

the probe depend on the measurement task.

4.9. Tranz-Tel sp. z o.o. [28]

Centralna 37, 43-210 Kobiór, http://www.tranztel.com.pl.

TranzTel designs, implements and maintains advanced—intrinsically safe—systems and devices for various industries. The Company offers one isotopic meter of its own production—density gauge. Installation on pipes with different diameters is possible. Wide application in industry: chemical, petrochemical, food and pharmaceutical industry, mining, environmental protection, etc. For example, together with other meters, it is used in the automatic regulation of heavy liquid in mining industry.

Technical specifications:

- Closed gamma radiation source: Cs-137,
- Source activity selected individually: 0.5 - 15 GBq,
- Outer diameter of pipes: 50 - 500 mm,
- Measuring range: 0.5 - 5.0 g/cm^3.

Companies involved in non-destructive testing, including gamma radiography.

- NDT System S. Twardowskiego 21, 01-643 Warszawa, http://www.ndt-system.com.pl,
- NDTEST Sp. z o.o. Sztabowa 10, 04-283 Warszawa, http://www.ndtest.com.pl,
- Badania Nieniszczące Górka Dawid Górka Podgórna 61, 62-064 Plewiska, http://www.ndtgorka.com.pl,
- "Energomontaż-Północ – Technika Spawalnicza i Laboratorium" Sp. z o.o., Chełmżyńska 194, 04-464 Warszawa, http://www.eptsil.pl,
- Laboratorium Badań Nieniszczących "H-GAZ" Sp. z o.o. Powstańców Listopadowych 2B, 35-606 Rzeszów, http://www.h-gaz.com.pl.

Acknowledgements

This paper has been prepared in the frame of International Atomic Energy Agency TC Regional Project RER1020 "Developing Radiotracer Techniques and Nuclear Control Systems for the Protection and Sustainable Management of Natural Resources and Ecosystems" and co-financed by Ministry of Science and Higher Education (Poland) project—416582/W81 /IAEA/2018.

Conflicts of Interest

The authors declare no conflicts of interest regarding the publication of this paper.

References

[1] Cameron, J.F. and Clayton, C.G. (1971) Radioisotope Instruments, Pergamon Press, Oxford. https://doi.org/10.1016/B978-0-08-015802-0.50007-0

[2] Chmielewski, A.G. (2008) Role of Nuclear and Radiation Technologies in Oil, Gas and Coal Mining, Distribution and Power Sector Applications. *Nukleonika*, **53**, 55-59.

[3] National Atomic Energy Agency (2017) Nnual Report Activities of the President of the National Atomic Energy Agency and Assessment of Nuclear Safety and Radiological Protection in Poland in 2016. Warsaw.

[4] Thereska, J., Rogowski, M. and Smolinski, T. (2018) IAEA-RER1020 Project to Enhance and Consolidate Regional Capabilty in Online Industrial Process Diagnosis, Optimization and Troubleshooting, Using Radiotracers and Sealed Source Techniques. Instytut Chemii I techniki Jądrowej. http://www.ichtj.waw.pl/ichtj/publ/REPOZYTORIUM/2018/konferencje/RER1020IAEA2018.pdf

[5] Smoliński, T., Rogowski, M., Pyszynska, M., Brykała, M. and Chmielewski, A.G. (2018) Nuclear Techniques for the Study Hydrometalurgical Procceses to Be Applided in Copper Industry; I. Application of 64Cu Radiotracer for Investigation of Copper Ore Leaching. *Nukleonika*, **63**, 123-129. https://doi.org/10.2478/nuka-2018-0015

[6] Rogowski, M., Smoliński, T., Pyszynska, M., Brykała, M. and Chmielewski, A.G. (2018) Nuclear Techniques for the Study Hydrometalurgical Procceses to Be Applided in Copper Industry; II. Application of Radiotracers for Copper Leaching from Flotation Tailings. *Nukleonika*, **63**, 131-137. https://doi.org/10.2478/nuka-2018-0016

[7] Miśkiewicz, A. and Zakrzewska-Kołtuniewicz, G. (2018) The Application of the Radiotracer Method for the Investigation of the Cake Layer Formation on the Membrane Surface in the Cross-Flow Flat-Sheet Membrane Module. *Desalination and Water Treatment*, **128**, 228-235. https://doi.org/10.5004/dwt.2018.22866

[8] POLATOM (2019). https://www.polatom.pl/en/produkty-uslugi

[9] National Centre for Nuclear Research (2019). https://www.ncbj.gov.pl/en/o-nas/maria-research-reactor

[10] Kraś, J., Nobis, C. and Myczkowski S. (2008) Leakage Control Methods for Metal Underground Tanks and Tanks Placed on Hardened Soil with the Use of Radioactive Tracers. *Nukleonika*, **53**, 137-140.

[11] Institute of Nuclear Chemistry and Technology (2019). http://www.ichtj.waw.pl/ichtj/market/m-eng/dep_01/leak.htm

[12] Palige, J., Roubinek, O., Wawryniuk, K., Modzelewski, Ł., Jakowiuk, A., Dobrowolski, A., Drewniak, ł. and Ciężkowska, M. (2014) Badania procesu fermentacji metanowej z wykorzystaniem metod radioznacznikowych i technik gamma skaningu [Research on the Methane Fermentation Process Using Radioactivity Methods and Gamma Scanning Techniques]. *Inżynieria i Aparatura Chemiczna*, **53**, 280-281

[13] http://www.cttemag.pl/

http://www.ibemag.pl/pl/

[14] Polish Atomic Law. http://prawo.sejm.gov.pl/isap.nsf/DocDetails.xsp?id=wdu20010030018

[15] OECD (2015) Nuclear Legislation in OECD and NEA Countries, Regulatory and Institutional Framework for Nuclear Activities. https://www.oecd-nea.org/law/legislation/

[16] PAA. http://www.paa.gov.pl/strona-40-prawo_krajowe.html

[17] PAA.

http://www.paa.gov.pl/strona-105-zezwolenia_na_dzialalnosc_ze_zrodlami.html

[18] Polish Norms and Radiological Standards. https://pzn.pkn.pl/pzn-share/page/

[19] http://www.ichtj.waw.pl/drupal/

[20] Smolinski, T., Wawszczak, D., Deptula, A., Lada, W., Olczak, T., Rogowski, M., Pyszynska, M. and Chmielewski, A.G. (2017) Solvent Extraction of Cu, Mo, V, and U from Leach Solutions of Copper Ore and Flotation Tailings. *Journal of Radioanalytical and Nuclear Chemistry*, **314**, 69-75. https://doi.org/10.1007/s10967-017-5383-y

[21] Smoliński, T., Rogowski, M., Pyszynska, M. and Chmielewski, A.G. (2017) Metal Recovery Optimized by Radioisotope Methods. Odzysk Metali Optymalizowany Metodami Radioizotopowymi. *GOSPODARKA ODPADAMI*, **2/2017**, 24-27.

[22] https://www.ncbj.gov.pl/en

[23] http://www.wilpo.pl/

[24] http://www.syskon.eu/firma/

[25] http://td-electronics.pl/

[26] http://www.polonizot.pl/

[27] http://www.polon-otj.pl/

[28] http://www.tranztel.com.pl/

World Journal of Nuclear Science and Technology, 2019, 9, 67-73
http://www.scirp.org/journal/wjnst
ISSN Online: 2161-6809
ISSN Print: 2161-6795

Natural Radioactivity Measurement and Dose Assessment in Soil Samples from Some Selected Areas of Mali

Issiaka Traoré[1*], Abdramane Ba[1], Abdel Mjid Nourreddine[2]

[1]Département de Physique, Université des Sciences, des Techniques et Technologies de Bamako, Bamako, Mali
[2]Institut Pluridisciplinaire Hubert Curien (IPHC), Université de Strasbourg, Strasbourg, France
Email: *amenotra@lossa-mali-edu.org

How to cite this paper: Traoré, I., Ba, A. and Nourreddine, A.M. (2019) Natural Radioactivity Measurement and Dose Assessment in Soil Samples from Some Selected Areas of Mali. *World Journal of Nuclear Science and Technology*, **9**, 67-73.
https://doi.org/10.4236/wjnst.2019.92004

Received: March 21, 2019
Accepted: April 20, 2019
Published: April 23, 2019

Abstract

This is the first time that a study applies the gamma ray spectroscopy using a high purity germanium to evaluate the terrestrial gamma radiation level by detector in selected regions of Mali. The results reveal that the activity concentrations of naturally occurring ^{226}Ra, ^{232}Th and ^{40}K radionuclides ranges between respectively 17.26 ± 1.81 and 105.43 ± 10.36; 20.41 ± 2.52 and 180.85 ± 19.69; 41.33 ± 8.26 and 627.63 ± 85.62 Bq·kg^{-1}. The measures of radium equivalent activity (Ra_{eq}), absorbed dose rates (ADR), annual effective dose rate (AEDR), external hazard index (H_{ex}), internal hazard index (H_{in}) and excess lifetime cancer risk (ELCR) were evaluated. Some of the obtained values exceed the recommended safe levels. Further studies are necessary to constitute a baseline reference data about the terrestrial radiation in Mali.

Keywords

Soil Radioactivity, Radiological Hazard, Population Exposure, Gamma Spectrometry, Mali

1. Introduction

Natural radionuclides of terrestrial origin, known as primordial radionuclides, are widespread in the earth's environment and exist in varying proportion in the entire natural environment, including the human body.

Only those radionuclides with half-lives comparable to the age of the earth such as ^{226}Ra, ^{232}Th, ^{40}K, and their decay products, exist in sufficient quantity to contribute significantly to population exposure [1].

To assess the health risk, it is important to estimate the radiation dose distri-

bution due to natural radionuclides that depend mainly on the local geological and geographical conditions.

In Mali, our previous study investigated on the natural radiological exposure for human being, focusing on the radon that is formed along with the ^{228}U decay disintegration chain [2].

In the same vein, our research team has collected some soil samples from four regions in Mali for gamma ray analysis.

The purpose of this study is to determine the concentration of soil radionuclides' activity and to evaluate the health risks via the gamma radiation parameters such as Radium equivalent activity (Ra_{eq}), external hazard index (H_{ex}), internal hazard index (H_{in}), absorbed dose rate (ADR), annual effective dose rate (AEDR) and excess lifetime cancer risk (ELCR). According to UNSCEAR (2000), only two African countries (Algeria and Egypt) were contributed to the 2000 report on the formulation of the world average radionuclide concentrations and the associated external exposure rates. This is the first time that such study is conducted to analyze the concentration of soils radionuclides in Mali. The results will help enrich the various studies reported in Africa since 2000 [3]-[8].

2. Materials and Methods

2.1. Geographical Description of the Study Area

Mali is a landlocked country in West Africa. It is the eighth largest country in Africa with an area of just over 1,240,000 square kilometres. This country is divided into eight regions and one capital district (see **Figure 1**). Each of the regions bears the name of its principal city. The regions are divided into 49 cercles. The cercles and the capital district are divided into 703 communes. The capital Bamako is administered separately and is in its own district.

Soil samples were collected from Bamako district (12˚38'21"N 8˚0'10"W), third region Sikasso (11˚19'N 5˚40'W), fourth region Ségou (13˚27'N 6˚16'W)

Figure 1. The sample collection areas on the Malian map.

and Faléa (12˚15'53"N 11˚16'30"W) a village located in the rural commune of the cercle of Kéniéba in the first region Kayes (**Figure 1**).

2.2. Sample Collection and Preparation

Soil samples were randomly collected by digging a half meter deep hole in different locations of the investigated areas: two samples from Bamako, Sikasso, and Segou, three samples from Falea (Kayes region). The distance between each site of collected sample was about 5 - 15 km. All the samples were dried, crushed, homogenised and passed through a 2 mm sieve and then oven-dried at 40˚C for 24 h. Before measuring the radioactivity, the conditioned samples were stored in cylindrical SG50 containers for one month to allow the short-lived daughters of ^{238}U and ^{232}Th decay series to reach a secular equilibrium.

2.3. Gamma Ray Detection System

The gamma-ray activities were measured by using a shielded planar Hyper-Pure Germanium (HPGe) detector and associated electronics. The detector, a BE 3830 model coupled to an 8192 channel analyser piloted by Genie 2000 software were supplied by Canberra [9]. The experimental detector resolution is 1.97 keV at 1332 keV and 0.65 keV at 122 keV. Each sample was counted for 200,000 s.

2.4. Calculation Formulae for Radiation Exposure Parameters

2.4.1. Radium Equivalent Activity (Ra_{eq})

Radium equivalent Ra_{eq} represents the sum of the specific activities of ^{226}Ra, ^{232}Th, and ^{40}K based on the assumption that 370 Bq·kg^{-1} of ^{226}Ra, 259 Bq·kg^{-1} of ^{232}Th, and 4810 Bq·kg^{-1} of ^{40}K would produce the same dose rate of gamma radiation.

Radium equivalent activity is calculated through the following relation [10]:

$$Ra_{eq} = A_{\mathrm{Ra}} + 1.43 \times A_{\mathrm{Th}} + 0.077 \times A_{\mathrm{K}} \tag{1}$$

where A_{Ra}, A_{Th} and A_{K} are the activity concentrations respectively of ^{226}Ra, ^{232}Th and ^{40}K expressed in in Bq·kg^{-1}.

2.4.2. Absorbed Dose Rate (ADR)

The absorbed gamma dose rate ADR (nGy·h^{-1}) due to the activity of ^{226}Ra, ^{232}Th and ^{40}K in the air at 1 m above the ground is defined by the following expression:

$$\mathrm{ADR}\left(\mathrm{nGy}\cdot\mathrm{h}^{-1}\right) = 0.462A_{\mathrm{Ra}} + 0.604A_{\mathrm{Th}} + 0.042A_{\mathrm{K}} \tag{2}$$

where A_{Ra}, A_{Th} and A_{K} are defined in the above equation.

2.4.3. Annual Effective Dose Rate (AEDR)

The annual effective dose rate received by the population is calculated using the following equation according to UNSCEAR [1]:

$$\mathrm{AEDR}\left(\mathrm{mSv}\cdot\mathrm{y}^{-1}\right) = \mathrm{ADR} \times 8760 \times 0.2 \times 0.7 \times 10^{-6} \tag{3}$$

where ADR is the estimated absorbed dose rate (nGy·h^{-1}) given in Equation (2), 0.7 Sv·Gy^{-1} the conversion coefficient from absorbed dose in the air to effective

dose received by adults, 0.2 is the fraction of time spent indoors and 8760 is the time in hours in 1 year.

2.4.4. External Hazard Index (H_{ex}) and Internal Hazard Index (H_{in})

The external hazard index is a criterion used to assess soil radiation exposure rate on a human body. The maximum value of H_{ex} equal to unity corresponds to the upper limit of Ra_{eq} (370 Bq·kg^{-1}) and the maximum of the annual radiation dose (1.5 mSv·y^{-1}). The external hazard index H_{ex} is calculated by the following formula:

$$H_{ex} = \frac{A_{Ra}}{370} + \frac{A_{Th}}{259} + \frac{A_{K}}{4810} \quad (4)$$

The internal exposure to radon and its daughter progenies is quantified by the internal hazard index H_{in}, which is given by the equation:

$$H_{in} = \frac{A_{Ra}}{185} + \frac{A_{Th}}{259} + \frac{A_{K}}{4810} \quad (5)$$

2.4.5. Excess Lifetime Cancer Risk (ELCR)

The excess lifetime cancer risk (ELCR) gives the probability of developing cancer during the life of a human being at a given exposure level. The ELCR is calculated using the following equation [7] [11] [12] [13]:

$$\mathrm{ELCR} = \mathrm{AEDR} \times \mathrm{RF} \times \mathrm{DL} \quad (6)$$

where AEDR is the annual effective dose rate, DL the average duration of life for human being (70 years) and RF is the mortal cancer risk factor (Sv^{-1}). For stochastic effects, ICRP 60 uses RF values of 0.05 for the public [14].

3. Results and Discussion

Table 1 summarizes the measured concentrations of the specific activity of ^{226}Ra,

Table 1. Measured activity levels (Bq·kg^{-1}) of specific radionuclides for soil samples at various locations of Mali.

Sample No.	Sector	^{226}Ra	^{232}Th	^{40}K
S1	Bamako 1	22.67 ± 2.95	37.78 ± 5.02	622.28 ± 85.36
S2	Bamako 2	22.67 ± 2.48	35.56 ± 4.10	627.63 ± 85.62
S3	Ségou 1	17.26 ± 1.81	20.41 ± 2.52	52.06 ± 15.49
S4	Ségou 2	22.66 ± 2.35	26.02 ± 2.97	41.33 ± 8.26
S5	Sikasso 1	28.20 ± 2.63	36.81 ± 3.92	245.34 ± 27.37
S6	Sikasso 2	25.95 ± 2.82	34.03 ± 4.10	210.93 ± 30.62
S7	Kayes 1	105.43 ± 10.36	180.85 ± 19.69	76.71 ± 14.96
S8	Kayes 2	77.01 ± 7.91	68.41 ± 8.20	185.16 ± 28.88
S9	Kayes 3	85.93 ± 8.35	85.65 ± 9.41	143.46 ± 21.38
Range		17.26 - 105.43	20.41 - 180.85	41.33 - 627.63
Average		45.31 ± 4.63	58.39 ± 6.66	244.99 ± 35.33

^{232}Th, ^{40}K, which ranges respectively, from 17.26 ± 1.81 to 105.43 ± 10.36 Bq·kg^{-1}, 20.41 ± 2.52 to 180.85 ± 19.69 Bq·kg^{-1}, 41.33 ± 8.26 to 627.63 ± 85.62 Bq·kg^{-1} in the selected soil samples. The mean activity of ^{40}K observed (244.99 ± 35.33 Bq·kg^{-1}) in the present study is below the recommended limit (400 Bq·kg^{-1}) [1]. Meanwhile, the mean activity concentration levels of ^{226}Ra (45.31 ± 4.63 Bq·kg^{-1}) and ^{232}Th (58.39 ± 6.66 Bq·kg^{-1}) are higher than the worldwide mean reported values (35 and 30 respectively).

The radium equivalent activity, the gamma absorbed dose rate, the annual effective dose rate, the external, and internal hazard index, the excess lifetime cancer risk due to ^{226}Ra, ^{232}Th and ^{40}K in the soil samples was calculated from respectively Equations (1)-(6) and are presented in column 3, 4, 5, 6, 7, 8 of **Table 2**.

As can be seen from **Table 2** the calculated radium equivalent (Ra_{eq}) is between 50.45 ± 6.61 and 369.95 ± 39.67 with the average of 266 Bq/kg. None of those values exceeded the suggested maximal admissible value of 370 Bq/kg that is acceptable as safe limit.

The absorbed dose rate (ADR) obtained by equation (2) indicated that the lowest dose rate was 22.49 ± 3.01 nGy/h for the soil sample S4, while the highest dose rate was 161.16 ± 17.31 nGy/h for the soil represented by sample S7. Except the dose rates of samples S7, S8, S9, all the calculated dose rates were lesser than the global average value 57 nGy/h according to UNSCEAR,2000 report.

The annual effective dose rates (AEDR) in the air varied from 0.028 ± 0.004 to 0.198 ± 0.021 mSv/year with an average value of 0.082 ± 0.001 mSv/year which is higher than the world's mean (0.07 mSv/year).

For the external hazard index results showed that no soil sample exceed unity. It is noteworthy that only the internal hazard index value of soil represented by sample S7 is higher than the permissible value (unity).

Table 2. Radium equivalent activity (Ra_{eq}), absorbed dose rate (ADR), annual effective dose rate (AEDR), external hazard index (H_{ex}), internal hazard index (H_{in}) and excess lifetime cancer risk (ELCR) of selected soil samples in Mali.

Sample No.	Sector	Ra_{eq} (Bq·Kg^{-1})	ADR (nGy·h^{-1})	AEDR (mSv·y^{-1})	H_{ex}	H_{in}	ELCR (×10^{-3})
S1	Bamako 1	124.61 ± 16.70	59.43 ± 7.98	0.073 ± 0.009	0.34 ± 0.05	0.40 ± 0.05	0.26 ± 0.03
S2	Bamako 2	121.85 ± 14.94	58.31 ± 7.22	0.072 ± 0.009	0.33 ± 0.04	0.40 ± 0.05	0.25 ± 0.03
S3	Ségou 1	50.45 ± 6.61	22.49 ± 3.01	0.028 ± 0.004	0.14 ± 0.02	0.18 ± 0.02	0.10 ± 0.01
S4	Ségou 2	63.05 ± 7.23	27.92 ± 3.23	0.034 ± 0.004	0.17 ± 0.02	0.23 ± 0.03	0.11 ± 0.01
S5	Sikasso 1	99.73 ± 10.34	45.57 ± 4.73	0.056 ± 0.006	0.27 ± 0.03	0.35 ± 0.04	0.20 ± 0.02
S6	Sikasso 2	90.85 ± 11.04	41.40 ± 5.06	0.051 ± 0.006	0.25 ± 0.03	0.32 ± 0.04	0.18 ± 0.02
S7	Kayes 1	369.95 ± 39.67	161.16 ± 17.31	0.198 ± 0.021	0.99 ± 0.11	1.28 ± 0.14	0.69 ± 0.07
S8	Kayes 2	189.09 ± 21.86	84.67 ± 9.82	0.104 ± 0.012	0.51 ± 0.06	0.72 ± 0.08	0.36 ± 0.04
S9	Kayes 3	219.46 ± 23.45	97.46 ± 10.44	0.120 ± 0.013	0.60 ± 0.06	0.83 ± 0.09	0.42 ± 0.04
Range		50.45 - 369.95	22.49 - 161.16	0.028 - 0.198	0.14 - 0.99	0.18 - 1.28	0.10 - 0.69
Average		147.676 ± 16.87	66.49 ± 7.64	0.082 ± 0.001	0.40 ± 0.05	0.52 ± 0.06	0.29 ± 0.032
Safe level		370	57	0.07	1	1	0.29

Except samples S7, S8, and S9, it was found that the life cancer risk value is lesser than the world average of 0.29×10^{-3}. In the first region Kayes there is a possibility of developing cancer cases among people.

A more detailed analysis of the overall results from calculated radiological parameters shows that soil samples collected in the fourth region Ségou presented the lowest value and those in Kayes region the highest value. More investigations were undertaken to understand the exceeded value obtained in the cercle of Falea located in western Mali approximately 350 km west of the capital, Bamako. The information collected showed that the cercle of Falea is a uranium, silver and copper deposit. The current resource estimate is approximately 45 million pounds of U_3O_8 [~17,300 t U] at an average grade of ~ 0.07% U_3O_8 [~0.06% U]. The deposit also contains ~37 million Oz Ag and ~70,000 t Cu. The dominant uranium mineral is uraninite; copper is present mainly as chalcopyrite and silver mainly as argentite, and in its native form. Only 5% of the property has been explored to date, and all zones remain open [15] [16].

In sum, the nature of the Falea deposit (an unconformity-associated uranium deposit) may explain the high values of the radium and thorium concentrations, impacting those of the radiological parameters.

4. Conclusions

In the present work, we used gamma spectrometry to determine natural radioactivity in 9 soil samples in Mali. The specific activities of the ^{226}Ra, ^{232}Th and ^{40}K radionuclides measured in these samples vary respectively from 17.26 ± 1.81 to 105.43 ± 10.36 $Bq{\cdot}kg^{-1}$, 20.41 ± 2.52 to 180.85 ± 19.69 $Bq{\cdot}kg^{-1}$, 41.33 ± 8.26 to 627.63 ± 85.62 $Bq{\cdot}kg^{-1}$.

The level of the natural radiation in the studied areas does not exceed the norm, except in Falea location where samples S7, S8 and S9 were collected.

Although the study did not cover the entire country of Mali, however, the findings reported in this workpaper provide relevant information and data which would document and enrich the world database on natural radioactivity emitted from soil and their effects on human bodies.

Acknowledgements

The authors acknowledge ISP for granting financial assistance. Special thanks to Nouhoum Keita for help in sample collection at Falea.

Conflicts of Interest

The authors declare no conflicts of interest regarding the publication of this paper.

References

[1] UNSCEAR (2000) Sources and Effects of Ionizing Radiation. United Nations Scientific Committee on the Effects of Atomic Radiation, United Nations Publication, New York.

[2] Traore, I., Nachab, A., Bâ, A., Nourreddine, A. and Togo, V. (2013) Assessment of Activity and Effective Dose Rate of ^{222}Rn in Several Dwellings in Bamako, Mali. *Radioprotection*, **2**, 277-284.

[3] Yeboah, J., Boadu, M. and Darko, E.O. (2001) Natural Radioactivity in Soils and Rocks within the Greater Accra Region of Ghana. *Journal of Radioanalytical and Nuclear Chemistry*, **249**, 629-632. https://doi.org/10.1023/A:1013262702436

[4] Murty, V.R.K. and Karunakara, N. (2008) Natural Radioactivity in the Soil Samples of Botswana. *Radiation Measurements*, **43**, 1541-1545. https://doi.org/10.1016/j.radmeas.2008.10.004

[5] Agbalagba, E.O. and Onoja, R.A. (2011) Evaluation of Natural Radioactivity in Soil, Sediment and Water Samples of Niger Delta (Biseni) Flood Plain Lakes, Nigeria. *Journal of Environmental Radioactivity*, **102**, 667-671. https://doi.org/10.1016/j.jenvrad.2011.03.002

[6] Olufunmbi, A., Akinjide, O., Moromoke, O. and Oluwafunmito, O. (2016) The Concentration of Natural Radionuclides in Soil Samples from the Practical Year Agricultural Farmland, University of Ibadan. *Journal of Applied Physics*, **8**, 60-68.

[7] Kassi, B., Boukhair, A., Azkour, K., Fahad, M., Benjelloun, M. and Nourreddine, A.-M. (2018) Assessment of Exposure Due to Technologically Enhanced Natural Radioactivity in Various Samples of Moroccan Building Materials. *World Journal of Nuclear Science and Technology*, **8**, 176-189. https://doi.org/10.4236/wjnst.2018.84015

[8] Engola, L.N., *et al.* (2018) Air Absorbed Dose Rate Measurements and External Dose Assessment by Car-Borne Survey in the Gold Mining Areas of Betare-Oya, Eastern-Cameroon. *Japanese Journal of Health Physics*, **53**, 5-11.

[9] Canberra, Genie (2000) Version 3.2.1. Canberra Industries, Inc.

[10] Beretka, J. and Mathew, P.J. (1985) Natural Radioactivity of Australian Building Materials, Industrial Wastes and By-Products. *Health Physics*, **48**, 87-95. https://doi.org/10.1097/00004032-198501000-00007

[11] Assie, A., Oudah, A.-J.A., Jassim, A.S. and Al-Mashhadani A.H. (2016) Determination of Natural Radioactivity by Gamma Spectroscopy in Balad Soil, Iraq. Pelagia Research Library. *Advances in Applied Science Research*, **7**, 35-41.

[12] Cengiz, G.B. and Çağlar, A. (2017) Evaluation of Natural Radioactivity Levels and Radiological Hazards in Soil Samples of Sarıkamış Province, Kars, Turkey. *Radiation Science and Technology*, **3**, 68-73.

[13] Taskin, H., Karavus, M., Ayb, P., Topuzoglu, A., Hidiroglu, S. and Karahan, G. (2009) Radionuclide Concentrations in Soil and Excess Lifetime Cancer Risk Due to Gamma Radioactivity in Kirklareli, Turkey. *Journal of Environmental Radioactivity*, **100**, 49-53. https://doi.org/10.1016/j.jenvrad.2008.10.012

[14] International Commission on Radiological Protection (1990) Recommendations of the International Commission on Radiological Protection. *Annals of the ICRP*, **21**, 1-3.

[15] Ring, R. and Freeman, P. (2014) Development of the Falea Polymetallic Uranium Project, Mali. IAEA-CN-261.

[16] Jerome, M.R., Issoumaila, M.S. and Robert, M.B. (2018) Falea: An Unconformity-Type Polymetallic Deposit, Mali, West Africa. *International Symposium on Uranium Raw Material for the Nuclear Fuel Cycle*: *Exploration*, *Mining*, *Production*, *Supply and Demand*, *Economics and Environmental Issues*, IAEA-CN-261.

World Journal of Nuclear Science and Technology, 2019, 9, 74-83
http://www.scirp.org/journal/wjnst
ISSN Online: 2161-6809
ISSN Print: 2161-6795

Analysis of Neutronics and Thermal-Hydraulic Behavior in a Fuel Pin of Pressurized Water Reactor (PWR)

Md. Ghulam Zakir*, M. A. Rashid Sarkar, Altab Hossain

Nuclear Science and Engineering (NSE) Department, Military Institute of Science and Technology (MIST), Dhaka, Bangladesh
Email: *paban81@gmail.com

How to cite this paper: Zakir, Md.G., Sarkar, M.A.R. and Hossain, A. (2019) Analysis of Neutronics and Thermal-Hydraulic Behavior in a Fuel Pin of Pressurized Water Reactor (PWR). *World Journal of Nuclear Science and Technology*, **9**, 74-83.
https://doi.org/10.4236/wjnst.2019.92005

Received: January 25, 2019
Accepted: April 20, 2019
Published: April 23, 2019

Abstract

This paper presents a comparative analysis of different parameters such as enthalpy, moderator temperature, moderator density, flow velocity, pressure, and fuel temperature profile at the fuel pin cell level of PWR. Moreover, in this paper pitches to fuel pin radius ratio are varied from 2.3 to 4. The methods and implementation strategy are such that the coupled neutronic and thermal-hydraulic analysis is executed in a fully one dimensional (1D) manner. The thermal hydraulic is based on moderator/coolant mass and enthalpy equation together with one group diffusion equation for fuel pin. Modelling of fuel pin cell and subchannel is executed in two steps. First, the governing equations are derived assuming that all the parameters appearing in the equations are temperature independent. Fuel pin centerline temperature and radially averaged temperature equations are derived from Fourier laws of thermal conductivity. Finally, diffusion coefficient, fission cross-section and absorbing cross-section are evaluated with respect to the fuel pin temperature. The outcome will be helpful for further neutronics and thermal analysis of PWR. Thermal hydraulics parameter varies the maximum 30 percentage from the lowermost value.

Keywords

Fuel Pin, Pitch, Sub-Channel, Neutronics and Thermal Hydraulics

1. Introduction

The Light Water Reactor (LWR) Nuclear Fuel Development Research and Development (R & D) is mainly focused on improving reactor core economics and safety margins through the development of fuel design. To obtain significant economical improvements while remaining safety boundaries, significant steps

beyond improvements in the current generation of nuclear fuel are required. Primary improvements in the field of fuel pin and pallet design, cladding interaction with coolant, enhanced fuel burn up; fuel composition is highly essential. To achieve massive development within next 20 - 25 years in nuclear industry, advanced fuel design should be introduced by today and those designs must be implemented with confidence [1].

For LWR, strong economic incentives exist with higher fuel consumption by maintaining its reliability. One of the most effective ways to increase fuel consumption and to use fuel pin more efficiently is raising the fuel volume fraction in the core, which in terms of thermal hydraulic and structural design can be done by increasing the fuel pin diameter and by decreasing the fuel pitch. Under certain operating condition, small fuel pitch can cause fuel pin damage or distortion, thus examining in some detail the fuel pin pitch optimization of a large LWR, taking these problems into consideration [2].

2. Objective

The aim of this work is to analysis both thermal-hydraulic and neutronic behavior along the channel of the fuel pins. The overall objectives are divided into several steps:

- To vary the fuel pitch to pin radius ratio;
- To investigate thermal hydraulic behavior by analyzing coolant temperature, pressure, density and enthalpy inside fuel assembly.

3. Methodology

The entire methodology is performed on three steps. Firstly, neutron flux is calculated from one group diffusion equation. Volumetric heat source is determined from this equation as well.

Thus, other parameters such as temperature of the fluid from fuel cladding are also determined. Finally, an equation of enthalpy is developed from the Gauss theorem and enthalpy conservation equation.

Enthalpy is determined for four different fuel pin pitch to radius ratio. Thus, other parameters such as temperature profile and moderator density profile are determined.

However, several assumptions have been made:

Pressure throughout the reactor is assumed to be constant and it is 15.5 bar. Moreover, no pressure drop will occur in the reactor.

Finally, using above two properties and implementing all values from steam table leads to determine moderator temperature and density. Those two parameters are determined for four distinct fuel pin pitch to radius ratio. Thus, other parameters: diffusion coefficient, macroscopic cross-section, fuel radially averaged temperature, coolant velocity and pressure are also determined by using Matlab.

4. Model and Equation

In this work, uranium-235 is used which is 3.957% enriched. The thermal hy-

draulics behaviors along the channel of two adjacent fuel pins are properly analyzed. The parameters relevant to the fuel pins are mentioned in Table 1 and Table 2. The pitch between two fuel pins is varied to investigate the change in enthalpy, coolant temperature, coolant velocity. Radius of the pin remained constant. It is assumed that the higher pitch to fuel pin radius ratio reflects more distance between two pins. Thus, more space can be added for coolants between the two fuel pins and the volume for the coolant can be increased as well.

$$\nabla^2\varphi(z)+\frac{\left(\upsilon\Sigma_f-\Sigma_a\right)}{D}\varphi(z)=0 \tag{1}$$

$$\varphi(z)=C\sin\left(\frac{\pi z}{H}\right) \tag{2}$$

φ is defined as neutron flux, υ, Σ_f, Σ_a are the neutron released per fission, macroscopic fission cross-section, macroscopic absorbing cross-section and D is diffusion coefficient. The solution of Equation (1) is Equation (2). Volumetric heat flux and moderator enthalpy is determined from Equation (2).

$$q''(z)=-\frac{R_{fp}^2}{2R_{co}}k\Sigma_f C\sin\left(\frac{\pi z}{H}\right) \tag{3}$$

$$\bar{h}(z)=\bar{h}(0)-\frac{P_w}{GA}\frac{R_{fp}^2}{2R_{co}}k\Sigma_f C\frac{H}{\pi}\left(\cos\left(\frac{\pi z}{H}\right)-1\right) \tag{4}$$

$$C=\frac{Q}{2K\Sigma_f HR_{fp}^2} \tag{5}$$

q'' is noted as heat dissipated to fluid from the cladding. R_{fp} is the radius of the fuel pin, k is recoverable energy per fission event, h is the enthalpy, H is the total height of the fuel pin. R_{co} is defined radius of the pin including the cladding. z defines any parameter value along the z axis or along the vertical axis. Q is power produced by one fuel pin. Enthalpy is defined in Equation (4).

$$T_{mod}=\frac{\left(h(z)-h_0\right)}{\left(h_1-h_0\right)}\times\left(T_1-T_0\right)+T_0 \tag{6}$$

T_{mod} is moderator temperature, h_1 is the updated enthalpy at the end of node, h_0 initial enthalpy at the beginning of node, T_1 temperature at the end of node, T_0 initial temperature at the beginning of the node. Total height is discretized into 37 nodes. By Equation (6) temperature of the moderator is updated from the moderator enthalpy.

$$T_{fp}^{\max}=R_{eff}R_f^2\pi q'''+\bar{T}_{mod} \tag{7}$$

$T_f^{\max}$ is noted as maximum fuel centerline temperature, R_{eff} is effective thermal resistance, q''' is volumetric heat flux.

The assumptions are made:

- the system is considered to be at steady-state conditions;
- the fluid contains no volumetric heat source/sink;

- the coolant is always assumed to remain in single-phase (PWR example);
- the flow is assumed to be mono-dimensional along the vertical *z*-axis;
- the neutron transport will be described by using one-group diffusion theory;
- the thermal conductivity of the fuel is assumed to be temperature-independent;
- the effective thermal resistance is assumed to be constant along the channel;
- the friction factor is assumed to be constant along the channel;
- Fuel pin radius measured including the cladding, however, cladding material has not been taken into account.

Fuel Pin Diameter including cladding is 8 mm.

A nuclear reactor core is the portion of a nuclear reactor containing the nuclear fuel components where the nuclear reactions take place and the heat is generated.

A structured group of fuel pins (long, slender, metal tubes containing pellets of fissionable material, which provide fuel for nuclear reactors). Depending on the design, each reactor vessel may have dozens of fuel assemblies (also known as fuel bundles), each of which may contain 200 or more fuel pins. A long, slender, zirconium metal tube contains pellets of fissionable material, which provide fuel for nuclear reactors. Fuel pins are assembled into bundles called fuel assemblies, which are loaded individually into the reactor core. Table 1 presents fuel pin pitch and pitch to radius ratio which are used to determine different parameters. Moreover, Table 2 presents specific initial conditions and other parameters related to the problem. Figure 1 presents core, fuel assembly and fuel pin with pitch between two adjacent pins. Apart from this, subchannel among four pins and subchannel among three pins are shown in Figure 2. In this paper, subchannel among the four pins is implemented.

Table 1. Fuel pin and pitch design data.

Pitch (mm)	Pitch to radius ratio
9.2	2.3
10.4	2.6
11.6	2.9
16	4.0

Table 2. Problem specification.

Parameters	**Data**
Axial Height (m)	4.20
Fuel Pin Radius without cladding (mm)	3.5
Power produced by one fuel pin (W)	6.5×10^{4}
Recoverable energy per fission event (J)	3.2×10^{-11}
Flow velocity at the inlet of the channel (ms^{-1})	4.34
Flow temperature at the inlet of the channel (K)	556.51
Macroscopic fission cross-section (cm^{-1})	0.028

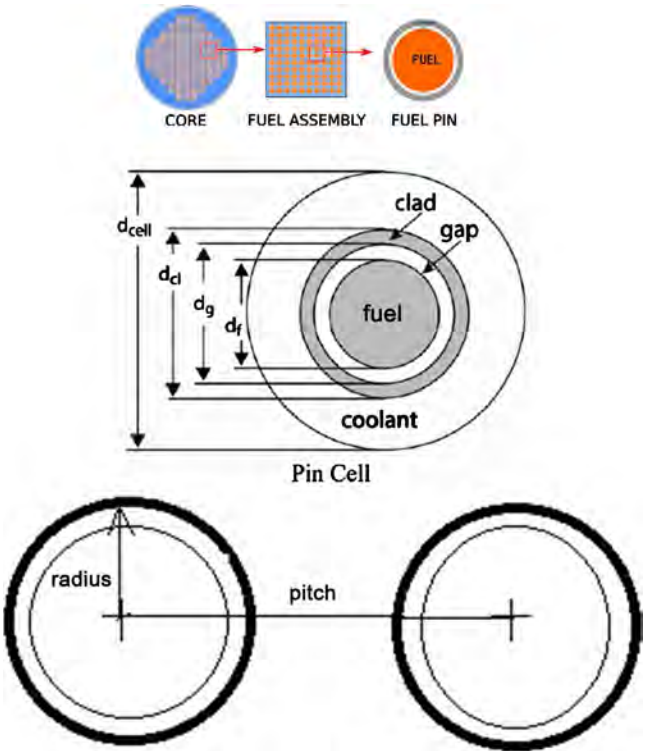

Figure 1. The radius and pitch between two pins.

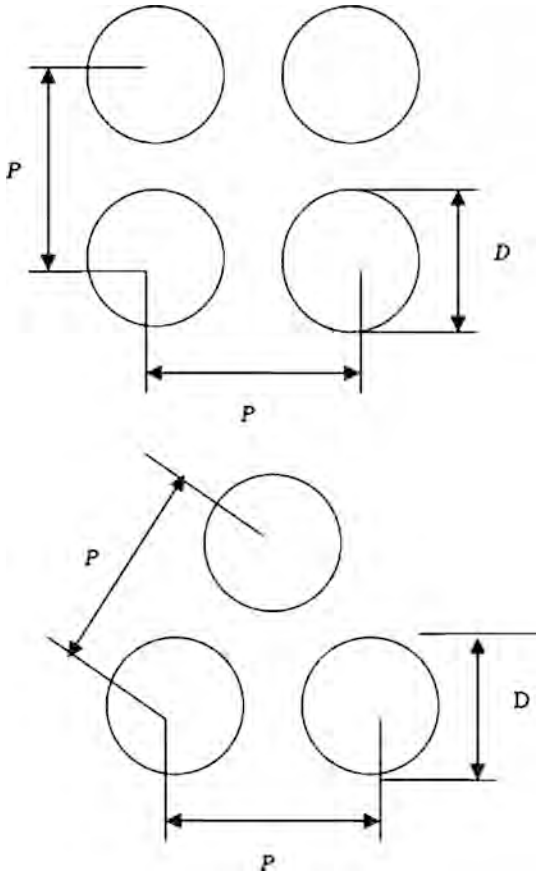

Figure 2. Different design for various fuel assembly.

5. Result and Discussions

It is found in Figure 3 that maximum enthalpy of the coolant is determined for lowest fuel pitch to pin radius ratio and minimum enthalpy is determined for maximum fuel pitch to pin radius ratio. More enhancement of pitch will result in more flatten of the enthalpy curve. However, an optimum range between 2.6 to 2.9 shows better results from both the power generation and safety aspects. Maximum enthalpy for minimum pitch to radius ratio 2.3 is a concern from the safety aspects. On the other hand, less enthalpy to the coolant results in lower power generation. An enthalpy range from 1500 KJ to 1200 KJ is desired value for PWR. As a result, a fuel pitch to radius ratio 2.9 to 4 is desirable for PWR.

Figure 4 shows the change in moderator temperature and moderator density respectively. For steady state condition, inlet moderator temperature is set at 556 K. Since, melting point of moderator in PWR is 615 K and single-phase flow is desirable for PWR and the optimum value of fuel pin pitch to radius ratio is 2.9 to 4. For four different ratios the temperature of moderator increases from 550 K to 650 K along the vertical axis. All three except the ratio 2.3 show satisfactory result. On the other hand, moderator density reduces along the axis as temperature along the axis increases. Moderator density remains almost constant for ratio 4 and it changes rapidly for ratio 2.3. Maximum density is found almost 770 kg/m^3 and minimum density is 505 kg/m^3.

Figure 5 shows gradual decrease of coolant pressure. Several pressure drops such as: gravitational pressure drop, frictional pressure drop, acceleration pressure drop are taken into account which causes a fall of pressure along the verticle axis inside the reactor. Pressure range is found from 15.5 MPa to 15.65 MPa for all four pitch to radius ratio. In PWR maximum pressure can be raised upto 15.5 MPa [3]. So, all the pressure range lie in optimum level.

Figure 6 shows increase of coolant velocity along the vertical axis. A significant

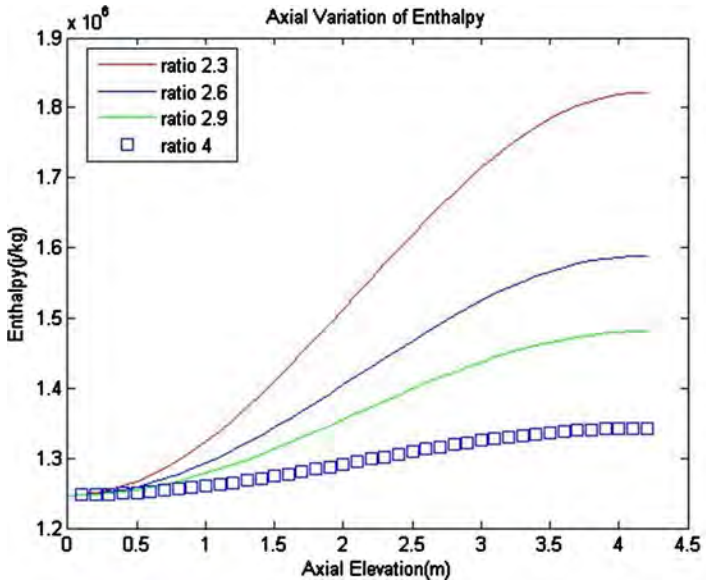

Figure 3. Enthalpy along the axial elevation.

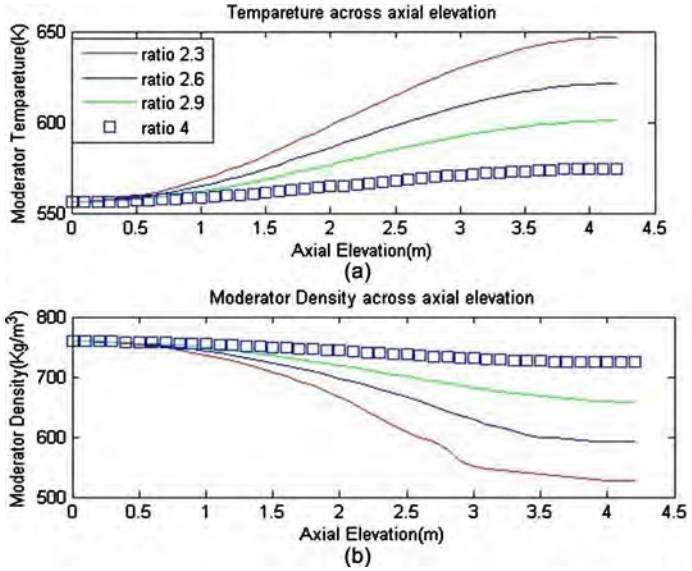

Figure 4. A variation on moderator temperature (a) and moderator density (b) along the channel.

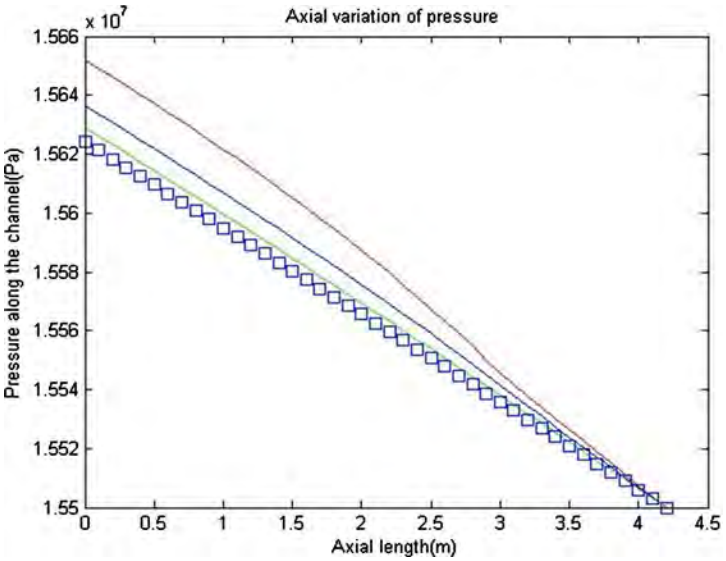

Figure 5. Axial variation of the coolant pressure.

increment has been found for 2.3 ratio. Maximum allowable coolant velocity is found 6.4 ms^{-1} for this ratio. The rest of the ratio shows increment from 4.4 ms^{-1} to 5.5 ms^{-1}. No significant flow velocity is found for the ratio 4.

In Figure 7, radially averaged fuel temperature is presented. As it can be seen, maximum temperature has been found for 2.3 ratio is 1580 K. The fuel temperature is almost 50 K higher than the lowest value for the pin pitch to radius ratio 4. The profile seems symmetrical.

The pellet radial temperature profile at the hottest location in fuel pin is depicted in Figure 7. In the fuel pin the hottest location is found at the fuel rod position at active height of 1.5 to 2.5 m. The thermal conductivity from 500˚C to 2000˚C is 4 W(m·K) to 2 W(m·K) [4].

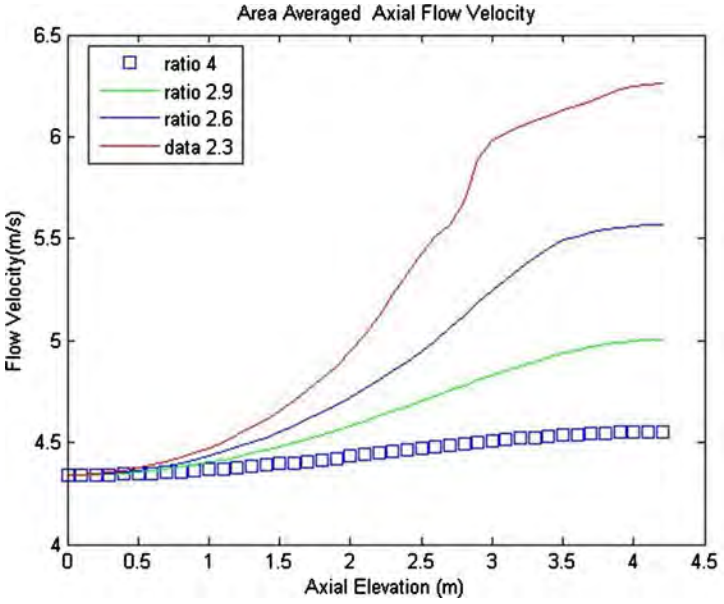

Figure 6. Coolant flow velocity along the vertical axis.

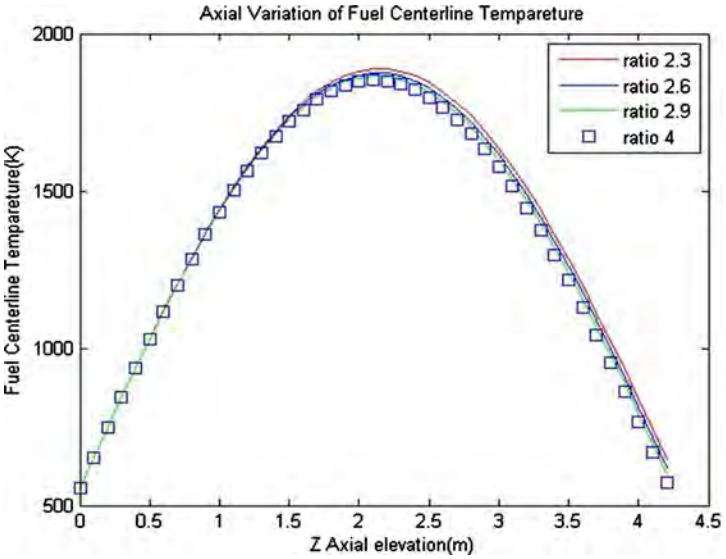

Figure 7. Fuel centerline temperature along the vertical axis.

Thermal-hydraulic behavior along the channel has been observed. This analysis has been performed on the pin cell level by varying pitch to fuel pin radius ratio. It has been found from overall all figures that ratio 2.6 is optimum and acceptable ratio. As coolant higher enthalpy results in more rise in the temperature and lowers the coolant density.

The first important constraint is that the core temperatures remain below the melting points of core components. This is particularly important for the fuel and clad materials.

There are also limits on heat transfer rate between the fuel elements and coolant, since if this heat transfer rate becomes too large, critical heat flux may be approached leading to boiling transition. This, in turn, will result in a rapid in-

crease of the clad temperature.

In case of exceeding limit of a certain wall heat flux, there heat transfer rate will become progressively worse [5].

Critical heat flux is the primary concern for the Pressurized Water Reactors (PWR), since such reactors operate with subcooled and low quality coolants. Even for Boiling Water Reactors (BWR), which have a significantly bottom-peaked axial power profile, the DNB-risk have to be taken into account.

6. Conclusion

In this study, fuel pin optimization is performed for Pressurized Water Reactor. The results are specifically dependent on design specification and design criteria. The pitch to fuel pin radius ratio is better optimized from 2.6 to 2.9 which is desirable for PWR. A certain temperature limit is maintained to keep the reactor in subcooled condition. Moreover, a PWR fuel pitch and radius should be designed in such a way that will result in higher neutron economy which rises the enthalpy, and thus efficiency of the reactor. The results are obtained very preliminary. These may be used in future modelling of reactor core.

Acknowledgements

The author would like to thank Prof. Christopher Demezair from Dept of Nuclear Engineering, Chalmers University of Technology, Gothenburg, Sweden for useful discussions on the interpretation of the results.

Conflicts of Interest

The authors declare no conflicts of interest regarding the publication of this paper.

References

[1] Barrett, K. and Bragg-Sitton, S. (2012) Advanced LWR Nuclear Fuel Cladding System Development Trade-Off Study. No. INL/EXT-12-27090. Idaho National Laboratory (INL), Idaho Falls.

[2] Miki, K., Kawashima, K. and Inoue, K. (1981) Effect of Fuel Pin Pitch on Core Characteristics of Large LMFBR. *Journal of Nuclear Science and Technology*, **18,** 71-73. https://doi.org/10.1080/18811248.1981.9733224

[3] Cooper, J.R., London, E.Ns. and Dooley, R.B. (2007) International Association for the Properties of Water and Steam.

[4] (1957) Thermal Conductivity of Uranium Dioxide. *Nuclear Power.*

[5] (2003) Applied Reactor Technology and Nuclear Safety.

Nomenclature

D	diffusion coefficient
q''	heat dissipated to fluid from the cladding
R_{fp}	radius of the fuel pin
k	recoverable energy per fission event
h	the enthalpy
H	the total height of the fuel pin
R_{co}	radius of the pin including the cladding
z	the any parameter value along the z axis or along the vertical axis
T_{mod}	moderator temperature
h_1	updated enthalpy at the end of node
h_0	initial enthalpy at the beginning of node
T_1	temperature at the end of node
T_0	initial temperature at the beginning of the node
$T_{fp}^{\max}$	is noted as maximum fuel centerline temperature
R_{eff}	is effective thermal resistance
q'''	is volumetric heat flux

Greek Letters

φ	neutron flux
υ	neutron released per fission
Σ_f	macroscopic fission cross-section
Σ_a	macroscopic absorbing cross-section

Subscripts

fp	fuel pin
mod	moderator
f	fission
a	absorbing cross-section
co	cladding
eff	effective

World Journal of Nuclear Science and Technology, 2019, 9, 84-95
http://www.scirp.org/journal/wjnst
ISSN Online: 2161-6809
ISSN Print: 2161-6795

Study of Radionuclides and Radon Exhalation Rate in Soil and Sand Samples from Tiba, Luxor, Governorate

Hani H. Negm[1], Nour K. Ahmed[2], Abdelbaset Abbady[2], Maha M. Reda[3]

[1]Faculty of Science, Assiut University, Assiut, Egypt
[2]Faculty of Science, South Valley University, Qena, Egypt
[3]High Institute of Engineering and Technology at El-Tod, Luxor, Egypt
Email: negm_sci@yahoo.com, nkahmed54@yahoo.com, mousa_19@yahoo.com, mahareda2015@yahoo.com

How to cite this paper: Negm, H.H., Ahmed, N.K., Abbady, A. and Reda, M.M. (2019) Study of Radionuclides and Radon Exhalation Rate in Soil and Sand Samples from Tiba, Luxor, Governorate. *World Journal of Nuclear Science and Technology*, **9**, 84-95.
https://doi.org/10.4236/wjnst.2019.92006

Received: March 10, 2019
Accepted: April 22, 2019
Published: April 25, 2019

Abstract

In this study, the natural radionuclides in soil and sand have been measured by using high purity germanium (HPGe) detector. While, radon exhalation rate has been measured by Alpha GUARD. The data analysis is performed to determine ^{226}Ra, ^{232}Th, and ^{40}K activity concentrations in addition to ^{222}Rn exhalation rate. The values of radium equivalent activity (R_{aeq}), external hazard index (H_{ex}), internal hazard index (H_{in}), and absorbed dose rate were ranged from 46.46 to 124.16 Bq·kg^{-1}, 0.07 to 0.33 Bq·kg^{-1}, 0.09 to 0.42 Bq·kg^{-1}, and 13.24 to 58.37 nGy·h^{-1} respectively in all samples. The area and mass exhalation rates were increased from 9.16 ± 2.83 to 16.18 ± 2.83 Bq·m^{-2}·h^{-1} and 1.8 ± 1.34 to 11.35 ± 0.98 Bq·kg^{-1}·h^{-1} respectively.

Keywords

HPGe Detector, Alpha GUARD, Natural Radionuclides, Hazard Index, Radon Gas

1. Introduction

In soil and sand, the natural radionuclides consist mainly of ^{232}Th and ^{238}U and isotopes with their daughter products in addition to ^{40}K. The natural radioactivity may vary from one type of soil to another; the sources of radioactivity in soil other than those of natural origin are mainly due to extensive use of fertilizers rich in phosphates for agricultural purposes [1]. The information of the concentrations and distribution of the radionuclides in these materials enable one to assess any possible radiological risks to human health [2] [3], and provide useful

information in the monitoring of environmental contamination by natural radioactivity. Nationwide surveys have been carried out to determine the radium equivalent activity of building materials in many countries [4] [5] [6]. The reason for current interest is due to the fact that external radiation exposures from naturally occurring radionuclides materials (NORM) contribute, on average, of about 10% of the average annual dose to the human body from all radiation sources. It has been observed that naturally occurring radionuclides are present in soil [7] [8] [9] and sand which constitute a lived-in radioactive environment. In this study, we used The HPGe detector N-type for determining the activity levels of ^{226}Ra, ^{232}Th and ^{40}K in soil and sand samples collected from Tiba area. ALPHA GUARD has been used for evaluating radon exhalation rate. It is well known that radon exhalation of soil samples is higher than sand samples because of the presence of relatively high uranium content in its natural formation [10]. The formatter will need to create these components, incorporating the applicable criteria that follow.

2. Materials and Methods

2.1. Sampling and Samples Preparation

In this study, 36 samples have been collected from Tiba city Luxor governorate, as presented in **Figure 1**, for more detailed descriptions. The soil sampling sites were randomly selected for the two types of samples (soil and sand) and samples were collected by a core method, in which cores of 10 cm diameter and 25 cm in depth were used to take samples (ASTM, 1986, 1983) [11]. Samples with large grain size were crushed to small pieces using mechanical crusher. Afterwards, the samples were ground to a fine grain size powder. Every powdered sample was mixed using electric shaker to obtain a homogeneous powdered sample. The reason of choosing this region because it is a new reclaimed area and there are no enough researches in it. The samples were divided to, 15 samples of soil and

Figure 1. Sampling location (Tiba, Luxor).

21 samples of sand. Some processes have been done on the samples before measuring the activity concentration for them, like the following: First, the samples dried in an oven at 105˚C, to get rid of moisture and water inside samples. Second, the samples sieved through 200 mesh, to optimize the grain size of the heavy mineral [12]. Third, each sample has been placed in a plastic container, which was sealed to avoid the escape of ^{222}Rn and ^{220}Rn from the samples. Moreover, the samples were left for one month at least to achieve equilibrium between ^{232}Th, ^{226}Ra, and their daughter products before radiometric analysis [13].

2.2. Measuring Systems

1) Measurement activity concentration

Gamma-ray spectrometry is a commonly used technique for direct determination of the radionuclides in crustal and extra-terrestrial materials. The radioactive analysis in environmental samples often encounters with difficulty in measuring low levels of radioactivity. However, gamma spectrometry is a useful tool in the analysis of natural radionuclides at environmental concentrations. It is a relative method of assay and has the merit of being simple and essentially non-destructive technique. The method is based on the fact that the decay of the radioelements is accompanied by the emission of high energy gamma-rays in order of Kev to few-MeV. The applied low-level gamma-ray spectrometer is based on the high purity germanium (HPGe) detector with its electronic instrumentation. The detector is the coaxial closed end, closed facing window geometry with vertical dipstick cryostat with carbon composite window.

The detector-crystal has been shielded in a chamber of three layers starting with copper (30 mm thick), lead (100 mm thick) and finally cadmium (3 mm thick). This shield serves in reducing the background-radiation for the measuring sample to less than 1%. Figure 2 shows the block diagram of a low-level gamma-rays spectrometer, which consists of; the preamplifier, the main amplifier, multichannel analyzer, and the scalar or PC. Each sample was placed in face to face geometry over the detector for about 8 hours or more for the natural radionuclide's (^{226}Ra, ^{232}Th and ^{40}K) in soil and sand samples. Signals produced by the gamma-ray detector are amplified, stored and displayed by the multichannel analyzer as well as the energy spectra, *i.e.* the number of counts per unit time per energy interval.

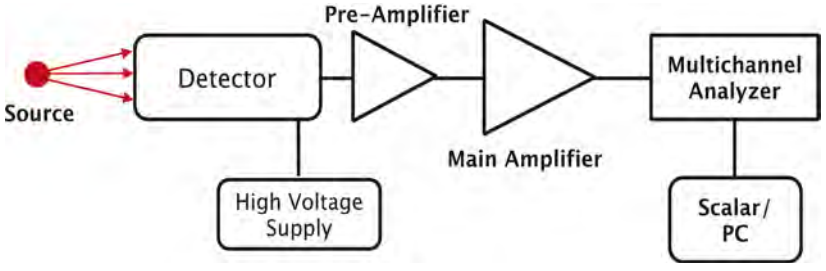

Figure 2. Block diagram of a gamma-ray spectrometer.

The activity concentrations have been calculated from the intensity of each line considering the size and mass of the sample, the branching ratio for the gamma-decay, and the efficiency of the detector. The branching ratio is the statistical chance that a gamma-ray is emitted per decaying nucleus. The efficiency of the detector represents the probability that the emitted gamma-ray contributes to the line in the spectrum. Activity concentrations calculated from the intensity of several gamma-rays emitted by a nucleus are grouped together to produce a weighted average activity per nuclide. For activity concentrations of nuclides in the same decay series, the activity concentrations are grouped in a similar way.

The analysis of ^{226}Ra and ^{232}Th is based on the gamma-lines of the decay products in equilibrium with their parent nuclides. The specific activity of ^{226}Ra of the samples has been determined through its daughters (^{214}Pb and ^{214}Bi) via the intensity of the 295.2 keV, 351.9 keV for ^{214}Pb gamma-lines, and 609.3 keV, 1120.3 keV, 1764.5 keV for ^{214}Bi gamma-lines. The specific activity of ^{232}Th of the samples has been determined from its daughters (^{228}Ac, ^{212}Pb, and ^{208}Tl) via the intensity of 209.3 keV, 338.3 keV, 911.2 keV, 969.0 keV gamma-lines for ^{228}Ac, 238.6 keV gamma line of ^{212}Pb, and 583.2 keV, 2614.6 keV gamma-lines of ^{208}Tl, while the specific activity of ^{40}K has been determined from the emission of 1460.7 keV gamma-line.

Before using the gamma-ray spectrometer for measurements, the following considerations have been made: energy calibration, detection efficiency calibration, and background measurements.

The specific activity concentration $A(E_i)$ with Bq·kg^{-1}, of a nuclide and for a gamma-line (i) with energy E, is given by:

$$A(E_i) = \frac{N(E_i)/T - n(E_i)/t}{\varepsilon(E_i) \cdot P(E_i) \cdot M} \tag{1}$$

where, $N(E_i)$ is the counts in a given peak (i) area, T is the sample counting lifetime, $n(E_i)$ is the number of counts in background peak (i), t is the background counting time, $P(E_i)$ is the number of gammas per disintegration of this nuclide (emission probability), M is the mass in kg of the measured sample, $\varepsilon(E_i)$ is the detection efficiency of the measured gamma-line energy.

If there is more than one peak in the energy analysis range for a nuclide, then an attempt to average the peak activities is made by using the weighted average nuclide activity. Moreover, the concentrations of the radiological hazard indices in the collected samples have been estimated, based on the measured gamma-ray photo-peaks, that emitted from the specific radionuclides in the ^{232}Th and ^{226}Ra decay series as well in ^{40}K. The calculations depend on the establishment of secular-equilibrium for each sample, due to the much smaller lifetime of daughter radionuclides in the decay series of ^{232}Th and ^{226}Ra. More specifically, the ^{232}Th concentration was determined from the average activity concentrations of ^{212}Pb, ^{208}Tl, and ^{228}Ac in the samples, and that of ^{226}Ra was determined from the average activity concentrations of the ^{214}Pb and ^{214}Bi decay products. Therefore, an accu-

rate measurement of ^{232}Th and ^{226}Ra radiological activity concentrations has been made, whereas a true measurement of ^{40}K concentration was achieved.

2) Measurement of the radon exhalation rate

To determine the ^{222}Rn exhalation activity concentration in soil and sand samples, the ionization chamber Alpha GUARD PQ2000PRO along with the additional special equipment [14] has been used. The background of the detection system, without a sample, is measured for a few minutes before achieving any measuring. About 200 g of each sample was put into the degassing vessel. The Alpha-pump was switched on with the flow rate 1.0 min and 10.0 min flow, thus the ^{222}Rn activity concentration will be recorded every 10 min. At equilibrium state, the buildup activity of exhaled radon inside the emanation container is as follows:

$$A = A_0\left(1 - e^{-\lambda t}\right) \tag{2}$$

where A_0 is the total value of the activity concentration in Bq/m^3 and λ is the decay constant of the radon nuclide. The radon exhalation rate of the concerned sample per unit area, E_S, which known as the radon flux that released via the surface of the material, can be calculated using the following formula [15] [16]:

$$E_S = A_0 \frac{V}{S}\lambda \tag{3}$$

where V is the effective volume of the emanation container (2400×10^{-6} m^3) and S is the total surface area of the sample (0.01130 m^2), which equals the cross-sectional area of the emanation container. By analogy of Equation (3), the radon exhalation rate per unit mass of the concerned sample E_M is also calculated using the following formula:

$$E_M = A_0 \frac{V}{M}\lambda \tag{4}$$

where M is the sample mass.

3. Results and Discussions

3.1. Natural Activity Concentration

The activity concentrations of ^{226}Ra and ^{232}Th series, and ^{40}K acquired from sand samples are ranged from 18.34 ± 4.24 Bq·kg^{-1}, 14.06 ± 3.66 Bq·kg^{-1}, 210.99 ± 14.467 Bq·kg^{-1}, respectively, and for soil samples vary from 15.916 ± 4.769 to 34.3073 ± 5.85 Bq·kg^{-1}, 12.9314 ± 3.59 to 40.244 ± 6.34 Bq·kg^{-1} and 135.36 ± 11.63 to 528.144 ± 22.98 Bq·kg^{-1}, respectively. The measured activities values have been found within the acceptable range of radioactive concentrations reported by UNSCEAR [17]. A summary of measurements for the activity concentration in Bq·kg^{-1} of the natural radioactivity due to ^{226}Ra, ^{232}Th, and ^{40}k of different samples is presented in **Table 1**. The distribution of ^{226}Ra, ^{232}Th, and ^{40}k activity concentrations in all samples are given in **Figure 3** & **Figure 4**.

3.2. Radiation Hazard Indices

Radium equivalent activity (R_{aeq}), Internal hazard index (H_{in}), External hazard

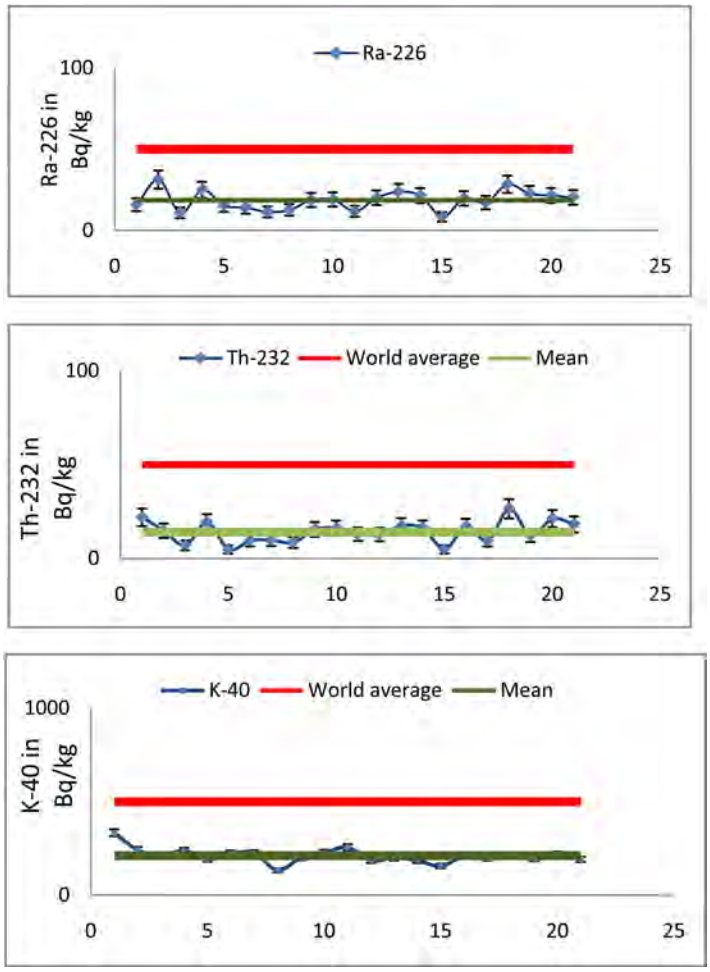

Figure 3. Distribution activity concentration (Bq·Kg^{-1}) of ^{226} Ra, ^{232}Th and ^{40}K for Tiba sand samples.

index (H_{ex}) and Gamma activity concentration index ($I_{\gamma r}$), can be estimated by following equations respectively [18] [19] [20] [21]:

$$Ra_{eq} = A_{Ra} + \frac{10}{7} A_{Th} + \frac{10}{130} A_K \tag{5}$$

$$H_{ex} = \frac{1}{370} A_{Ra} + \frac{1}{259} A_{Th} + \frac{1}{4810} A_K \tag{6}$$

$$H_{in} = \frac{1}{185} A_{Ra} + \frac{1}{259} A_{Th} + \frac{1}{4810} A_K \tag{7}$$

$$I_{\gamma r} = \frac{1}{150} A_{Ra} + \frac{1}{100} A_{Th} + \frac{1}{1500} A_K \tag{8}$$

3.3. Absorbed Dose Rate

The absorbed dose rate of gamma-ray, D, in nGy·h^{-1} in the outdoor air at a height 1.0 m above the ground level can be calculated using the activity concentrations of ^{226}Ra and ^{232}Th series as well ^{40}K isotope that measured in Bq·kg^{-1} as the following equation of UNSCEAR-2000 [17]:

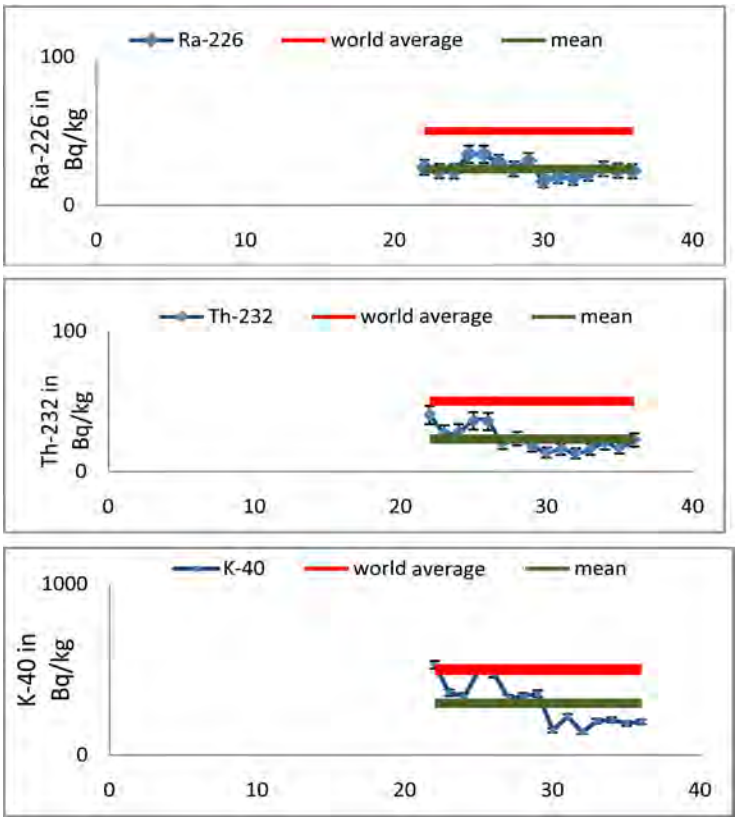

Figure 4. Distribution activity concentration (Bq/Kg) of ^{226} Ra,^{232}Th and ^{40}K for Tiba soil samples.

$$D(\text{nGy/h}) = 0.462A_{Ra} + 0.604A_{Th} + 0.0416A_{K} \quad (9)$$

The calculated absorbed doses in air for soil samples are ranged from 21.58 to 58.37 nGy·h^{-1} with an average value 37.98 nGy·h^{-1}, while it for sand samples are ranged from 13.24 to 37.84 nGy·h^{-1} with an average value of 25.85 nGy·h^{-1}. However, according to UNSCEAR-2000 [17], the dose rate in outdoor air from terrestrial gamma-rays in normal circumstances is about 57 nGy·h^{-1}. Consequently, the evaluated doses obtained in this study for all samples are lower than the worldwide average value of 57 nGy·h^{-1}, which attributed to the low of activity concentrations of ^{226}Ra and ^{232}Th series, as well ^{40}K isotope.

While the results of R_{aeq}, I_{yr}, H_{in}, H_{ex} and D are given in Table 1.

3.4. Calculation Radium Content and Exhalation Rates in Soil and Sand Samples Collected from Tiba Region

Table 2 shows the average values for radium content in Bq·kg^{-1}, mass exhalation rate in Bq·kg^{-1}·h^{-1}, and area exhalation rate in Bq·m^{-2}·h^{-1}, for soil and sand samples collected from Tiba region. Figure 5 shows the average value for Radium content (a), mass exhalation rate (b), and area exhalation rate(c), for soil and sand samples. As results of the evaluation of these parameters, the average values for radium content, mass exhalation rate and area exhalation rate for soil samples are higher than of the corresponding values of the sand samples.

Table 1. Average radionuclide concentrations, radium equivalent activity, external hazard index, internal hazard index, representative level index and absorbed dose rate in different samples from Tiba, Luxor governorate.

Sample No.	Type of sample	Activity concentration (Bq/Kg)			R_{aeq}	H_{ex}	H_{in}	I	Absorbed dose rate
		^{226}Ra	^{232}Th	^{40}K					
22	Soil	25.50 ± 5	40.24 ± 6.3	528.1 ± 22.9	123.71	0.33	0.4	0.92	58.11
23		22.95 ± 4.7	27.74 ± 5.2	364.7 ± 19.1	90.77	0.24	0.3	0.67	42.59
24		22.74 ± 4.7	28.57 ± 5.3	343.7 ± 18.5	90.07	0.24	0.3	0.66	42.1
25		34.30 ± 5.8	36.05 ± 6	497.4 ± 22.3	124.1	0.33	0.42	0.92	58.37
26		34.29 ± 5.8	35.57 ± 5.9	476.6 ± 21.8	121.8	0.32	0.42	0.9	57.2
27		28.54 ± 5.3	20.70 ± 4.5	333.1 ± 18.3	83.54	0.22	0.3	0.61	39.58
28		24.41 ± 4.9	23.59 ± 4.8	344.2 ± 18.6	84.66	0.22	0.29	0.62	39.88
29		29.66 ± 5.4	18.60 ± 4.3	358.8 ± 18.9	83.9	0.22	0.3	0.62	39.9
30		15.91 ± 3.9	13.59 ± 3.6	144.30 ± 12	46.46	0.12	0.16	0.33	21.58
31		19.10 ± 4.3	16.01 ± 4	224.8 ± 14.9	59.3	0.16	0.21	0.43	27.86
32		17.87 ± 4.2	12.93 ± 3.5	135.3 ± 11.6	46.79	0.12	0.17	0.33	21.71
33		21.04 ± 4.5	16.01 ± 4	198.2 ± 14.1	59.21	0.15	0.21	0.43	27.66
34		24.52 ± 4.9	20.30 ± 4.5	205.4 ± 14.3	69.37	0.18	0.25	0.5	32.15
35		23.31 ± 4.8	17.03 ± 4.1	185.0 ± 13.6	61.93	0.16	0.23	0.44	28.78
36		22.83 ± 4.7	22.60 ± 4.7	194.2 ± 13.9	70.11	0.18	0.25	0.5	32.3
Max		34.30 ± 5.8	40.24 ± 6.3	528.1 ± 22.9	124.16	0.33	0.42	0.92	58.37
Min		15.91 ± 4.7	12.93 ± 3.5	135.3 ± 11.6	46.46	0.12	0.16	0.33	21.58
Aver		24.46 ± 5.2	23.30 ± 4.7	302.29 ± 17	81.07	0.21	0.28	0.59	37.98
1	Sand	15.88 ± 3.9	21.9 ± 4.6	333.5 ± 18.2	56.07	0.19	0.23	0.54	34.47
2		31.28 ± 5.5	14.78 ± 3.8	241.7 ± 15.5	55.57	0.19	0.27	0.51	33.46
3		10.78 ± 3.2	6.97 ± 2.6	213.9 ± 14.6	85.14	0.1	0.12	0.28	18.11
4		24.9 ± 4.9	19.2 ± 4.3	237.2 ± 15.4	53.17	0.19	0.25	0.51	32.99
5		15.3 ± 3.9	4.78 ± 2.1	192.3 ± 13.8	91.52	0.09	0.14	0.27	17.97
6		14.01 ± 3.7	9.5 ± 3.1	223.4 ± 14.9	73.62	0.12	0.15	0.33	21.52
7		11.4 ± 3.3	9.7 ± 3.1	225.0 ± 15.1	76.04	0.11	0.14	0.32	20.51
8		12.6 ± 3.5	8.5 ± 2.9	132.2 ± 11.5	77.88	0.09	0.12	0.25	16.47
9		18.72 ± 4.3	15.45 ± 3.9	200.8 ± 14.1	60.03	0.15	0.2	0.41	26.35
10		19.01 ± 4.3	16.16 ± 4	226.9 ± 15.1	59.01	0.16	0.21	0.43	28
11		11.8 ± 3.4	12.9 ± 3.5	255.3 ± 15.9	69.4	0.13	0.16	0.37	23.89
12		20.11 ± 4.4	12.72 ± 3.5	185.4 ± 13.6	62.96	0.14	0.19	0.38	24.7
13		23.75 ± 4.8	17.31 ± 4.1	199.5 ± 14.4	55.43	0.17	0.23	0.46	29.74
14		21.45 ± 4.6	16.2 ± 4	185.4 ± 13.6	57.68	0.15	0.21	0.42	27.42
15		8.34 ± 2.8	4.8 ± 2.1	155.6 ± 12.5	100.51	0.07	0.09	0.2	13.24

Continued

16	19.72 ± 4.4	17.04 ± 4.1	209.9 ± 14.5	57.69	0.16	0.21	0.44	28.15
17	17.12 ± 4.1	9.4 ± 3.1	198.3 ± 14.1	71.35	0.12	0.17	0.34	21.85
18	28.39 ± 5.3	26.45 ± 5.1	209.9 ± 14.5	47.1	0.22	0.29	0.59	37.84
19	22.67 ± 4.7	12.27 ± 3.5	195.3 ± 13.9	62.37	0.14	0.21	0.4	26.02
20	21.51 ± 4.6	21.20 ± 4.6	217.3 ± 14.7	53.13	0.18	0.24	0.5	31.8
21	20.29 ± 4.5	18.11 ± 4.2	191.3 ± 13.8	56.35	0.16	0.21	0.44	28.29
Max	31.28 ± 5.5	26.45 ± 5.1	333.5 ± 18.2	100.51	0.22	0.29	0.59	37.84
Min	18.34 ± 2.8	4.78 ± 2.1	232.2 ± 11.5	47.1	0.07	0.09	0.2	13.24
Aver	18.52 ± 4.2	14.06 ± 3.6	210.9 ± 14.4	65.81	0.14	0.19	0.4	25.85

Table 2. The average values for radium content ($Bq \cdot kg^{-1}$), mass exhalation rate ($Bq \cdot kg^{-1} \cdot h^{-1}$) and area exhalation rate ($Bq \cdot m^{-2} \cdot h^{-1}$) for soil and sand samples collected from Tiba region.

Type of samples	Radium content ($Bq \cdot kg^{-1}$)	Radon exhalation rate	
		Mass ($Bq \cdot Kg^{-1} \cdot h^{-1}$)	Surface area ($Bq \cdot m^{2} \cdot h^{-1}$)
Soil	240.25 ± 15.46	1.816 ± 1.34	16.18 ± 4.012
Sand	152.39 ± 11.35	1.1 ± 0.98	9.16 ± 2.83

4. Conclusion

High purity germanium was exploited to determine activity concentration for naturally occurring ^{226}Ra, ^{232}Th, and ^{40}K radioisotopes in two types of samples (soil, sand) from Tiba area in Luxor governorate. Results show the average activity concentrations of ^{226}Ra, ^{232}Th, and ^{40}K are 24.4 ± 1.4 $Bq \cdot kg^{-1}$, 23.3 ± 1.1 $Bq \cdot kg^{-1}$ and 302.2 ± 6 $Bq \cdot kg^{-1}$, respectively for soil and 18.52 ± 0.8, 14.06 ± 0.5 and 210.9 ± 6 for sand. The results indicate that soil generally has higher natural radioactivity than sand in the same region. These values fall in the lowest range of the world values 30.35 and 400 $Bq \cdot kg^{-1}$ for ^{226}Ra, ^{232}Th, and ^{40}K respectively [16]. The radium equivalent activity (R_{aeq}), internal hazard indexes (H_{in}), external hazard indexes (H_{ex}), absorbed dose rate (D) and representative level index (I), for all samples under studying (soil-sand) were 81.07, 0.28, 0.21, and 0.59 respectively for soil samples, 65.81, 0.19, 0.14, and 0.40 for sand. The results indicate that the dose rates at 1 m above the ground from terrestrial sources in all samples under investigation were 37.98 and 25.85 $nGy \cdot h^{-1}$ for soil and sand samples respectively. These values agree with the world average value reported by UNSCEAR [17]. These values present no hazards to human. The surface exhalation and mass exhalation rates for radon from these different samples were reflected by their radium contents. The result indicates that the exhalation rates are higher for soil samples from than sand samples. The overall average of mass exhalation rate for samples under investigation is 1.69 ± 0.12 $Bq \cdot kg^{-1} \cdot h^{-1}$ and the average value for surface exhalation rate for radon in different samples is 29.86 ± 0.35 $Bq \cdot m^{-2} \cdot h^{-1}$.

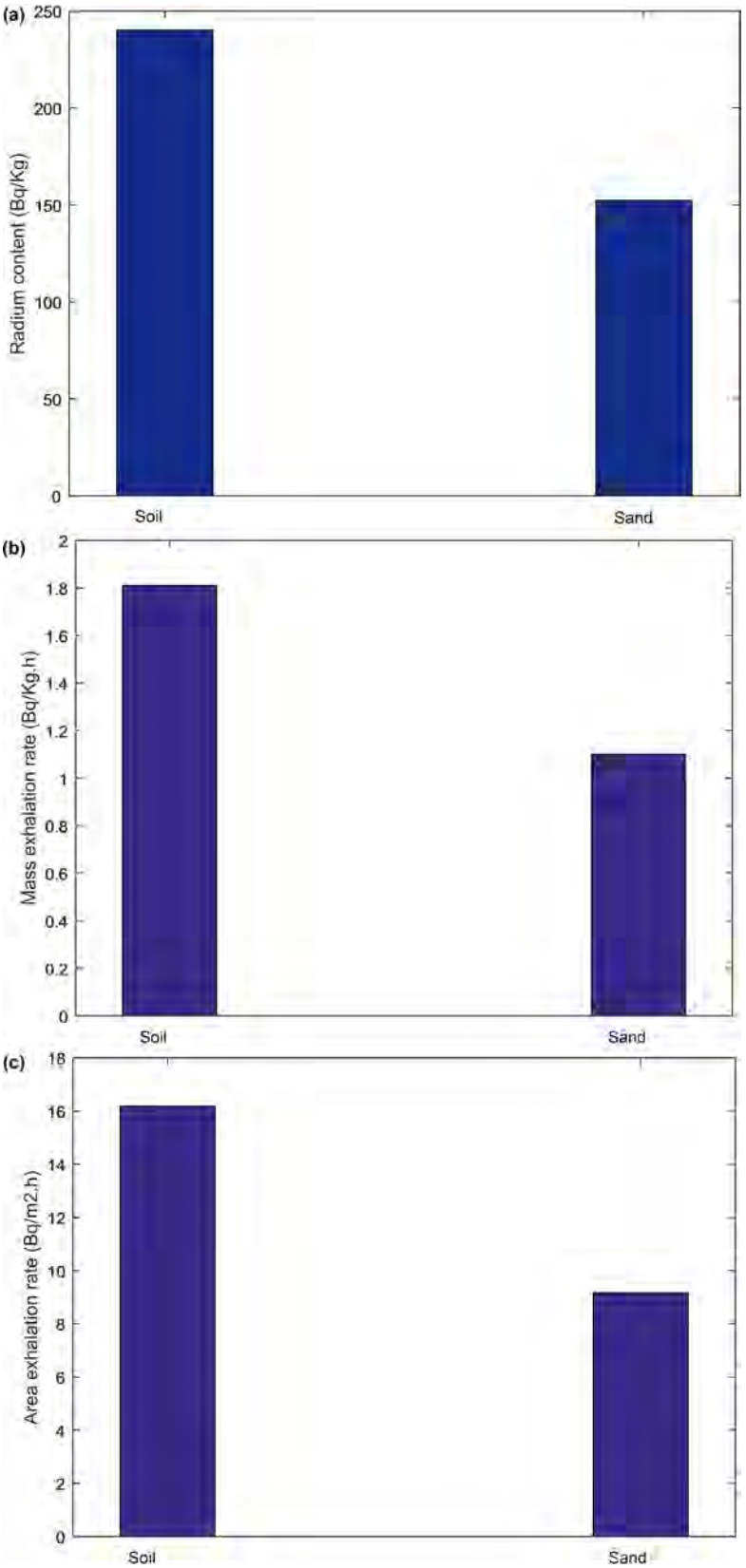

Figure 5. Average value for Radium content (a), mass exhalation rate (b), and area exhalation rate (c), for soil and sand samples.

Acknowledgements

The author would like to thank the staff of High Institute of Engineering and Technology at Eltod for their support.

Conflicts of Interest

The authors declare no conflicts of interest regarding the publication of this paper.

References

[1] Abbady, A., El-Arabi, A.M., Abbady, A.G.E. and Taha, S. (2006) Gamma-Ray Measurements of Natural Radioactivity in Cultivated and Reclaimed Soil. *Seventh Internal National Radiation Physics Conference*, Beni Suef, 13-15 November 2006, 223-231.

[2] Ahmed, N.K. and El-Arabi, A.M. (2005) Natural Radioactivity in Farm Soil and Phosphate Fertilizer and Its Environmental Implications in Qena Governorate, Upper Egypt. *Journal of Environmental Radioactivity*, **84**, 51-64. https://doi.org/10.1016/j.jenvrad.2005.04.007

[3] Altschuler, Z.S. (1980) The Geochemistry of Trace Elements in Marine Phosphorites. 1. Charac Teristic Abundances and Enrichment. Society of Economic Paleontologists and Mineralogists Special Publication, Vol. 29, 19-30. https://doi.org/10.2110/pec.80.29.0019

[4] Amrani, D. and Tahtat, M. (2001) Natural Radioactivity in Algerian Building Materials. *The International Journal of Applied Radiation and Isotopes*, **54**, 687-689. https://doi.org/10.1016/S0969-8043(00)00304-3

[5] Hayumbu, P., Zaman, M.B., Lubaba, N.C.H., Munsanje, S.S. and Nuleya, D. (1995) Natural Radioactivity in Zambian Building Materials Collected from Lusaka. *Journal of Radioanalytical and Nuclear Chemistry*, **199**, 229-238. https://doi.org/10.1007/BF02162371

[6] Mollah, A.S., Ahmed, G.U., Hussain, S.R. and Rahman, M.M. (1986) The Natural Radioactivity of Some Building Materials Used in Bangladesh. *Health Physics*, **50**, 849-851.

[7] UNSCEAR (1993) Exposures from Natural Sources of Radiation. Report to the General Assembly, with Scientific Annexes, United Nations, New York.

[8] Radhakrishna, A.P., Somashekarappa, H.M., Narayana, Y. and Siddappa, K.A. (1993) New Natural Background Radiation Area on the Southwest Coast of India. *Health Physics*, **65**, 390-395. https://doi.org/10.1097/00004032-199310000-00006

[9] P. Ziqiang, Y. Yang, G. Mingqiang, (1988) Natural Radiation and Radioactivity in China. *Radiation Protection Dosimetry*, **24**, 29-38.

[10] Durrani, S.A. and Ilic, R. (1997) Radon Measurements by Etched Track Detectors: Applications in Radiation Protection, Earth Sciences and the Environment. World Sci. Publ. Co., Ltd., London. https://doi.org/10.1142/3106

[11] American Society for Testing and Materials (1986) Annual Book of ASTM Standards; 420. ASTM, Philadelphia, Report No. D, 109-113.

[12] Saad, A.F. (2008) Radium Activity and Radon Exhalation Rates from Phosphate Ores Using CR-39 On-Line with an Electronic Radon Gas Analyzer "Alpha Guard". *Radiation Measurements*, **43**, S463-S466. https://doi.org/10.1016/j.radmeas.2008.04.052

[13] Walley El-Dine, N., El-Sharsha, A., Ahmed, F. and Abdel-Haleem, A.S. (2001) Measurement of Radioactivity and Radon Exhalation Rate in Different Kinds of Marbles and Granites. *Applied Radiation and Isotopes*, **55**, 853-860. https://doi.org/10.1016/S0969-8043(01)00107-5

[14] AquaKIT Manual (1999) Genitron Instruments GmbH, Germany 09/97.

[15] Mustonen, R. (1984) Natural Radioactivity in and Radon Exhalation from Finnish Building Materials. *Health Physics*, **46**, 1195-1203. https://doi.org/10.1097/00004032-198406000-00003

[16] Barton, T.P. and Ziemer, P.L. (1986) The Effects of Plastic Size and Moisture Content on the Emanation of RN from Coal Ash. *Health Physics*, **50**, 518-528. https://doi.org/10.1097/00004032-198605000-00001

[17] United Nations Scientific Committee on the Effects of Atomic Radiation (2000) Sources, Effects and Risk of Ionizing Radiation. United Nations, New York.

[18] Beretka, J. and Mathew, P.J. (1985) Natural Radioactivity of Australian Building Materials, Industrial Wastes and By-Products. *Health Physics*, **48**, 87-95. https://doi.org/10.1097/00004032-198501000-00007

[19] NEA-OECD (1979) Nuclear Energy Agency-Organization for Economic Cooperation and Development. Exposure to Radiation from Natural Radioactivity in Building Materials. Report by NEA Group of Experts, OECD, Paris.

[20] Mantazul, I.C., Alam, M.N. and Hazari, S.K.S. (1999) Distribution of Radionuclides in the River Sediments and Coastal Soils of Chittagong, Bangladesh and Evaluation of the Radiation Hazard. *Applied Radiation and Isotopes*, **51**, 747-755. https://doi.org/10.1016/S0969-8043(99)00098-6

[21] Krieger, R. (1981) Radioactivity of Construction Materials. *Betonwerk Fertigteil Technology*, **47**, 468-473. https://doi.org/10.1016/S0160-3450(16)31258-2

World Journal of Nuclear Science and Technology, 2019, 9, 96-111
http://www.scirp.org/journal/wjnst
ISSN Online: 2161-6809
ISSN Print: 2161-6795

New Formulation for Semi-Empirical Correlations for Penetration Jets

R. R. Pacheco[1*], L. O. Freire[2], M. S. Rocha[2], N. L. Scuro[2], M. O. Menezes[2], D. A. Andrade[2*]

[1]Centro Tecnológico da Marinha em São Paulo, São Paulo, Brazil
[2]Instituto de Pesquisas Energéticas e Nucleares, São Paulo, Brazil
Email: *rafaelrade@gmail.com, *delvonei@ipen.br

How to cite this paper: Pacheco, R.R., Freire, L.O., Rocha, M.S., Scuro, N.L., Menezes, M.O. and Andrade, D.A. (2019) New Formulation for Semi-Empirical Correlations for Penetration Jets. *World Journal of Nuclear Science and Technology*, **9**, 96-111.
https://doi.org/10.4236/wjnst.2019.92007

Received: January 22, 2019
Accepted: April 27, 2019
Published: April 30, 2019

Abstract

Correlations for the extension of a water vapor jet injected in a liquid pool were historically proposed considering the mass flux (kg/m^2/s) as a constant. The results were satisfactory, however adjusting the values by linear regression. Although, it presents the following drawbacks: 1) the formulation is only valid for the specific range of data for what it was created; 2) it does not allow the analytical evaluation of the heat transfer coefficient from the extension equation. This paper proposes a new formulation for the calculation of the mass flux, in such a way to remove both of these drawbacks.

Keywords

Direct Contact Condensation, Vapor Jet, Steam Jet, Steam Mass Flux, Vapor Cavity, Reynolds Number, Jet Radius, Rate of Condensation, Non-Dimensional Jet Length, Liquid Pool, Dimensionless Transport Modulus, Condensation Driving Potential

1. Introduction

The phenomenon of Direct Contact Condensation (DCC) has been discussed in the literature since Kerney [1], due to its importance as a solution of engineering, where large values of heat transfer coefficient are needed. Through the DCC, several different sets of equipment can be designed, when, for example, condensation is in a small frame of time, or when reduced space is required.

DCC is the natural solution for applications where superheated vapor must be discharged in the atmosphere. Within this scope, DCC offers a safe alternative to reduce the heat and pressure up to the threshold where the discharge to the atmosphere is plausible, as it occurs in relief tanks.

For the nuclear industry, it emerges as a solution for containing the discharge

of the high energetic water contained in a primary loop of a Pressure Water Reactor (PWR), and also, to direct it to the chemical and radiological plant treatment facilities.

For Boiling Water Reactors (BWR), DCC emerges as a solution to recollect the water vaporized within the reactor vessel. For this, BWR plants prescribe Suppression Pools in their projects, where the DCC phenomenon takes place.

The DCC phenomenon reached well-established economic importance and has become an object of research since it is related to the safety of nuclear power plants, where it occurs as a high energetic vapor injection in a tank containing liquid compressed water. The heat transfer coefficient is increased due to the turbulent character of the interface of the jet and the bath, and this is the key to the efficiency of thermal exchange [2].

The design of devices where the DCC may occur determined the interest in the research of the phenomenon. The research focused mainly on the determination of a model for the extension of the jet, and another model for the determination of the heat transfer coefficient.

Nevertheless, the highly complex physics of this phenomenon restrains the development of a full analytical model for the extension of the jet and for its heat transfer coefficient. Experimental data are supplied to fulfill the gaps in the analytical development and semi-empirical correlations have been proposed, observing the following restrictions: 1) these correlations are valid only for the specific range of experimental data; 2) the analytical evaluation of the heat transfer directly from the length correlation was not possible, considering the available formulation.

The present work proposes a new formulation for the flux of mass in the currently presented correlations in the literature, in such a way that their validity would extend to any set of data, and which would allow a direct deduction of the heat transfer coefficient from the adjusted correlation of the dimensionless extension. This proposition grounds itself in an analytical procedure considering the 1st and the 2nd law of the thermodynamics.

2. Literature Review

The first proposal to evaluate the extension of the jet, as in [1], is a development of the mass conservation, applied to a simple model, in which a superheated vapor jet produces a cavity full of vapor, discharged in an atmospheric water bath, as presented in **Figure 1**. In Equation (1), the vapor flow rate ("$\dot{m}$") along the injection axis "x" is related to the jet radius "r" and the rate of condensation "R".

$$\frac{\mathrm{d}\dot{m}}{\mathrm{d}x'} = -2\pi r' R \tag{1}$$

Figure 2 presents the basic configuration of the experimental set. A pressure chamber (P_C) supplies superheated vapor. After the restriction by a valve, the vapor is injected in the water pool. The setting of the experiment allows a choked flow injection since it would reduce fluctuations in the jet.

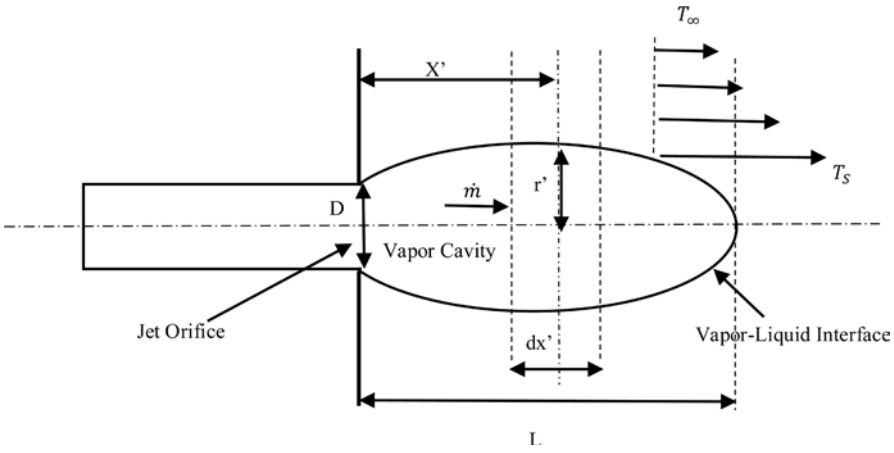

Figure 1. Dimensional variables [1].

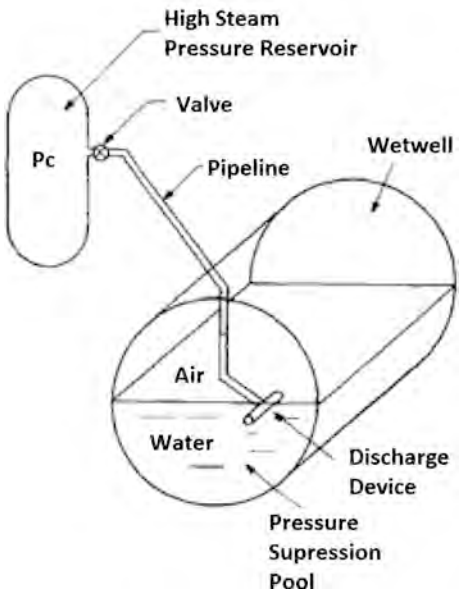

Figure 2. Illustration of the Experiment from (Sonin, 1981).

The dimensions r' and dx' are depicted in **Figure 1**. According to this proposal, there is an outflow of water along the lateral vapor-liquid interface of the jet. This amount of water, crossing the jet interface, promptly freezes, assuming the properties of the surrounding water bath. This condensation is governed by R, which takes the following form:

$$R = h\frac{\left(T_S - T_\infty\right)}{h_{gf}} \tag{2}$$

The mass flow (Equation (3)) also takes part in this development. Initial conditions are applied in Equation (4).

$$\dot{m} = \pi r'^2 G \tag{3}$$

$$\dot{m}_0 = \pi r_0'^2 G_0 \tag{4}$$

After some algebraic effort, Equation (1) and Equation (4) produce Equation

(5):

$$X = \int_1^0 \left[-\left(\frac{G_0}{G}\right)^{1/2} \cdot B^{-1} \cdot S^{-1} \right] \mathrm{d}Y \tag{5}$$

where B is defined as the driving potential for condensation (Equation (6)), and S as the dimensionless transport modulus, which is analogous to the Stanton Number (Equation (7)), although it presents some unorthodoxy, since the heat transfer coefficient (h) and the specific heat (C_P) are related to the liquid phase, and the mass flow rate (G) is related to the vapor phase. X is defined as the dimensionless jet length, Equation (8). For sake of clarity, Y replaces the term presented Equation (9).

$$B = C_P \frac{\left(T_S - T_\infty\right)}{h_{gf}} \tag{6}$$

$$S = \frac{h}{C_P \cdot G} \tag{7}$$

$$X = L/r_0 \tag{8}$$

$$Y = \left(\dot{m}/m_0\right)^{1/2} \tag{9}$$

At this point, namely Equation (5), [1] comes to a crossroad, since G and S depend on Y, and for this, Equation (5) cannot be integrated. A pure analytic result is not achievable. However, assuming G_M and S_M as constant, this author proposed the correlation, Equation (10):

$$X = \left(\frac{G_0}{G_M}\right)^{1/2} \cdot S_M^{-1} \cdot B^{-1} \tag{10}$$

And S_M is described by Equation (11):

$$S_M = \frac{h}{C_P \cdot G_M} \tag{11}$$

Considering the results of their experiment, treated by linear regression, the numeric format of Equation (12) was proposed, within 13.6% accuracy.

G_M was arbitrarily chosen as 275 kg/m^2/s, constant value, related to the critical vapor mass rate of the nozzle, as a representative value of the order of the magnitude of the mass rate. The value of 1.932 for S_M in Equation (12), is partially originated from the arbitrarily chosen value of 275 kg/m/s^2 and the conditions of the experiment (h, and C_P), which Kerney [1] derived in their experiment, considering a linear fit of the achieved data.

$$X = \frac{1}{1.932}\left(\frac{G_0}{G_M}\right)^{1/2} \cdot B^{-1} \tag{12}$$

In [3], a method to extend the semi-empirical correlation scope, in order to present results considering fluids other than water, and pressures other than ambient in the pool was presented. To achieve it, the proposed correlation considers the influence of the fluid density.

The development is not analogous to that in [3] since it uses a full set of equation (continuity of mass, linear momentum, and energy) while [1] used only the continuity of mass. Another theoretical remark is that the former considered that there is a cross flow of vapor to the bath, which is condensed within it, while the latter considered the opposite entrainment of water into the vapor jet, which is partially evaporated, and creates a two-phase flow zone.

This development also presented a point where the integration of the continuity of the mass is not possible since the integrand is not a defined function of the mass cross flow. An approximated correlation is considered, and this further development, considering experimental data, yields:

$$X = 35.5\left(\frac{G_0}{G_W}\right)^{1/2} \cdot B^{-1} \cdot \left(\frac{\rho_\infty}{\rho_w}\right)^{-1/2} \tag{13}$$

where G_W is not an arbitrary fixed value since it was considered the mass flux in the point where the jet finishes an isentropic expansion. After that, the jet allows entrained water in. The "W" properties are calculated considering the laws of the Thermodynamics, for the depth in which the jet starts the two-phase flow. The average absolute deviation found was 21.9%, higher than the value found in the precedent work.

A slightly better average absolute deviation is found both by Kerney [1] and Weimer [3], when they depart of the condition to have *a* priori fixed value exponents, and consider them a free product of the regression. No further development of the latter was found in the literature.

Based on previous work, Chun [4], consider that the characteristics of the jet are mainly dependent on 1) the degree of subcooling of the bath, 2) the steam mass flux, 3) the nozzle direction and 4) the depth of the nozzle. The efficiency of the Direct Contact Condensation as a mechanism of heat transfer is also praised, although attention is called to the fact that no reliable correlation to determine the length of the jet exists. According to this paper, much of the disagreement is related to the fact that, experimentally, the length of the jet is obtained by a visual method, what raises issues related to the geometric limits of the jet. In this paper, the end of the jet was considered as the interface between pure vapor and two-phase flow regions. Theoretical development was not presented, and this paper focused on the development of new values for old parameters. The theoretical expression has its roots in Kerney [1], as shown in Equation (14).

$$X = F\left(\frac{G_0}{G_M}, B, S_M\right) \tag{14}$$

Empirically, through visual method, the values of X are determined, which allows Chun [4] propose Equation (15), within a 20% dispersion,

$$X = 0.5923 \cdot \left(\frac{G_0}{G_M}\right)^{0.3444} \cdot B^{-0.66} \tag{15}$$

In sequence, as product of a regression, it is also proposed a correlation for the heat transfer coefficient, Equation (16):

$$\frac{h}{C_P \cdot G_M} = 0.8012 \cdot \left(\frac{G_0}{G_M}\right)^{0.3444} \cdot X^{-1.0079} B^{-0.6247} \tag{16}$$

The value of G_M is also not mentioned throughout the work, for what is supposed that in [4], Chun considered the fixed value of 275 kg/m^2/s as formerly proposed.

Proceeding a similar experiment (vapor injection in a subcooled water pool, atmospheric pool), reference Kim, *et al.* (2001) produced the correlation as presented in Equation (17) and Equation (18):

$$X = 0.503 \cdot \left(\frac{G_0}{G_M}\right)^{0.47688} \cdot B^{-0.70127} \tag{17}$$

$$\frac{h}{C_P \cdot G_M} = 1.4453 \cdot \left(\frac{G_0}{G_M}\right)^{0.13315} \cdot B^{0.03587} \tag{18}$$

The value of G_M was again considered 275 kg/m^2/s, as originally proposed. It is worth to notice that Equation (10), Equation (15) and Equation (17) are reasonably similar in their forms. Both are directly obtained from the original mathematical development.

Gulawani, in [5] and Kang, in [6] present CFD as a new tool to perform the geometric analysis of the jet, and its heat transfer coefficient. Shah, in [7], also by CFD analysis, found heat transfer coefficients ranging between 0, 6 and 08 MW/m^2/K and a dimensionless length ranging between 3.8 and 8.

In [8], it was experimentally proposed a different form of correlation. For instance, this model includes a pressure correction factor, as shown in Equation (21):

$$X = 0.868 \left(\frac{P_0}{P_a}\right)^{0.2} \cdot \left(\frac{G_0}{G_M}\right)^{0.5} \cdot B^{-0.60} \tag{21}$$

This correlation is within a 40% band of error.

This development leads to the proposal of another heat transfer correlation, as shown in Equation (22):

$$S_M = \frac{h}{C_P \cdot G_M} = 0.576 \left(\frac{P_0}{P_a}\right)^{0.2} \cdot \left(\frac{G_0}{G_M}\right)^{0.5} \cdot B^{-0.4} \tag{22}$$

Xu, in [9] proposed a different configuration of an experiment when a vertical pipe injected vapor in a flow of water instead of a pool. The extension and the heat transfer coefficient correlations were determined to have the Reynolds number as a parameter. The results presented the dimensionless extension between 0.29 and 4.64 and the heat transfer coefficient between 0.34 MW/m^2 K and 11.36 MW/m^2 K.

Chong, in [10] proposed a correlation for a straight-pipe nozzle, based on the original formulation. Under this work, the dimensionless extension correlation,

the geometry of the orifice nozzle was considered, through the imposition of a geometrical factor $(\varepsilon/\varepsilon')^2$, which represents the expansion ratio between a straight-line nozzle and actual orifice nozzle (for straight-line nozzle, $(\varepsilon/\varepsilon')^2 = 1$), as presented in Equation (21).

$$X = 0.3866\left(\frac{\varepsilon}{\epsilon}\right)^2 \cdot \left(\frac{G_0}{G_M}\right)^{0.78} \cdot B^{-0.80} \tag{23}$$

As a summary, Table 1 presents the main correlations for determining the dimensionless length in the literature, within the scope of this work.

One can notice that the constant value of $G_M = 275$ kg/s is broadly found (up to 2015) in the literature ([1] [4] [5] [7] [8] [9] [11] and [10]). For each one of these, S_M takes a different constant value, valid only for the respective correlation and for the respective range of data. A more realistic formulation of G_M would be of great interest since it directly impacts the formulation of X, S_M, and h.

3. Development

The experimental works under this scope are related to the development of a correlation for the non-dimensional length and heat transfer coefficient, through the propositions of variations of the originally proposed development from which results in the length correlation (Equation (10)). The extension of the works studied shows concern related to increasing the accuracy in a variety of experimental settings and parameters, in order to reduce the band of adjustment numerical error, since no fully analytical model is yet available.

The band of the error band is determined by fluctuations, which were neglected when Equation (5) was approximated. Sonin, in [12] experimentally investigated this phenomenon related to pressure waves propagating along the pool, while Youn [13] focused the particular case in which pressure waves are

Table 1. Extension correlation selected in the literature.

Dimensionless Extension	Equation Number
$X = 0.5200\left(\frac{G_0}{G_M}\right)^{1/2} \cdot B^{-1}$	(12)
$X = 35.5\left(\frac{G_0}{G_w}\right)^{1/2} \cdot B^{-1} \cdot \left(\frac{\rho_\infty}{\rho_w}\right)^{-1/2}$	(13)
$X = 0.5923 \cdot \left(\frac{G_0}{G_M}\right)^{0.3444} \cdot B^{-0.66}$	(15)
$X = 0.503 \cdot \left(\frac{G_0}{G_M}\right)^{0,4768878} \cdot B^{-0.70127}$	(17)
$X = 0.868\left(\frac{P_S}{P_a}\right)^{0.2} \cdot \left(\frac{G_0}{G_M}\right)^{0.5} \cdot B^{-0.60}$	(21)
$X = 0.3866\left(\frac{\varepsilon}{\epsilon}\right)^2 \cdot \left(\frac{G_0}{G_M}\right)^{0.78} \cdot B^{-0.80}$	(23)

created by a low mass flux of injection. The case where multiple jets are simultaneously created by different holes was explored by Cho [14]. The fluctuations related to turbulence, for example, were not originally considered in the analytical development of the semi-empirical correlations. This analysis indicates that some fluctuation is intrinsic to the process and offers an open field to research.

The experimental works follow a standard: the length of the jet is observed, what allows the definition of a correlation of length and the determination of the heat transfer coefficient. The experimental data collected supplies complementary information in order to complement the development of Equation (5).

In order to achieve a more realistic value of G_M, this paper proposes a new correlation. This value is developed through the application of the 1st and 2nd law of the thermodynamics in the jet, considering it an isentropic discharge, and a function of the conditions in the pressure chamber, as displayed from Equation (24) to Equation (30):

$$G_M = \rho_x \cdot V_{Crit} \tag{24}$$

$$V_{Crit} = \sqrt{2 \cdot \left(h_0 - h_{crit}\right)} \tag{25}$$

$$h_0 = h\left(P_0, T_0\right) \tag{26}$$

$$h_{crit} = h\left(P_{crit}, s_{crit}\right) \tag{27}$$

$$P_{crit} = 0.577 \cdot P_0 \tag{28}$$

$$\rho_x = \rho\left(101.3\ \text{kPa}, S_{Crit}\right) \tag{29}$$

$$s_{crit} = s_0 \tag{30}$$

Within the scope of this paper, the proposed correlations of G_M (Equation (24)) substituted the formerly constant value of G_M = 275 kg/m^2/s in those correlations presented in **Table 1**. The numerical analysis that follows considered the experimental data obtained from Kerney [1].

4. Results

1) *The Validity of G_M as Product of an Isentropic Process*

Table 2 presents some important data related to the numerical procedure. Item (i) presents the least square adjustment error when this procedure is applied to the correlation in the respective literature. All the correlations in item (i) were applied to the experimental data presented in Kerney [1]. Item (ii) presents the adjustment error found when the least square procedure is applied to the correspondent correlation when using the value of G_M as proposed in Equation (24), as suggested by this paper. The experimental data comes also from Kerney [1]. The percentage difference between (i) and (ii) is presented in item (iii). Item (iv) presents the value of S_M as found in the respective literature, while (v) presents S_M recalculated, where the data originally used by each respective author is swapped by the data presented in Kerney [1]. The difference from (iv) and (v) can be explained as a consequence of the fact that each correlation stands only for the range of data of the experiment for what it was developed. So,

changing the parameters of the experiment (e.g. the temperature of the pool, pressure of injection, mass flux, etc.), the correlation would also have to be changed in its parameters (S_M, and the exponents of G_0/G_M, B). This is evidenced with the small difference for the column of Equation (12), but greater for the remaining columns. Last item, (vi), evaluates the value of S_M as a product of the isentropic relation in Equation (24). The difference between correspondent values of references (v) and (vi) is small, indicating that the isentropic correlation stands for a broad range of parameters.

For the analysis of Table 2, it is evidenced by the dependence of S_M on the range of parameters employed in the experiment, since items (iv) and (v) present a large difference. When the isentropic formulation of G_M (Equation (24)) is used in item (vi), this difference is vastly reduced (see items (v) and (vi)).

The currently proposed distribution of G_M as an isentropic relation (Equation (24)), applied to the experimental data within Kerney [1], follows a logarithmic path along the pressure in the chamber axis (P_C), as presented in Figure 3. Equation (30) presents $G_M = G_M\left(P_C\right)$ as a product of regression.

$$G_M = 127.6367 + 26.4510 \cdot \ln\left(P_C\right) \tag{30}$$

The graphics in Figures 4-7 present comparisons between the correlations proposed by the respective authors, considering G_M = 275 kg/m^2/s constant, as originally proposed by Kerney [1] *versus* the currently proposed correlation for G_M, within the scope of this paper, Equation (24). The respective results were plotted against the experimental data.

As noticed, the correlations considering both propositions of G_M found a narrow agreement, what validates the use of G_M as the product of an isentropic assumption (Equation 24) as proposed by the present paper.

2) *Heat Transfer Coefficient*

Once the value of G_M is specified by Equation (24), the heat transfer coefficient (h) can be analytically derived from Equation (11), in conjunction with the adjusted value of S_M, which is obtained from the linear coefficient of the least square adjustment in the correlations of Table 1. In this section, this value of heat transfer coefficient, this way obtained, is compared with values found

Table 2. Numerical parameters of the method.

Item	Description	Equation (12)	Equation (15)	Equation (17)	Equation (21)
(i)	Adjustment Error (G_M = 275 kg/m^2/s)	2.268	2.762	2.241	2.949
(ii)	Adjustment Error (G_M as in Equation 24)	2.409	2.907	2.407	2.458
(iii)	Difference in Percentage (i) and (ii)	6.255%	5.273%	7.403%	16.65%
(iv)	S_M literature, calculate by the respective author, and with data from the respective author	1.923077	1.688334	1.988072	1.152074
(v)	S_M (G_M = 275 kg/m^2/s) recalculated with Kerney [1]	1.918281	0.59453	0.776398	0.534474
(vi)	S_M (G_M as in Equation 24), calculate with data from Kerney [1]	1.850481	0.581395	0.749625	0.514933

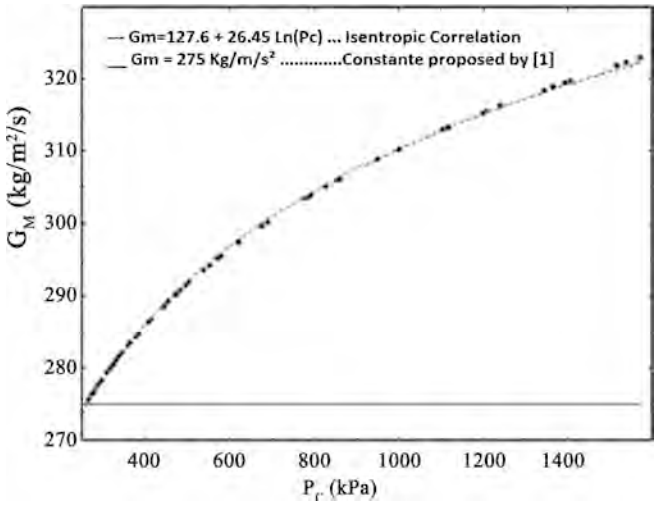

Figure 3. G_M as isentropic relation (Equation (24)) *vs.* pressure in the chamber (P_C) for Kerney [1], experimental data.

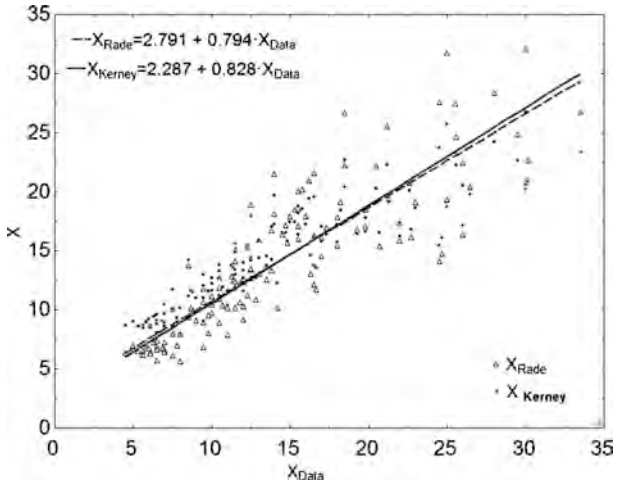

Figure 4. Correlation of Kerney [1], *vs.* Data X dispersion using G_M = 275 kg/m²/s constant and by G_M as an isentropic formulation (Equation (24)).

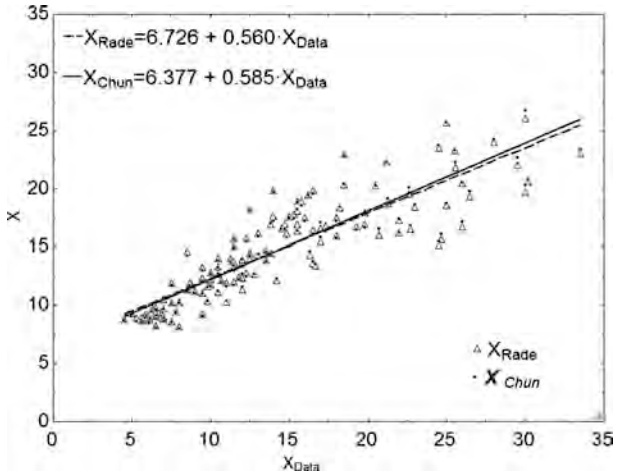

Figure 5. Correlation of Chun [4], *vs.* Data (X dispersion using G_M = 275 kg/m²/s constant and G_M as an isentropic formulation, Equation (24)).

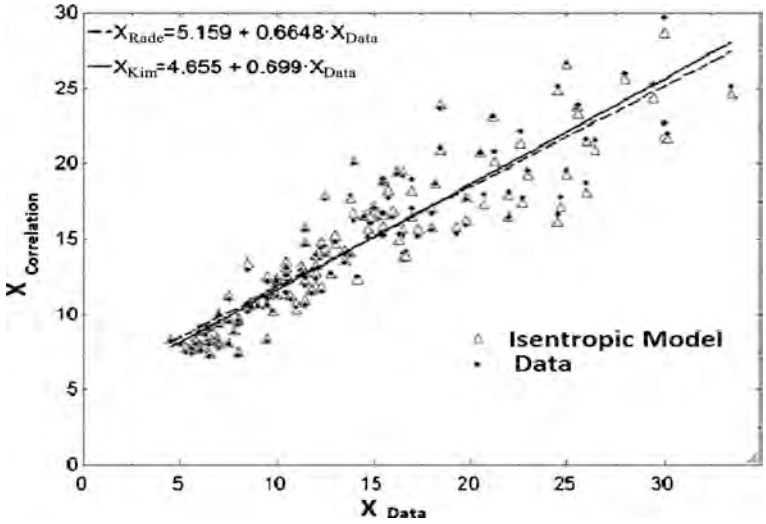

Figure 6. Correlation Kim [11], *vs.* Data (X dispersion using G_M = 275 kg/m^2/s constant and G_M as an isentropic formulation, Equation (24)).

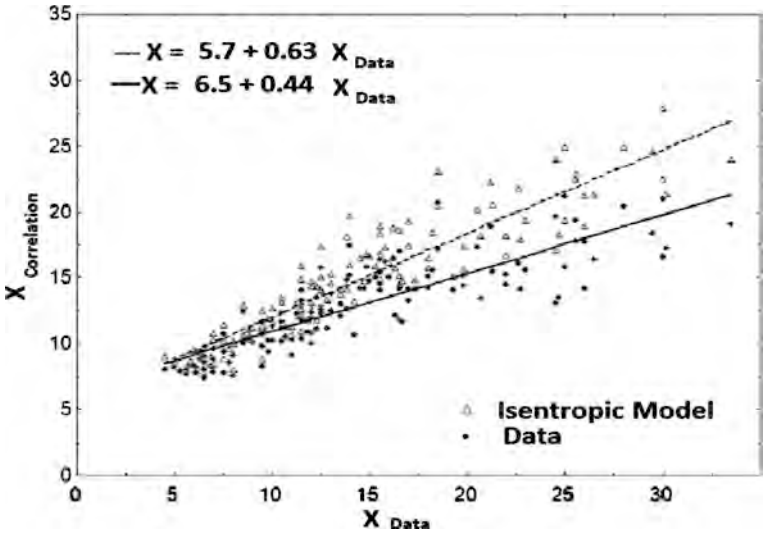

Figure 7. Correlation of Wu [8], *vs.* Data (X dispersion using G_M = 275 kg/m^2/s constant and G_M as an isentropic formulation, Equation (24)).

through the application of correlations in the literature (Equation (16) and Equation (18)).

Figure 8 and Figure 9 present h as a smooth function of P_C. Both sets of data belong to the same magnitude order, which indicates that this procedure to obtain h may be valid.

In Figure 9, difference decreases as long as the pressure in the chamber increases. On the other hand, Figure 10 and Figure 11 present the value of the heat transfer coefficient, found through the application of the least square procedure in an extension correlation in order to determine M with data from Kerney [1]. These values are plotted vs G_0. When "h" is represented as a function of "G_0", its smoothly dependence on "G_0" is easily observed. Once more, both results belong to the same magnitude order.

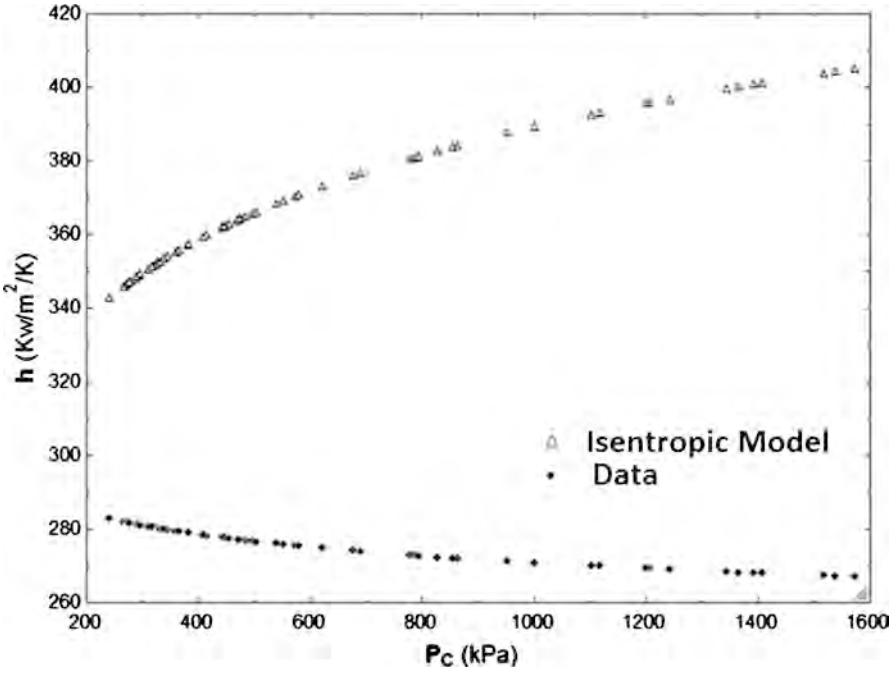

Figure 8. Heat Transfer Coefficient *vs* Pressure in the Chamber. G_M from an isentropic relation (Equation (24)); h from the correlation of Chun [4], Equation (16); Data from Kerney [1].

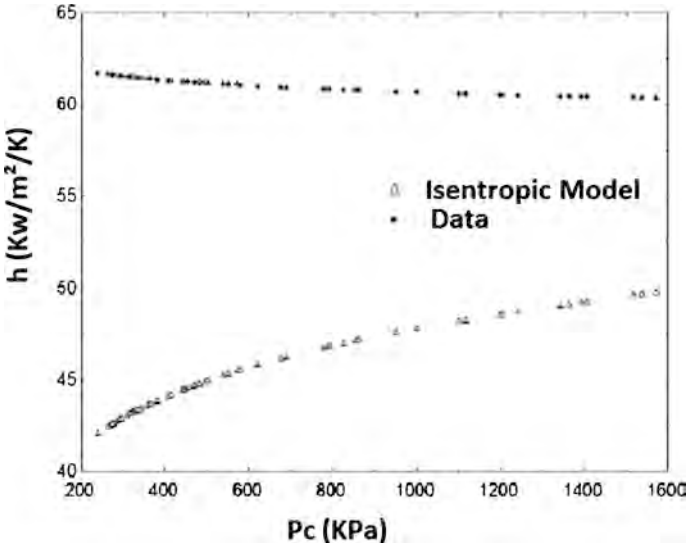

Figure 9. Heat Transfer Coefficient *vs* Pressure in the Chamber. G_M from an isentropic relation (Equation (24)); h from the correlation of Kim [11], Equation (18); Data from Kerney [1].

5. Conclusions

The decision to maintain S_M as a constant is numerically satisfactory since the chosen value is adjusted by the linear regression to fit the found data. Through this premise, any value proposed for G_M would generate the same adjustment error. This decision, proposed originally by Kerney [1], has been assumed up to works in 2015, although it does not depict the physics of the problem.

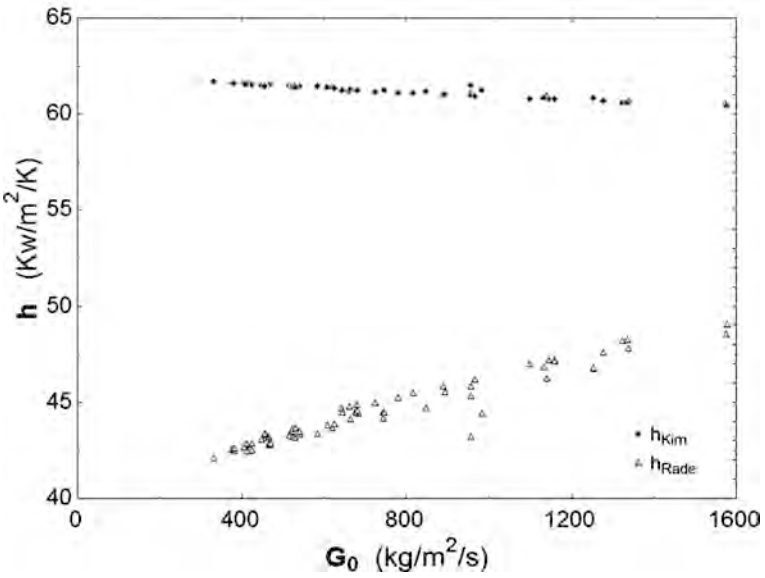

Figure 10. Heat Transfer Coefficient considering G_M from Equation (24) *vs.* mass flux ratio. *h* from correlation of Chun [4] *vs.* mass flux ratio. Data from Kerney [1].

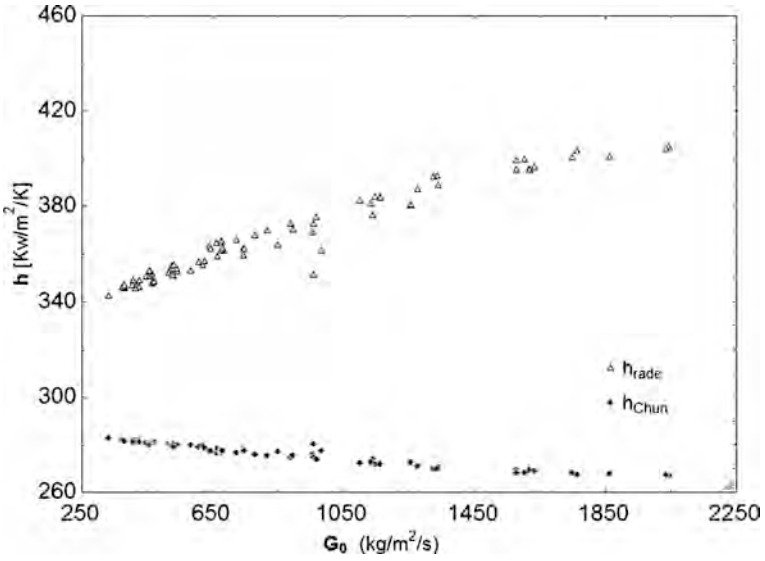

Figure 11. Heat Transfer Coefficient considering G_M from Equation (24) *vs.* mass flux ratio. *h* from the correlation of Kim [11] *vs.* mass flux ratio. Data from Kerney [1].

A full analytic function is not possible to be achieved since the area and the variation of major parameters as a function of the flux of mass in Equation (5) are unknown. These gaps have been fulfilled with experimental data, allowing the propositions of correlations, which present some degree of adjustment error, and are suitable only for the range of the experimented data.

This work presented satisfactory arguments to question the original formulation, where the mass flow rate (G_M) is constant. This original formulation stands as reasonable when a formulation for the extension of the jet is proposed since any constant value proposed fits when applied the linear regression. Although it presents the following drawbacks: 1) the formulation is only valid for the specific

range of data for what it was created; 2) it does not allow the analytical evaluation of the heat transfer coefficient from the extension equation, Equation (10).

This way, the isentropic formulation of G_M adds flexibility for the extension jet equation, once it is less dependent of experimental data, and allows the analytical evaluation of the heat transfer coefficient from the extension equation.

Considering the scope of correlations presented in this work, the proposed correlation of G_M as an isentropic function of the pressure chamber stands as reasonable and would apply to any extension of thermodynamical conditions.

Besides, the isentropic formulation of G_M allows the direct deduction of the heat transfer coefficient from the formulation of the extension, which reduces the dependence on experimental data. The present analysis indicates the possibility to reduce the dependence on experimental data to determine h, and points to a direction where more experimental efforts could be expended.

Further works could focus on the reinforcement of the presented correlation through the experimental analysis, considering a large range of parameters.

Acknowledgements

The authors would like to acknowledge Nuclear and Energy Research Institute, IPEN-CNEN/SP and CTMSP/SP for the infrastructure, particularly the computer laboratory.

Conflicts of Interest

The authors declare no conflicts of interest regarding the publication of this paper.

References

[1] Kerney, P.J., Faeth, G.M. and Olson, D.R. (1972) Penetration Characteristics of a Submerged Steam Jet. *AIChE Journal*, **18**, 548-553. https://doi.org/10.1002/aic.690180314

[2] van Wissen, R.J.E., Schreel, K.R.A.M., van der Geld, C.W.M. and Wieringa, J. (2004) Turbulence Production by a Steam-Driven Jet in a Water Vessel. *International Journal of Heat and Fluid Flow*, **25**, 173-179. https://doi.org/10.1016/j.ijheatfluidflow.2003.11.013

[3] Weimer, J.C., Faeth, G.M. and Olson, D.R. (1973) Penetration of Vapor Jets Submerged in Subcooled Liquids. *AIChE Journal*, **19**, 552-558. https://doi.org/10.1002/aic.690190321

[4] Chun, M.-H., Kim, Y.-S. and Park, J.-W. (1996) An Investigation of Direct Condensation of the Steam Jet in Subcooled Water. *International Communications in Heat and Mass Transfer*, **23**, 947-958. https://doi.org/10.1016/0735-1933(96)00077-2

[5] Gulawani, S.S., Joshi, J.B., Shah, M.S., RamaPrasad, C.S. and Shukla, D.S. (2006) CFD Analysis of Flow Pattern and Heat Transfer in Direct Contact Steam Condensation. *Chemical Engineering Science*, **61**, 5204-5220. https://doi.org/10.1016/j.ces.2006.03.032

[6] Kang, H.-S. and Song, C.-H. (2008) CFD Analysis for Thermal Mixing in a Sub-

cooled Water Tank under a High Steam Mass Flux Discharge Condition. *Nuclear Engineering and Design*, **238**, 492-501.
https://doi.org/10.1016/j.nucengdes.2007.02.044

[7] Shah, A., Chughtai, I.R. and Ham, M. (2010) Numerical Simulation of Direct-Contact Condensation from a Supersonic Steam Jet in Subcooled Water. *Chinese Journal of Chemical Engineering*, **18**, 577-587.
https://doi.org/10.1016/S1004-9541(10)60261-3

[8] Wu, X.-Z., Yan, J.-J., Shao, S.-F., Cao, Y. and Liu, J.-P. (2007) Experimental Study on the Condensation of Supersonic Steam Jet Submerged in Quiescent Subcooled Water: Steam Plume Shape and Heat Transfer. *International Journal of Multiphase Flow*, **33**, 1296-1307. https://doi.org/10.1016/j.ijmultiphaseflow.2007.06.004

[9] Xu, Q., Guo, L., Zou, S., Chen, J. and Zhang, X. (2013) Experimental Study on Direct Contact Condensation of a Stable Steam Jet in Water Flow in a Vertical Pipe. *International Journal of Heat and Mass Transfer*, **66**, 808-817.
https://doi.org/10.1016/j.ijheatmasstransfer.2013.07.083

[10] Chong, D.-T., Zhao, Q.-B., Yuan, F., Wang, W., Chen, W. and Yan, J.-J. (2015) Research on the Steam Jet Length with Different Nozzle Structures. *Experimental Thermal and Fluid Science*, **64**, 134-141.
https://doi.org/10.1016/j.expthermflusci.2015.02.015

[11] Kim, H.-Y., Bae, Y.-Y., Song, C.-H. and Park, J.-K. (2001) Experimental Study on Stable Steam Condensation in a Quenching Tank. *International Journal of Energy Research*, **25**, 239-252. https://doi.org/10.1002/er.675

[12] Sonin, A.-A. (1981) Scaling Laws for Small-Scale Modeling of Steam Relief into Water Pools. *Nuclear Engineering and Design*, **65**, 17-21.
https://doi.org/10.1016/0029-5493(81)90115-1

[13] Youn, D.-H., Ko, K.-B., Lee, Y.-Y., Kim, M.-H., Bae Y.-Y. and Park, J.-K. (2012) The Direct Contact Condensation of Steam in a Pool at Low Mass Flux. *Journal of Nuclear Science and Technology*, **40**, 881-885.
https://doi.org/10.1080/18811248.2003.9715431

[14] Cho, S., Chun, S.-Y., Baek, W.-P. and Kim, Y. (2004) Effect of Multiple Holes on the performance of Sparger during Direct Contact Condensation of Steam. *Experimental Thermal and Fluid Science*, **28**, 629-638.
https://doi.org/10.1016/j.expthermflusci.2003.10.002

Nomenclature

A Heat Transfer Area (m^2)

B Condensation Driving Potential

C_p Water Specific Heat (J/kg/˚C)

G Steam Mass Flux ($kg/m^2/s$)

h Average Heat Transfer Coefficient (W/m^2˚C)

h_{fg} Condensation Enthalpy (kJ/kg)

L Steam Jet Length (m)

$\dot{m}$ Vapor Flow Rate (kg/s)

P Pressure (kPa)

r Jet Radius (m)

R Rate of Condensation ($kg/m/s^2$)

S Dimensionless Transport Modulus

T Temperature (˚C)

x Axial Coordinate (m)

X Non-Dimensional Jet Length

ρ Density (kg/m^3)

Subscripts

A Atmospheric Conditions

C Conditions in the Pressure Chamber

f Conditions of Saturated Liquid

S Conditions in the Vapor-Bath Interface

g Conditions of Saturated Vapor

∞ Average Conditions in the Pool, Far Away from the Jet

0 Conditions in the Nozzle

M Average Conditions over the Interface Surface

W Developed as [3]

Call for Papers

World Journal of Nuclear Science and Technology (WJNST)

ISSN 2161-6795 (Print) ISSN 2161-6809 (Online)
http://www.scirp.org/journal/wjnst

World Journal of Nuclear Science and Technology **(WJNST)** is an international peer-reviewed, open access journal publishing in English original research studies, reviews in all aspects of nuclear science and technology and its applications. Symposia or workshop papers may be published as supplements.

Editor-in-Chief

Prof. Andrzej Grzegorz Chmielewski

Editorial Board

Subject Coverage

This journal invites original research and review papers that address the following issues. Topics of interest include, but are not limited to:

- Fuel Cycle and Isotopes
- Global Nuclear Security Technology
- Nonreactor Nuclear Facilities
- Nuclear and Chemical Waste Management
- Nuclear and Particle Physics
- Nuclear Cardiology
- Nuclear Energy
- Nuclear Engineering and Design
- Nuclear Fusion
- Nuclear Instruments and Methods
- Nuclear Magnetic Resonance Spectroscopy
- Nuclear Materials
- Nuclear Medicine and Biology
- Nuclear Medicine and Molecular Imaging
- Nuclear Physics
- Nuclear Science and Techniques
- Nuclear Structural Engineering
- Nuclear Track Detection
- Nuclear Tracks and Radiation Measurements
- Radiation Applications and Instrumentation
- Radioanalytical and Nuclear Chemistry
- Reactor and Nuclear Systems
- Reactor Science and Technology

We are also interested in short papers (letters) that clearly address a specific problem, and short survey or position papers that sketch the results or problems on a specific topic. Authors of selected short papers would be invited to write a regular paper on the same topic for future issues of the WJNST.

Notes for Intending Authors

Submitted papers should not have been previously published nor be currently under consideration for publication elsewhere. Paper submission will be handled electronically through the website. All papers are refereed through a peer review process. For more details about the submissions, please access the website.

Website and E-mail

http://www.scirp.org/journal/wjnst **E-mail: wjnst@scirp.org**

What is SCIRP?

Scientific Research Publishing (SCIRP) is one of the largest Open Access journal publishers. It is currently publishing more than 200 open access, online, peer-reviewed journals covering a wide range of academic disciplines. SCIRP serves the worldwide academic communities and contributes to the progress and application of science with its publication.

What is Open Access?

All original research papers published by SCIRP are made freely and permanently accessible online immediately upon publication. To be able to provide open access journals, SCIRP defrays operation costs from authors and subscription charges only for its printed version. Open access publishing allows an immediate, worldwide, barrier-free, open access to the full text of research papers, which is in the best interests of the scientific community.

- High visibility for maximum global exposure with open access publishing model
- Rigorous peer review of research papers
- Prompt faster publication with less cost
- Guaranteed targeted, multidisciplinary audience

Scientific Research Publishing

Website: http://www.scirp.org

Subscription: sub@scirp.org

Advertisement: service@scirp.org